

Published in final edited form as:

Chem Rev. 2013 July 10; 113(7): 5322–5363. doi:10.1021/cr300503r.

Visible Light Photoredox Catalysis with Transition Metal Complexes: Applications in Organic Synthesis

Christopher K. Prier, Danica A. Rankic, and David W. C. MacMillan*

Merck Center for Catalysis at Princeton University, Princeton, New Jersey 08544, United States

1. INTRODUCTION

A fundamental aim in the field of catalysis is the development of new modes of small molecule activation. One approach toward the catalytic activation of organic molecules that has received much attention recently is visible light photoredox catalysis. In a general sense, this approach relies on the ability of metal complexes and organic dyes to engage in single-electron-transfer (SET) processes with organic substrates upon photoexcitation with visible light.

Many of the most commonly employed visible light photocatalysts are polypyridyl complexes of ruthenium and iridium, and are typified by the complex tris(2,2'-bipyridine) ruthenium(II), or $\text{Ru}(\text{bpy})_3^{2+}$ (Figure 1). These complexes absorb light in the visible region of the electromagnetic spectrum to give stable, long-lived photoexcited states.^{1,2} The lifetime of the excited species is sufficiently long (1100 ns for $\text{Ru}(\text{bpy})_3^{2+}$) that it may engage in bimolecular electron-transfer reactions in competition with deactivation pathways.³ Although these species are poor single-electron oxidants and reductants in the ground state, excitation of an electron affords excited states that are very potent single-electron-transfer reagents. Importantly, the conversion of these bench stable, benign catalysts to redox-active species upon irradiation with simple household lightbulbs represents a remarkably chemoselective trigger to induce unique and valuable catalytic processes.

The ability of $\text{Ru}(\text{bpy})_3^{2+}$ and related complexes to function as visible light photocatalysts has been recognized and extensively investigated for applications in inorganic and materials chemistry. In particular, photoredox catalysts have been utilized to accomplish the splitting of water into hydrogen and oxygen⁴ and the reduction of carbon dioxide to methane.⁵ $\text{Ru}(\text{bpy})_3^{2+}$ and its analogues have been used (i) as components of dye-sensitized solar cells⁶ and organic light-emitting diodes,⁷ (ii) to initiate polymerization reactions,⁸ and (iii) in photo-dynamic therapy.⁹

Until recently, however, these complexes had been only sporadically employed as photocatalysts in the area of organic synthesis. The limited exploration of this area is

perhaps surprising, as single-electron, radical processes have long been employed in C–C bond construction and often provide access to reactivity that is complementary to that of closed-shell, two-electron pathways.¹⁰ In 2008, concurrent reports from the Yoon group and our own lab detailed the use of Ru(bpy)₃²⁺ as a visible light photoredox catalyst to perform a [2 + 2] cycloaddition¹¹ and an α -alkylation of aldehydes,¹² respectively. Shortly thereafter, Stephenson and co-workers disclosed a photoredox reductive dehalogenation of activated alkyl halides mediated by the same catalyst.¹³ The combined efforts of these three research groups have helped to initiate a renewed interest in this field, prompting a diversity of studies into the utility of photoredox catalysis as a conceptually novel approach to synthetic organic reaction development.

Much of the promise of visible light photoredox catalysis hinges on its ability to achieve unique, if not exotic bond constructions that are not possible using established protocols. For instance, photoredox catalysis may be employed to perform overall redox neutral reactions. As both oxidants and reductants may be transiently generated in the same reaction vessel, photoredox approaches may be used to develop reactions requiring both the donation and the reception of electrons at disparate points in the reaction mechanism. This approach stands in contrast to methods requiring stoichiometric chemical oxidants and reductants, which are often incompatible with each other, as well as to electrochemical approaches, which are not amenable to redox neutral transformations. Furthermore, single-electron-transfer events often provide access to radical ion intermediates having reactivity patterns fundamentally different from those of their ground electronic or excited states.¹⁴ Access to these intermediates using other means of activation is often challenging or requires conditions under which their unique reactivity cannot be productively harnessed.

At the same time, photoredox catalysts such as Ru(bpy)₃²⁺ may also be employed to generate radicals for use in a diverse range of established radical chemistries. Photoredox reactions occur under extremely mild conditions, with most reactions proceeding at room temperature without the need for highly reactive radical initiators. The irradiation source is typically a commercial household light bulb, a significant advantage over the specialized equipment required for processes employing high-energy ultraviolet (UV) light. Additionally, because organic molecules generally do not absorb visible light, there is little potential for deleterious side reactions that might arise from photoexcitation of the substrate itself. Finally, photoredox catalysts may be employed at very low loadings, with 1 mole % or less being typical.

This Review will highlight the early work on the use of transition metal complexes as photoredox catalysts to promote reactions of organic compounds (prior to 2008), as well as cover the surge of work that has appeared since 2008. We have for the most part grouped reactions according to whether the organic substrate undergoes reduction, oxidation, or a redox neutral reaction and throughout have sought to highlight the variety of reactive intermediates that may be accessed via this general reaction manifold.¹⁵

Studies on the use of transition metal complexes as visible light photocatalysts for organic synthesis have benefited tremendously from advances in the related fields of organic and semiconductor photocatalysis. Many organic molecules may function as visible light

photocatalysts; analogous to metal complexes such as $\text{Ru}(\text{bpy})_3^{2+}$, organic dyes such as eosin Y, 9,10-dicyanoanthracene, and triphenylpyrylium salts absorb light in the visible region to give excited states capable of single-electron transfer. These catalysts have been employed to achieve a vast range of bond-forming reactions of broad utility in organic synthesis.¹⁶ Visible light photocatalysis has also been carried out with heterogeneous semiconductors such as mesoporous carbon nitride¹⁷ and various metal oxides and sulfides.¹⁸ These approaches are often complementary to photoredox catalysis with transition metal-polypyridyl complexes, and we have referred to work in these areas when it is similar to the chemistry under discussion. However, an in-depth discussion of the extensive literature in these fields is outside the scope of this Review, and readers are directed to existing reviews on these topics.^{16–18}

2. PHOTOCHEMISTRY OF $\text{Ru}(\text{bpy})_3^{2+}$

Before we discuss organic transformations enabled by photo-redox catalysis, it is instructive to consider the photochemistry of the prototypical photoredox catalyst $\text{Ru}(\text{bpy})_3^{2+}$. Upon absorption of a photon in the visible region, an electron in one of the photocatalyst's metal-centered t_{2g} orbitals is excited to a ligand-centered π^* orbital (Scheme 1).^{1,19} This transition is thus termed a metal to ligand charge transfer (MLCT) and results in a species in which the metal has effectively been oxidized to a Ru(III) oxidation state and the ligand framework has undergone a single-electron reduction.²⁰ The initially occupied singlet MLCT state undergoes rapid intersystem crossing (ISC) to give the lowest-energy triplet MLCT state. This triplet state is the long-lived photoexcited species that engages in single-electron transfer; its long lifetime derives from the fact that decay to the singlet ground state is spin-forbidden.

The photoexcited species has the remarkable property of being both more oxidizing and more reducing than the ground-state species. To quantify this phenomenon, we refer to standard reduction potentials, which describe the potential associated with an electrochemical half reaction written in the direction from the oxidized to the reduced species. For instance, the half-reaction $\text{Ru}(\text{bpy})_3^{3+} + e^- \rightarrow {}^*\text{Ru}(\text{bpy})_3^{2+}$ is described by the reduction potential $E_{1/2}^{\text{III}/*{\text{II}}} = -0.81 \text{ V}$ vs the saturated calomel electrode (SCE).²¹ This potential signifies that the excited-state ${}^*\text{Ru}(\text{bpy})_3^{2+}$ is a much more potent electron donor than ground-state $\text{Ru}(\text{bpy})_3^{2+}$ ($E_{1/2}^{\text{III}/\text{II}} = +1.29 \text{ V}$ vs SCE). At the same time, the reduction potential of the excited state ($E_{1/2}^{*{\text{II}}/\text{I}} = +0.77 \text{ V}$ vs SCE) indicates that this species is a much stronger oxidant than the ground state ($E_{1/2}^{\text{II}/\text{I}} = -1.33 \text{ V}$ vs SCE).²² The dual nature of the excited state as both oxidant and reductant may be rationalized on the basis of the molecular orbital diagram, as depicted in Scheme 1. Photoexcitation of $\text{Ru}(\text{bpy})_3^{2+}$ generates a higher-energy electron, which may be expelled from the π^* orbital when the photocatalyst acts as a reductant. Simultaneously, photo-excitation reveals a lower-energy hole in the t_{2g} orbital, which may accept an electron when the photocatalyst acts as an oxidant.

As a result of this unique property of the $\text{Ru}(\text{bpy})_3^{2+}$ photoexcited state, redox transformations of ${}^*\text{Ru}(\text{bpy})_3^{2+}$ may proceed either by oxidative or by reductive quenching (Scheme 2). In the oxidative quenching cycle, ${}^*\text{Ru}(\text{bpy})_3^{2+}$ functions as a reductant,

reducing some electron acceptor (**A**) by a single electron. The products of this single-electron-transfer event are the radical anion of **A** and the oxidized form of the photocatalyst, $\text{Ru}(\text{bpy})_3^{3+}$. This species is a strong oxidant ($E_{1/2}^{\text{III/II}} = +1.29 \text{ V vs SCE}$) and may accept an electron from some donor **D** to give the radical cation of **D** and return the catalyst to the $\text{Ru}(\text{II})$ ground-state species, completing the photocatalytic cycle. A compound that accepts an electron from $^*\text{Ru}(\text{bpy})_3^{2+}$ is said to be an oxidative quencher of the photocatalyst; common oxidative quenchers are viologens, polyhalomethanes, dinitro- and dicyanobenzenes, and aryldiazonium salts. Alternatively, in the reductive quenching cycle, $^*\text{Ru}(\text{bpy})_3^{2+}$ functions as an oxidant, accepting an electron from **D** to give the reduced species $\text{Ru}(\text{bpy})_3^+$. This $\text{Ru}(\text{I})$ intermediate is a good reductant ($E_{1/2}^{\text{II/I}} = -1.33 \text{ V vs SCE}$) and may donate an electron to **A** to afford the ground-state species $\text{Ru}(\text{bpy})_3^{2+}$. The most common reductive quenchers are tertiary amines. Of particular relevance to the use of these complexes as catalysts for SET reactions, the redox potentials at each step of the cycle may be significantly altered via ligand substitution; as a general rule, electron-donating substituents on the ligands render the complex more strongly reducing, while electron-withdrawing substituents render the complex more strongly oxidizing.²³ Redox potentials and selected photo-physical properties for a number of commonly utilized visible light photoredox catalysts are given in Table 1; the catalysts are arranged by their excited-state potentials $E_{1/2}(\text{M}^+/\text{M}^*)$, from the least reducing excited species (entry 1) to the most reducing (entry 8).

To determine whether a reductive or oxidative quenching cycle is operative in a particular reaction, fluorescence quenching (or Stern–Volmer) studies are commonly employed.²⁴ This technique examines the competition between two deactivation pathways of the photoexcited state: quenching via electron transfer and emission (Figure 2). In the absence of a quencher, $^*\text{Ru}(\text{bpy})_3^{2+}$ undergoes emission, emitting radiation at $\lambda_{\text{max}} = 615 \text{ nm}$ with an inherent intensity.³ Increasing concentrations of a quencher, however, additionally deactivate $^*\text{Ru}(\text{bpy})_3^{2+}$ via electron-transfer pathways and decrease the intensity of the observed emission. This relationship between quencher concentration and emission intensity is given by the Stern–Volmer equation, $I_0/I = 1 + k_q \tau_0 [\text{Q}]$, where I_0 and I are the emission intensity in the absence and presence of quencher, respectively, k_q is the quenching rate constant, τ_0 is the excited-state lifetime in the absence of quencher, and $[\text{Q}]$ is the concentration of quencher. Plotting the ratio I_0/I against the quencher concentration thus gives a straight line having a y-intercept equal to 1 and a slope, termed the Stern–Volmer constant (K_{SV}), equal to $k_q \tau_0$. The observation of this relationship between concentration of a putative quencher and emission intensity constitutes evidence that the molecule engages in single-electron transfer with the photocatalyst.

In addition to the electron-transfer pathways described here, the $\text{Ru}(\text{bpy})_3^{2+}$ photoexcited state may also engage in energy transfer with organic substrates. This pathway, which accounts for a relatively minor subset of organic transformations achieved using visible light photocatalysts, is discussed in detail in section 6. It should be noted that energy transfer pathways, like electron-transfer pathways, diminish the emission intensity of the photoexcited species and may be evaluated using the Stern–Volmer analysis.

3. NET REDUCTIVE REACTIONS

3.1. Reduction of Electron-Poor Olefins

The first reactions demonstrating the potential utility of visible light photoredox catalysis in organic synthesis were net reductive reactions, in which an electron donor is required to serve as the stoichiometric reductant. Among the earliest reports was a contribution by Pac and co-workers in 1981 describing the $\text{Ru}(\text{bpy})_3^{2+}$ -mediated reduction of electron-deficient olefins.²⁵ The terminal reductant employed in these studies, 1-benzyl-1,4-dihydronicotinamide (BNAH, **1**), was of interest for its analogy to the biological reductant 1,4-dihydronicotinamide adenine dinucleotide (NADH), with both molecules sharing the redox-active 1,4-dihydropyridine moiety. It was found that a catalyst system comprising 2 equiv of BNAH and catalytic quantities of $\text{Ru}(\text{bpy})_3^{2+}$ was capable, upon irradiation with visible light, of reducing dimethyl maleate (**2**) to the saturated product dimethyl succinate (**3**) (Scheme 3). As in all photoredox reactions, this process is initiated by absorption of visible light by the photocatalyst $\text{Ru}(\text{bpy})_3^{2+}$ to give the photoexcited species $^*\text{Ru}(\text{bpy})_3^{2+}$. Photoexcitation renders this species sufficiently oxidizing ($E_{1/2}^{*\text{II/I}} = +0.77 \text{ V vs SCE}$) to accept an electron from BNAH ($E_{1/2}^{\text{red}} = +0.76 \text{ V vs SCE}$), generating the BNAH radical cation **4** and concurrently reducing the photocatalyst to $\text{Ru}(\text{bpy})_3^+$. This Ru(I) intermediate is highly reducing ($E_{1/2}^{\text{II/I}} = -1.33 \text{ V vs SCE}$), enabling transfer of an electron to dimethyl maleate. This event oxidizes the photocatalyst back to $\text{Ru}(\text{bpy})_3^{2+}$ and completes the photocatalytic cycle. Meanwhile, single-electron reduction of **2** gives the radical anion **5**, which may be protonated to yield α -carbonyl radical **6**. This radical is then believed to undergo a second single-electron reduction followed by protonation to give dimethyl succinate (**3**). The single-electron donor for this step may be another equivalent of $\text{Ru}(\text{bpy})_3^+$, or it may be dihydropyridyl radical **7**, the product of deprotonation of radical cation **4** and itself a strong reductant ($E_{1/2}^{\text{red}} = -0.94 \text{ V vs SCE}$).²⁶ Upon loss of an electron, radical **7** is converted to pyridinium **8**, the ultimate product of two-electron oxidation of BNAH.

The catalytic cycle proposed here is supported by Stern–Volmer studies: BNAH (**1**) is observed to quench $^*\text{Ru}(\text{bpy})_3^{2+}$, while dimethyl maleate (**2**) does not. This observation provides strong evidence that the reaction proceeds via reductive quenching of $^*\text{Ru}(\text{bpy})_3^{2+}$ to give a $\text{Ru}(\text{bpy})_3^+$ intermediate, rather than via oxidative quenching to give a $\text{Ru}(\text{bpy})_3^{3+}$ intermediate. The reaction was additionally found to be amenable to the reduction of alkenes bearing a range of electron-withdrawing groups, such as esters, ketones, arenes, and nitriles (Scheme 3).^{27,28}

3.2. Reductive Dehalogenation

Much early work was conducted in the area of reductive dehalogenation reactions, in which a C–X bond is reduced to a C–H bond. An early contribution from Fukuzumi in 1990 was the reduction of phenacyl bromides using visible light, $\text{Ru}(\text{bpy})_3^{2+}$ as a photocatalyst, and 9,10-dihydro-10-methylacridine as the stoichiometric reductant.²⁹ In the net transformation, the phenacyl bromide (**9**) is reduced by two electrons to give acetophenone (**10**), while the dihydroacridine **11** is oxidized by two electrons to give the acridinium byproduct **12** (Scheme 4). The reaction is initiated by single-electron transfer from 9,10-dihydro-10-

methylacridine (**11**, $E_{1/2}^{\text{red}} = +0.8 \text{ V vs SCE}$)³⁰ to $^*\text{Ru}(\text{bpy})_3^{2+}$ to give the radical cation **13** and the reduced species $\text{Ru}(\text{bpy})_3^+$. The Ru(I) intermediate may then reduce phenacyl bromide ($E_{1/2}^{\text{red}} = -0.49 \text{ V vs SCE}$),³¹ returning the catalyst to its Ru(II) oxidation state. Upon undergoing single-electron reduction, α -bromocarbonyls such as **9** are known to undergo mesolysis, the fragmentation of a radical anion to afford an anion (bromide) and a radical (the α -carbonyl radical **14**). Radical **14** must then accept an electron and a proton to furnish the acetophenone product (**10**). This conversion may occur in two separate events, as is proposed for Pac's olefin reduction, or in one event via the abstraction of a hydrogen atom from radical cation **13** (as shown in Scheme 4).

As in the olefin reduction chemistry, dihydroacridine **11** is observed to quench the emission of the photocatalyst, while phenacyl bromide (**9**) does not, providing support for the described catalytic cycle. Interestingly, added perchloric acid improves the efficiency of the debromination reaction. Quenching studies indicated that the addition of acid enables the reduction of phenacyl bromide by $^*\text{Ru}(\text{bpy})_3^{2+}$, suggesting that under these conditions the reaction may also be proceeding via an oxidative quenching cycle involving proton-coupled electron transfer. This ability to change the nature of the photocatalytic cycle via simple changes in reagents and conditions is a common feature of photoredox catalysis.

In 1984 Tanaka and co-workers similarly employed $\text{Ru}(\text{bpy})_3^{2+}$ as a catalyst for the reduction of benzyl bromide.³² Instead of reducing benzyl bromide to toluene, however, the major product observed is the dimerized product 1,2-diphenylethane (**15**, Scheme 5). Analogous to the phenacyl bromide reduction, single-electron reduction of benzyl bromide induces fragmentation to give the benzyl radical **16**. Tanaka suggests that the product **15** may be formed by the radical–radical dimerization of **16**, or alternatively by a second reduction of **16** to the benzyl carbanion, which may react with benzyl bromide via a nucleophilic $\text{S}_{\text{N}}2$ mechanism to give **15**.

Kern and Sauvage have shown that bibenzyl products can also be obtained upon single-electron reduction of a benzyl bromide by a copper photocatalyst (Scheme 6).³³ The bis(diimine)copper(I) complex $\text{Cu}(\text{dap})_2^+$ ($\text{dap} = 2,9\text{-bis}(p\text{-anisyl})\text{-1,10-phenanthroline}$) has photophysical properties similar to those of $\text{Ru}(\text{bpy})_3^{2+}$; upon irradiation with visible light, $\text{Cu}(\text{dap})_2^+$ undergoes photoexcitation to give a long-lived excited species $^*\text{Cu}(\text{dap})_2^+$ ($\tau = 270 \text{ ns}$). This species is a strong reductant ($E_{1/2}^{\text{II}/\text{I}} = -1.43 \text{ V vs SCE}$), capable of donating an electron to 4-nitrobenzyl bromide (**17**, $E_{1/2}^{\text{red}} = -1.1 \text{ V vs SCE}$).³⁴ Thus, while $\text{Ru}(\text{bpy})_3^{2+}$ must be reduced to its Ru(I) oxidation state before it can transfer an electron to benzyl bromide, the substantially more reducing $\text{Cu}(\text{dap})_2^+$ can perform the reduction directly from its photoexcited state. Reduction of **17** induces fragmentation to afford benzyl radical **18**, which may dimerize to give bibenzyl **19** (or, as suggested by Tanaka, undergo a second reduction followed by $\text{S}_{\text{N}}2$ attack on benzyl bromide). Triethylamine ($E_{1/2}^{\text{red}} = +1.0 \text{ V vs SCE}$)³⁵ serves as a stoichiometric reductant to regenerate $\text{Cu}(\text{dap})_2^+$ from the oxidized photocatalyst $\text{Cu}(\text{dap})_2^{2+}$. In the process, the amine is oxidized to the corresponding aminium radical cation.

Having the foresight and creativity to recognize the potential utility of these transformations, Stephenson has developed a general photoredox reductive dehalogenation protocol.¹³ The

reaction conditions developed employ the tertiary amine Hünig's base (*i*-Pr₂NEt) as the stoichiometric reductant in concert with either formic acid or Hantzsch ester. Single-electron oxidation of the amine by *Ru(bpy)₃²⁺ generates the aminium radical cation **20** and Ru(bpy)₃⁺, which may reduce an α -chloroester **21** to the α -carbonyl radical **22** (Scheme 7). Significantly, single-electron oxidation of an amine dramatically lowers the bond strength of the α -C–H bonds; Dinnocenzo has estimated the bond dissociation energy of this bond to be 47 kcal/mol, or over 30 kcal/mol less than that of the parent amine ($\Delta H_{\text{BDE}}^\circ = 80$ kcal/mol for the α -C–H bond of triethylamine).³⁶ The radical **22** may thus abstract a hydrogen atom at one of the α -positions of **20**, converting **22** to the reduced product **23** and the amine radical cation to iminium ion **24**. Although deuterium-labeling studies implicated the amine radical cation as the primary source of the hydrogen atom added in **23**, the formate ion and Hantzsch ester employed in the reaction are also likely hydrogen atom donors. These conditions could be applied to the reduction of both alkyl bromides and chlorides and are selective for the dehalogenation of benzylic and α -carbonyl halides over aryl and vinyl halides (Scheme 7).

A significant limitation of dehalogenation protocols employing Ru(bpy)₃²⁺ is the requirement for activated (benzylic or α -carbonyl) halides. Subsequent to his initial report, Stephenson disclosed the reductive dehalogenation of alkyl, alkenyl, and aryl iodides using the iridium photocatalyst *fac*-Ir(ppy)₃ (ppy = 2-phenylpyridine).³⁷ This complex is rendered highly reducing by virtue of its three strongly electron-donating cyclometalated 2-phenylpyridine ligands.³⁸ Thus, despite the difficulty of reducing alkyl iodides ($E_{1/2}^{\text{red}} = -1.67$ V vs SCE for ethyl iodide),³⁹ Ir(ppy)₃ was found to be a sufficiently strong electron donor to reduce these substrates directly from its photoexcited state ($E_{1/2}^{\text{IV}^*/\text{III}} = -1.73$ V vs SCE). Using a reductant system comprising tributylamine and either Hantzsch ester or formic acid, alkyl as well as alkenyl and aryl iodides undergo reductive dehalogenation in high yields (Scheme 8). As in the Ru(bpy)₃²⁺-mediated dehalogenation, the stoichiometric reductants serve to both turn over the photocatalytic cycle and act as a source of hydrogen atoms for the alkyl, alkenyl, and aryl radicals generated upon reduction and mesolysis of the iodide starting materials. Remarkably, these conditions allowed for the selective dehalogenation of aryl iodides in the presence of aryl bromides and chlorides.⁴⁰

In a conceptually distinct contribution, Willner and coworkers have conducted the reduction of vicinal dibromides in a biphasic system by merging photoredox catalysis with viologen catalysis.⁴¹ 4,4'-Bipyridinium salts (viologens) are well-known electron acceptors and electron carriers. The prototypical species *N,N'*-dimethyl-4,4'-bipyridinium, known as dimethyl viologen (MV²⁺), undergoes facile single-electron reduction at $E_{1/2}^{\text{red}} = -0.4$ V vs SCE to give the methyl viologen radical cation (MV^{•+}) (Scheme 9).⁴² This species may be further reduced at $E_{1/2}^{\text{red}} = -0.8$ V vs SCE to give a neutral dihydrobipyridyl species (MV). The facility with which dimethyl viologen may accept and donate electrons has led to its frequent employment as a mediator of electron-transfer reactions.

Willner utilized viologens to develop a unique catalytic system in which a Ru(bpy)₃²⁺ photocatalyst is localized in an aqueous phase, the organic components are localized in an organic (ethyl acetate) phase, and a viologen serves as an electron relay, effectively carrying electrons between the two phases. The viologen employed is *N,N'*-dioctyl-4,4'-bipyridinium

(C_8V^{2+}), which shows significantly differing solubilities depending on its oxidation state; while the C_8V^{2+} species is soluble only in the aqueous phase, the $\text{C}_8\text{V}^{\bullet+}$ and C_8V species are soluble only in the organic layer (Scheme 10). Thus, single-electron reduction of C_8V^{2+} by $^*\text{Ru}(\text{bpy})_3^{2+}$ in the aqueous layer generates $\text{C}_8\text{V}^{\bullet+}$, which is then extracted into the organic layer. The radical cation $\text{C}_8\text{V}^{\bullet+}$ has the additional property of undergoing disproportionation; two molecules of $\text{C}_8\text{V}^{\bullet+}$ may exchange an electron to return one molecule to the C_8V^{2+} oxidation state and reduce the other to the C_8V oxidation state. In a monophasic system, the equilibrium for this disproportionation lies far on the side of the radical cations. In the biphasic system, however, because C_8V is soluble only in the organic layer and C_8V^{2+} is soluble only in the aqueous layer, the continued extraction of C_8V^{2+} out of the organic layer drives the disproportionation reaction forward, resulting in the buildup of substantial quantities of C_8V in the organic layer.

This highly reducing species is then capable of effecting the reductive dehalogenation of *meso*-1,2-dibromostilbene (**25**) to stilbene (**26**). This reaction presumably proceeds first via reduction of **25** to benzylic radical **27**, followed by a second single-electron reduction and elimination to ultimately deliver **26** (notably, $\text{C}_8\text{V}^{\bullet+}$ is not sufficiently reducing to reduce **25**).⁴³ Reduction of the substrate returns the viologen to its C_8V^{2+} oxidation state, enabling it to be used in substoichiometric quantities. The stoichiometric reductant for this reaction is $(\text{NH}_4)_3\text{EDTA}$, which serves to reduce the $\text{Ru}(\text{bpy})_3^{3+}$ intermediate generated upon reduction of C_8V^{2+} . Interestingly, when this reaction is carried out in a monophasic system, stilbene (**26**) is formed predominantly as the *trans* isomer but undergoes isomerization to the *cis* isomer as the reaction progresses, presumably via energy transfer from the photo-catalyst (see section 6). By contrast, in the biphasic system the organic components and the photocatalyst are isolated from each other, and only *trans*-stilbene is produced.⁴⁴

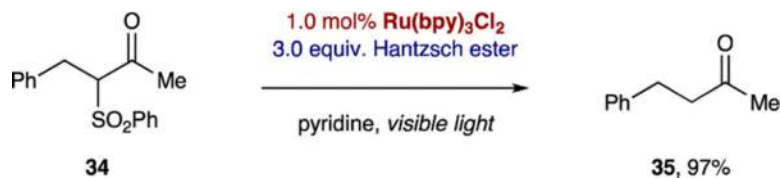
A potential drawback of these net reductive photoredox reactions is the requirement for a stoichiometric quantity of a terminal reductant, which may be prohibitive if the reductant is costly. As we have shown, several common stoichiometric reductants are analogues of the biological reductant 1,4-dihydronicotinamide adenine dinucleotide (NADH), which contains as its key functional group a dihydropyridine moiety. Willner and co-workers demonstrated that NADH itself may be employed as a reductant for the photoredox reductive dehalogenation of *vic*-dibromides, and furthermore showed that it may be recycled *in situ* via enzymatic catalysis.⁴⁵ Their approach makes use of the enzyme alcohol dehydrogenase, which performs the oxidation of ethanol to acetaldehyde, in the process reducing the pyridinium NAD^+ to the dihydropyridine NADH (Scheme 11). When combined with the conditions for the biphasic *vic*-dibromide reduction, NADH turns over the photocatalyst, donating an electron to $\text{Ru}(\text{bpy})_3^{3+}$ to give $\text{Ru}(\text{bpy})_3^{2+}$ and radical cation **28**. Deprotonation of **28** yields dihydropyridyl radical **29**, which may reduce a second equivalent of $\text{Ru}(\text{bpy})_3^{3+}$. This process regenerates NAD^+ , the substrate for alcohol dehydrogenase, closing the catalytic cycle. The generated $\text{Ru}(\text{bpy})_3^{2+}$ then presumably performs the reduction of **25**. In this process, ethanol serves as the stoichiometric reductant, donating the electrons that are ultimately transferred to the *vic*-dibromide substrate. This work additionally demonstrates that photoredox catalysis may be carried out in concert with enzymatic catalysis, overcoming potential pitfalls such as redox degradation of the enzyme.

Conceptually similar reactions have been reported in which photoredox catalysis is employed to generate NADH or NADPH and drive the reactions of several NAD(P)H-dependent dehydrogenases.⁴⁶

3.3. Reductive Cleavage of Sulfonium and Sulfonyl Groups

In one of the earliest works on photoredox-catalyzed transformations of organic molecules, Kellogg and co-workers in 1978 identified $\text{Ru}(\text{bpy})_3^{2+}$ as an effective catalyst for the reduction of phenacyl sulfonium salts by 1,4-dihydropyridines (Scheme 12).⁴⁷ In the context of their studies on 1,4-dihydropyridines as mimics of NADH, it was observed that the reduction of phenacylsulfonium **30** by *N*-methyl Hantzsch ester (**31**) could be accomplished in the presence of visible light. This process was found to be dramatically accelerated using various photosensitizers, with $\text{Ru}(\text{bpy})_3^{2+}$ providing the greatest rate enhancement. Although this reaction is superficially similar to reactions employing 1-benzyl-1,4-dihydronicotinamide (BNAH) as the stoichiometric reductant, **31** is significantly more difficult to oxidize than BNAH ($E_{1/2}^{\text{red}} = +1.0$ V vs SCE for **31** vs $E_{1/2}^{\text{red}} = +0.76$ V vs SCE for BNAH),⁴⁸ and in Stern–Volmer quenching studies Kellogg and coworkers found that neither **31** nor sulfonium **30** quench the photocatalyst. The reaction may thus proceed via direct abstraction of a hydrogen atom from **31** by α -carbonyl radical **14**. This step affords the dihydropyridyl radical **32**, which readily undergoes oxidation ($E_{1/2}^{\text{red}} = -0.60$ V vs SCE)⁴⁸ by $^*\text{Ru}(\text{bpy})_3^{2+}$ to generate $\text{Ru}(\text{bpy})_3^+$ and the pyridinium byproduct **33**. Reduction of the sulfonium by $\text{Ru}(\text{bpy})_3^+$ generates the α -carbonyl radical and completes the photocatalytic cycle. As the proposed quencher for the photocatalyst, **32**, is a catalytically generated intermediate that is not present at the start of the reaction, it must be initially generated via an alternative pathway; a likely route is direct photoexcitation of **31**, which itself absorbs in the visible region, followed by SET to sulfonium **30**. The quenching of the photocatalyst by a catalytically generated intermediate is a feature of many photoredox reactions.

Hantzsch ester has also been employed as a stoichiometric reductant to achieve the desulfonylation of β -ketosulfones (eq 1).⁴⁹ As in the reduction of phenacylsulfonium salts, the reaction likely proceeds via formation of $\text{Ru}(\text{bpy})_3^+$, which may reduce the β -ketosulfone **34** to an α -carbonyl radical analogous to **14**. Abstraction of a hydrogen atom from Hantzsch ester then yields the reduced ketone product **35**.



(1)

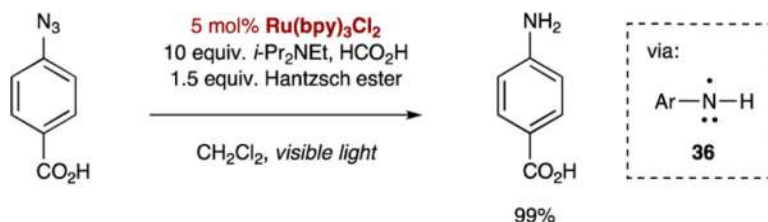
3.4. Nitrogen Functional Group Reductions

Photoredox catalysis has been employed in the reduction of numerous nitrogen-containing functional groups. Hirao and co-workers have reported the reduction of nitrobenzenes to

anilines using either $\text{Ru}(\text{bpy})_3^{2+}$ or the related photocatalyst $\text{Ru}(\text{bpy})_2(\text{MeCN})_2(\text{PF}_6)_2$ (eq 2).⁵⁰ In these reactions, hydrazine is employed as the stoichiometric reductant, the source of the electrons that are ultimately transferred to the nitroarene. The reduction of nitrobenzenes to anilines has also been achieved using a resin loaded with the organic photocatalyst eosin Y.⁵¹ Additionally, the reduction of azides to amines has been accomplished by Liu using a catalytic system comprising $\text{Ru}(\text{bpy})_3^{2+}$, Hünig's base, and Hantzsch ester (eq 3).⁵² The reaction is proposed to proceed first via reductive quenching of $^*\text{Ru}(\text{bpy})_3^{2+}$ by the tertiary amine to give $\text{Ru}(\text{bpy})_3^+$. Single-electron reduction of the azide by $\text{Ru}(\text{bpy})_3^+$ gives an azide radical anion, which upon expulsion of dinitrogen and protonation affords the aminyl radical **36**. This intermediate may then abstract a hydrogen atom (from either Hantzsch ester or the radical cation of Hünig's base) to furnish the primary amine product. Aryl as well as aliphatic azides may be reduced following this protocol. The reaction was also shown to be compatible with biomolecules, as demonstrated by the reduction of an azide tethered to a DNA oligonucleotide. Willner has also made use of a biphasic redox system similar to that discussed in section 3.2 to achieve the reduction of an azobenzene derivative.⁵³



(2)



(3)

Finally, the reduction of hydrazides and hydrazines has been achieved by Zheng under visible light photoredox catalysis.⁵⁴ Using the photoredox catalyst $\text{Ru}(\text{bpz})_3^{2+}$, a tris(bipyrazyl) analogue of $\text{Ru}(\text{bpy})_3^{2+}$, *N*-phenyl-*N*-benzoylhydrazine (**37**) undergoes efficient reduction to *N*-phenylbenzamide (**38**), and *N*-methyl-*N*-phenylhydrazine (**39**) is reduced to *N*-methylaniline (**40**) (Scheme 13). The photoexcited species $^*\text{Ru}(\text{bpz})_3^{2+}$ is highly oxidizing ($E_{1/2}^{*\text{III/I}} = +1.45 \text{ V vs SCE}$)⁵⁵ by virtue of the strongly electron-withdrawing bipyrazine ligands, and it may accept an electron from the hydrazide or hydrazine **41** to give radical cation **42**. Deprotonation of this species furnishes aminyl radical **43**, which is proposed to add to dioxygen to give adduct **44**. A rearrangement of this intermediate may proceed to provide **45**, fragmentation of which would generate nitrous acid and aminyl radical **46**. Reduction of this species by $\text{Ru}(\text{bpz})_3^+$ followed by protonation would provide the reduced product **47**. In accord with the proposed mechanism, the

unsubstituted NH_2 group is required, and trisubstituted or tetrasubstituted hydrazines do not give the products of N–N bond cleavage.⁵⁶

3.5. Radical Cyclizations

In the reaction types presented thus far, photoredox catalysis has been shown to enable simple functional group manipulations. However, if the radicals generated via photoredox catalysis engage other functional groups in chemical reactions, the potential exists for building molecular complexity. As an example of this potential, photoredox catalysis has been employed by Stephenson to conduct reductive radical cyclization reactions. As in the reductive dehalogenation chemistry, reductive quenching of $^*\text{Ru}(\text{bpy})_3^{2+}$ by a tertiary amine generates the reductant $\text{Ru}(\text{bpy})_3^+$, which may reduce alkyl halides such as **48** to the alkyl radical **49** (Scheme 14).⁵⁷ If this radical is tethered to an alkene or alkyne, the alkyl radical may add to the pendent π -system to give adduct **50**. Hydrogen atom abstraction, likely from the amine radical cation, then furnishes the cyclized product **51**. Employing either $\text{Ru}(\text{bpy})_3^{2+}$ or the more reducing photocatalyst $\text{Ir}(\text{ppy})_2(\text{dtbbpy})^+$ (ppy = 2-phenylpyridine, dtbbpy = 4,4-di-*tert*-butyl-2,2'-bipyridine), a variety of α -bromocarbonyls could be engaged in radical cyclizations to form five- and six-membered rings.⁵⁸

As described earlier, less activated radical precursors such as alkyl iodides may be engaged in photoredox reactions by employing strongly reducing photocatalysts.³⁷ The iridium photocatalyst $\text{Ir}(\text{ppy})_3$ has thus been demonstrated to promote a variety of alkyl, alkenyl, or aryl iodide starting materials to undergo photoredox radical cyclizations to generate a range of carbocyclic and heterocyclic structures (Scheme 15).⁵⁹

Stephenson and co-workers have shown that these radical cyclization reactions are amenable to the development of cascade reactions, in which an initial radical cyclization step is coupled with a second bond-forming process. For instance, when cyclopentene **52** is exposed to the photoredox cyclization conditions, the tricyclic product **53** is obtained via a cascade of two radical cyclizations proceeding via the intermediate alkyl radical **54** (Scheme 16).⁵⁷ Alternatively, radical cyclization may be carried out in concert with a divinylcyclopropane rearrangement; use of bromocyclopropane **55** as a substrate for radical cyclization results in the formation of tricyclic product **56** in good yield.⁶⁰ Presumably, an initial radical cyclization proceeds to give vinylcyclopropane **57**, which may then undergo the Cope rearrangement followed by rearomatization to provide the observed product.

3.6. Reductive Epoxide and Aziridine Opening

The ability to reduce carbonyls using photoredox catalysis has been exploited to achieve the reductive opening of epoxides and aziridines. Although an epoxide functional group is not readily reduced, installation of the epoxide adjacent to the redox-active carbonyl group, as in α -ketoepoxide **58**, enables reductive opening of the epoxide using $\text{Ru}(\text{bpy})_3^{2+}$ as the photocatalyst and Hantzsch ester as the stoichiometric reductant.^{61,62} In the catalytic cycle, reductive quenching of $^*\text{Ru}(\text{bpy})_3^{2+}$ generates $\text{Ru}(\text{bpy})_3^+$ (Scheme 17). $\text{Ru}(\text{bpy})_3^+$ is sufficiently reducing to donate an electron to α -ketoepoxide **58** to give ketyl radical **59**. Subsequent C–O bond cleavage provides radical anion **60**, which after protonation and abstraction of a hydrogen atom gives the β -hydroxyketone product **61**. Hantzsch ester (HE)

may potentially act as a hydrogen atom donor and reductive quencher as described in Scheme 17, ultimately undergoing conversion to Hantzsch pyridine (HP). This reductive protocol was additionally found to ring-open α -ketoaziridines such as **62** to provide β -aminoketones such as **63**. In the case of both epoxide and aziridine ring-opening, an aryl substituent is required on the ketone, presumably to facilitate single-electron reduction to the ketyl radical.

Rather than simply undergo reduction, the radical intermediate **64** may also be engaged in C–C bond formation (Scheme 18). For instance, this intermediate may be intercepted by allylsulfone **65** to give β -hydroxy- α -allylketone **66**, the product of tandem ring-opening/allylation. The iridium photocatalyst Ir(ppy)₂(dtbbpy)PF₆ was found to be optimal for this transformation. The excellent levels of diastereoselectivity observed in this reaction may be rationalized according to Guindon's model for selectivity in the radical allylation of β -alkoxyesters, in which the key organizing element is stabilization of the α -carbonyl radical singly occupied molecular orbital (SOMO) by hyperconjugation.⁶³ As the phenyl C–C bond is most σ -donating bond at the β -position, this effect aligns the phenyl C–C bond with the α -carbonyl radical SOMO. Additionally, orientation of the β -heteroatom away from the carbonyl minimizes dipole–dipole repulsions. In this conformation (**67**), the phenyl group effectively shields one face of the α -carbonyl radical; approach of the allylsulfone opposite the phenyl group then provides the observed major diastereomer. As in the ring-opening reaction, α -ketoaziridines are also suitable substrates for this allylation protocol.

3.7. Reduction-Labile Protecting Groups

Photoredox catalysis has been employed to develop reduction-labile protecting groups, functional groups that are inert to most reaction conditions but that undergo cleavage upon single-electron reduction. In an early contribution, Okada and co-workers demonstrated in 1991 that *N*-(acyloxy)phthalimides may be used as a masking group for alkyl radicals.⁶⁴ Employing the familiar reductive quenching pathway, 1-benzyl-1,4-dihydronicotinamide (BNAH, **1**) quenches *Ru(bpy)₃²⁺ to give Ru(bpy)₃⁺ and the BNAH radical cation (**4**) (Scheme 19). Single-electron reduction of *N*-(acyloxy)phthalimide **68** by Ru(bpy)₃⁺ proceeds to give radical anion **69**, which upon protonation fragments to give phthalimide, carbon dioxide, and alkyl radical **70**. Alkyl radicals generated in this fashion were shown to undergo a range of subsequent reactions, including reduction, phenylselenenylation, and conjugate addition. Thus, alkyl radical **70** may abstract a hydrogen atom from *tert*-butylthiol to give reduction product **71**, while reaction of **70** with diphenyl diselenide generates phenylselenide **72**. Addition of alkyl radical **70** to a Michael acceptor gives an α -carbonyl radical, which may abstract a hydrogen atom (likely from the BNAH radical cation **4**) to give alkylated product **73** (see section 5.9 for additional radical conjugate addition reactions).

Reductive photocatalysis also enables the use of the *N*-methylpicolinium group as a protecting group for amines. In this chemistry, ascorbic acid (**74**) has been employed as a reductive quencher of *Ru(bpy)₃²⁺, donating an electron to provide Ru(bpy)₃⁺ and the ascorbate radical **75** (Scheme 20).⁶⁵ Single-electron reduction of *N*-methylpicolinium carbamate **76** by Ru(bpy)₃⁺ then gives dihydropyridyl radical **77**. Fragmentation of this

radical proceeds to reveal the primary amine **78**, carbon dioxide, and *N*-methylpicolinyl radical **79**. Benzylic radical **79** is then proposed to abstract a hydrogen atom from ascorbate radical **75** to generate pyridinium **80** and the oxidized species dehydroascorbic acid (**81**). Falvey and co-workers have similarly employed the *N*-methylpicolinium group as a protecting group for carboxylic acids, achieving deprotection with both Ru(bpy)₃²⁺ and organic dyes.^{66,67}

Finally, the *N*-alkoxyphthalimide group has been employed by Sammis as a photoredox-labile protecting group for aldehydes.⁶⁸ Hünig's base is employed as a reductive quencher for *Ru(bpy)₃²⁺, generating the Ru(bpy)₃⁺ species that transfers an electron to *N*-alkoxyphthalimide **82** (Scheme 21). The resulting radical anion **83** may undergo a fragmentation to cleave the labile N–O bond and give the benzaldehyde product and the phthalimide radical anion **84**. Single-electron oxidation of **84**, either by the photocatalyst or by the amine radical cation, then gives the phthalimide byproduct. Significant yields of the aldehyde product were also observed when the reaction was irradiated in the absence of photocatalyst, suggesting that the *N*-alkoxyphthalimide group itself may be undergoing photo-excitation and performing a single-electron oxidation of the tertiary amine. Additionally, as the phthalimide group first accepts an electron and then, after fragmentation, releases an electron, this reaction is redox neutral (see section 5).

4. NET OXIDATIVE REACTIONS

Just as photoredox catalysis may be used to perform net reductive reactions when a stoichiometric electron donor is present, it may also be used to perform net oxidative reactions provided some species is present to function as a stoichiometric electron acceptor. Reactions in this category typically hinge on the single-electron oxidation of particularly electron-rich functional groups, such as electron-rich arenes and amines.

4.1. Functional Group Oxidations

Single-electron oxidation pathways have enabled the oxidation of several common functional groups via photoredox catalysis. A report by Cano-Yelo and Deronzier in 1984 revealed that the ruthenium(II) photocatalyst **85** could effect the oxidation of benzylic alcohols to the corresponding aldehydes using aryldiazonium salts as sacrificial oxidants (Scheme 22).⁶⁹ Aryldiazonium salts readily undergo single-electron reduction ($E_{1/2}^{\text{red}} = -0.1$ V vs SCE for phenyldiazonium tetrafluoroborate),⁷⁰ and upon accepting an electron fragment to release dinitrogen and afford an aryl radical. Thus, the Ru(bpy)₃²⁺ analogue **85** undergoes photoexcitation and subsequent oxidation by aryldiazonium **86** to give a Ru(III) intermediate and the aryl radical **87**. The Ru(III) species is then capable of oxidizing the aromatic ring of the benzylic alcohol substrate **88**, removing an electron to provide the arene radical cation **89**. The aryl radical **87** is proposed to abstract one of the benzylic hydrogen atoms of **89**, converting **87** to benzophenone (**90**) and the arene radical cation to the oxocarbenium ion **91**. Loss of a proton then furnishes the aldehyde product. Fluorenone is also observed as a byproduct in the reaction and presumably arises from a Pschorr reaction of aryl radical **87** (see section 5.3.1).

The alcohol oxidation reaction highlights the utility of modulating the redox properties of the photocatalyst via the installment of substituents on the ligand framework. The installation of electron-withdrawing ester groups on the bipyridine ligands renders **85** significantly more oxidizing than $\text{Ru}(\text{bpy})_3^{2+}$ ($E_{1/2}^{\text{III/II}} = +1.59 \text{ V vs SCE}$ for **85** as compared to $E_{1/2}^{\text{III/II}} = +1.29 \text{ V vs SCE}$ for $\text{Ru}(\text{bpy})_3^{2+}$). Photocatalyst **85** is thus capable of oxidizing substrates possessing electron-rich arenes such as 4-methoxybenzyl alcohol ($E_{1/2}^{\text{red}} = +1.52 \text{ V vs SCE}$). However, less readily oxidized substrates, such as 4-methylbenzyl alcohol ($E_{1/2}^{\text{red}} = +1.89 \text{ V vs SCE}$) and benzyl alcohol ($E_{1/2}^{\text{red}} = +2.19 \text{ V vs SCE}$), provide the corresponding aldehydes in lower yields.

Jiao and co-workers have recently introduced a method for the photoredox oxidation of α -haloesters to α -ketoesters.⁷¹ In their mechanistically unique strategy, a pyridine derivative serves to activate the α -haloester substrate and molecular oxygen serves as the terminal oxidant and source of the oxygen atom incorporated into the product. Thus, ethyl α -bromophenylacetate (**92**), which does not react in the absence of a pyridine catalyst, is converted in good yield into ethyl benzoylformate (**93**) in the presence of catalytic amounts of 4-methoxypyridine (**94**) and $\text{Ru}(\text{bpy})_3^{2+}$ by running the reaction under air (Scheme 23). The pyridine catalyst is proposed to promote the reaction by displacing the bromide of **92** to give pyridinium **95**. This species may be reduced by a catalytically generated $\text{Ru}(\text{bpy})_3^+$ complex to give dihydropyridyl radical **96**. Homolysis of this intermediate regenerates the pyridine catalyst and provides benzylic radical **97**. Reaction of radical **97** with dioxygen is proposed to provide α -ketoester **93** via the intermediacy of alkoxyl radical **98**. This process generates reduced states of dioxygen, which potentially may quench $^*\text{Ru}(\text{bpy})_3^{2+}$ to achieve turnover of the photocatalytic cycle.⁷² Evidence for the proposed $\text{Ru}(\text{II})/\text{Ru}(\text{I})$ cycle is provided by the observation that neither α -haloester **92** nor the isolated pyridinium salt **95** quench the emission of $^*\text{Ru}(\text{bpy})_3^{2+}$. These aerobic oxidation conditions could be used to convert a variety of α -bromo- as well as α -chloroesters to the corresponding α -ketoesters. Moderate yields were obtained for the conversion of benzhydryl halides to the corresponding benzophenone derivatives.

Molecular oxygen has also been used as a stoichiometric oxidant in the photoredox-mediated oxidative hydroxylation of arylboronic acids.⁷³ A report from the laboratories of Jørgensen and Xiao detailed the conversion of arylboronic acids into phenols using $\text{Ru}(\text{bpy})_3^{2+}$ as the photocatalyst, Hünig's base as a sacrificial reductant, visible light, and air. The key reactive species in this reaction is superoxide ($\text{O}_2^{\bullet-}$), which may be generated via single-electron reduction of molecular oxygen by $\text{Ru}(\text{bpy})_3^+$, itself generated via reductive quenching of $^*\text{Ru}(\text{bpy})_3^{2+}$ by the tertiary amine (Scheme 24). Superoxide is believed to add to the vacant p orbital of the Lewis acidic boronic acid (**99**) to afford radical anion **100**. Abstraction of a hydrogen atom, potentially from the amine radical cation, then gives boroperoxide species **101**, which undergoes a 1,2-aryl shift to give **102**. Subsequent hydrolysis affords the observed phenol product **103**. In support of this mechanism, ¹⁸O labeling studies revealed that the oxygen in the phenol arises from molecular oxygen and not from added water. An oxidative quenching cycle, in which oxygen quenches $^*\text{Ru}(\text{bpy})_3^{2+}$ to generate superoxide and $\text{Ru}(\text{bpy})_3^{3+}$, may also be operative. Employing this protocol,

electron-rich as well as electron-poor arylboronic acids give the corresponding phenols in excellent yields.

Li and co-workers have shown that thiobenzanilides can also be converted to benzothiazoles under oxidative photoredox conditions.⁷⁴ Oxygen is proposed to act as an oxidative quencher of $^*\text{Ru}(\text{bpy})_3^{2+}$, accepting an electron from the photocatalyst to give superoxide and the strongly oxidizing $\text{Ru}(\text{bpy})_3^{3+}$ (Scheme 25). While no reaction of thiobenzanilide **104** occurs in the absence of base, added 1,8-diazabicycloundec-7-ene (DBU) deprotonates **104** to give the more readily oxidized imidothiolate anion **105**. Single-electron oxidation of **105** by $\text{Ru}(\text{bpy})_3^{3+}$ provides sulfur-centered radical **106**, which may add to the benzene ring to give dienyl radical **107**. Superoxide may then abstract a hydrogen atom from dienyl radical **107**, generating the benzothiazole product **108** and hydrogen peroxide. In the net redox reaction, the substrate **104** thus undergoes a two-electron oxidation to give **108** and molecular oxygen undergoes a two-electron reduction to give peroxide. Extensive substitution on both arenes of the substrate is well tolerated. Interestingly, substrates that have the potential for radical addition at two regiochemically distinct positions display high selectivity for addition ortho to a functional group (as in the reaction to give benzothiazole **109**). This selectivity is a hallmark of radical additions to arenes and is complementary to other transition metal-based methods for the construction of benzothiazoles.⁷⁵ This work may be of utility to many practitioners of medicinal chemistry.

4.2. Oxidative Removal of the PMB Group

Just as photoredox catalysis has been applied to the cleavage of reduction-labile protecting groups, it has also been used to oxidatively cleave the common *para*-methoxybenzyl (PMB) protecting group. Stephenson and co-workers demonstrated that the iridium photocatalyst $\text{Ir}[\text{dF}(\text{CF}_3)\text{ppy}]_2(\text{dtbbpy})\text{PF}_6$ ($\text{dF}(\text{CF}_3)\text{ppy}$ = 2-(2,4-difluorophenyl)-5-trifluoromethylpyridine) is an effective catalyst for the deprotection of PMB ethers using bromotrichloromethane as the stoichiometric oxidant.⁷⁶ Photoexcitation of the heteroleptic iridium complex provides a species that is sufficiently reducing ($E_{1/2}^{\text{IV}/\text{III}} = -0.89$ V vs SCE)⁷⁷ to transfer an electron to bromotrichloro-methane ($E_{1/2}^{\text{red}} = -0.18$ V vs SCE)⁷⁸ (Scheme 26). Reduction of bromotrichloromethane induces mesolysis to give bromide and trichloromethyl radical, while oxidation of the photoexcited Ir(III) species gives an Ir(IV) intermediate. This Ir(IV) species is very strongly oxidizing ($E_{1/2}^{\text{IV}/\text{III}} = +1.69$ V vs SCE)⁷⁷ and, as in the oxidation of benzylic alcohols (section 4.1), may oxidize the electron-rich aromatic ring of the PMB ether **110** to give radical cation **111**. The trichloromethyl radical may then abstract a hydrogen atom from the benzylic position of **111**, producing chloroform and oxocarbenium ion **112**. Hydrolysis of **112** releases deprotected alcohol **113** as well as the byproduct 4-methoxybenzaldehyde. These conditions were shown to successfully deprotect PMB ethers in the presence of a range of other common alcohol and amine protecting groups. Particularly noteworthy is the selective cleavage of the PMB ether in the presence of a less readily oxidized benzyl ether, providing access to alcohol **114**. A similar deprotection of benzylic amines has also been achieved using visible light flavin photocatalysis.⁷⁹

4.3. Oxidative Biaryl Coupling

As has been illustrated thus far, photoredox protocols often do not generate new stereocenters, and those that do typically proceed in a racemic fashion; a significant challenge in this area is the development of strategies whereby reactive radical intermediates may be engaged in enantioselective transformations. As a way of addressing this challenge, Ohkubo and co-workers sought to determine if chiral photocatalysts could induce enantioselectivity in photoredox reactions. Octahedral metal complexes such as $\text{Ru}(\text{bpy})_3^{2+}$ are chiral, possessing a Δ and a Λ enantiomer, defined by whether the ligands form a right-handed (Δ) or left-handed helix (Λ) around the C_3 symmetry axis (Figure 3).⁸⁰

Ohkubo synthesized the chiral photocatalyst $\Delta\text{-Ru}(\text{menbpy})_3^{2+}$ (menbpy = 4,4'-dimenthoxycarbonyl-2,2'-bipyridine) and investigated its ability to catalyze the oxidative dimerization of naphthol (Scheme 27).⁸¹ Although $\text{Ru}(\text{menbpy})_3^{2+}$ was prepared as a mixture of the Δ and Λ forms, the chiral menthol groups on the bipyridine ligands render the Δ and Λ complexes diastereomeric, enabling their separation by column chromatography. The complex $\Delta\text{-Ru}(\text{menbpy})_3^{2+}$ was then investigated for its ability to dimerize 2-naphthol. Using $\text{Co}(\text{acac})_3$ as the stoichiometric oxidant, this reaction proceeds under visible light irradiation to provide the binaphthol product **115**. The reaction is suggested to proceed via oxidative quenching of $^*\Delta\text{-Ru}(\text{menbpy})_3^{2+}$ ($E_{1/2}^{\text{III/II}^*} = -0.45$ V vs SCE) by $\text{Co}(\text{acac})_3$ ($E_{1/2}^{\text{red}} = -0.34$ V vs SCE) to give $\Delta\text{-Ru}(\text{menbpy})_3^{3+}$. In the process, the cobalt species is reduced and loses a ligand to afford $\text{Co}(\text{acac})_2$. $\text{Ru}(\text{menbpy})_3^{3+}$ ($E_{1/2}^{\text{III/II}} = +1.55$ V vs SCE) may then oxidize the naphthol substrate **116** ($E_{1/2}^{\text{red}} = +1.34$ V vs SCE for 2-naphthol) by a single electron, giving α -carbonyl radical **117** after loss of a proton. This species may react with another equivalent of **116** to forge the C–C bond and give ketyl radical **118**. A second single-electron oxidation followed by rearomatization then furnishes the biaryl product **115**.

Interestingly, the product **115** was formed in a nonracemic fashion, with 2-naphthol undergoing dimerization to form 1,1'-bi-2-naphthol (BINOL) in 16% ee and 3-methoxy-2-naphthol giving product in 4% ee, with the reaction in each case favoring the (*R*) enantiomer. While the exact origin of these selectivities is not clear, the observed enantiomeric excesses derive in part from the faster decomposition of the (*S*) enantiomer of the product by the photocatalyst, a phenomenon confirmed in separate experiments. Ohkubo suggests that van der Waals interactions between the chiral photocatalyst and its substrate play a critical role in the efficiency of electron transfer.

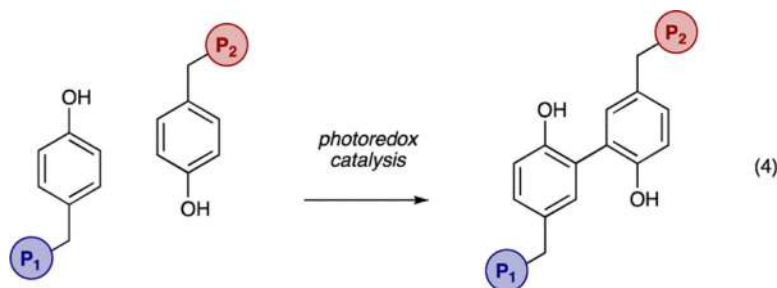
The low enantioselectivities obtained in this reaction reflect a general feature of photoredox catalysis—the catalyst typically serves only to generate a reactive radical species and does not serve as a catalyst for the bond-forming event. As it is not present in the transition state leading to bond formation, the photocatalyst may have no effect on the stereochemical outcome. Although the naphthol dimerization reaction constitutes a rare example of asymmetric induction from a chiral photocatalyst, the low enantioselectivities obtained also highlight the challenges inherent in this approach.

The dimerization of electron-rich arenes via photoredox catalysis has been employed in the biochemical arena by Kodadek to study protein–protein interactions.⁸² In these systems, a photocatalyst is employed to oxidize the phenol of a tyrosine residue to its radical cation. If

a second tyrosine (or other nucleophilic residue) is nearby, carbon–carbon bond formation will proceed analogously to the described naphthol dimerization (eq 4). As this reaction proceeds only between amino acids held in proximity to each other, it may be used to cross-link two proteins specifically at the protein–protein interface.

4.4. Oxidative Generation of Iminium Ions

A major area in which oxidative photoredox catalysis has been employed is the oxidation of amines. In particular, many



(4)

reactions have been developed that rely on the two-electron oxidation of an amine to its corresponding iminium ion. In a general sense, amines are very good electron donors, readily undergoing single-electron oxidation to yield an aminium radical cation **119** (Scheme 28). As described in section 3.2, oxidation of an amine has the effect of dramatically lowering the bond dissociation energy of the C–H bonds at the amine α -positions.³⁶ If a good hydrogen atom acceptor is present in the reaction, it may abstract a hydrogen atom from one of these positions, converting the aminium radical cation **119** to the iminium ion **120**. At the same time, however, single-electron oxidation to the radical cation also significantly lowers the pK_a of the protons at the α -positions: aminium radical cations have been estimated to have pK_a values between 3 and 13.⁸³ The aminium radical cation may thus be deprotonated at the α -position to yield an α -amino radical **121**, in which a radical at the α -position is stabilized by orbital overlap with the filled p orbital on nitrogen. This species is highly reducing, having a reduction potential of roughly -1.0 V vs SCE,³⁵ and may undergo a second single-electron oxidation, providing the iminium ion by a different route (for reactions of α -amino radicals, see sections 5.9 and 5.10).

As potent electrophiles, catalytically generated iminium ions may be trapped by nucleophiles to directly install new bonds at the α -position of amines. In the first report on the application of transition metal photoredox catalysis to this reaction type, Stephenson and co-workers achieved an aza-Henry reaction via the addition of nitromethane to a catalytically generated iminium ion.⁸⁴ The photocatalyst employed is the iridium complex $\text{Ir}(\text{ppy})_2(\text{dtbbpy})\text{PF}_6$, which upon photoexcitation is capable of oxidizing *N*-phenyltetrahydroisoquinoline (**122**) to its radical cation **123** (Scheme 29). The intermediate $\text{Ir}(\text{II})$ species is proposed to reduce dioxygen to complete the photoredox cycle. Superoxide may then abstract a hydrogen atom at the α -position of the amine to generate the key

iminium intermediate **124**. Addition of the nitromethane anion **125** yields the aza-Henry adduct **126**.⁸⁵

This reaction manifold has been used to accomplish a wide variety of α -functionalization reactions (Scheme 30). For example, α -cyanation reactions have been performed in which potassium cyanide serves as the cyanide source to provide the Strecker product **127**.⁸⁶ When enol silanes are employed as nucleophiles, Mannich products such as **128** are obtained.⁸⁷

Alternatively, similar products may be accessed directly from the corresponding ketones when proline is used as a cocatalyst; in this way, acetone may be employed to generate the Mannich adduct **129**. The reaction likely proceeds via the formation of a nucleophilic enamine intermediate that undergoes addition to the iminium ion.⁸⁸ Although the potential exists here for asymmetric induction from the chiral proline catalyst, only low enantiomeric excesses were observed. Catalytically generated iminium ions have also been intercepted by dialkyl phosphates such as **130** to give amino phosphonates such as **131**⁸⁹ and by allylsilanes to give α -allylamines such as **132**.⁹⁰ Indole may serve as a Friedel–Crafts nucleophile to give the α -arylated amine product **133**.^{90,91}

The iminium ion may also be intercepted by another catalytically generated intermediate; for instance, terminal alkynes react with a copper catalyst to provide a copper acetylide intermediate, which may add to the iminium to provide α -alkynylated amines such as **134**.⁹² Finally, α -trifluoromethylamines such as **135** may be accessed using the Ruppert–Prakash reagent (TMSCF₃) as the nucleophilic “CF₃–” source.⁹³ This amine α -trifluoromethylation reaction employs the organic photocatalyst rose bengal, which undergoes photoexcitation at $\lambda_{\text{max}} = 549$ nm to give a photoexcited state capable of oxidizing the amine to its iminium ion. Organic photocatalysts have also been successfully employed in the aza-Henry, α -cyanation, and α -alkynylation reactions,^{93,94} and cadmium sulfide has been shown to promote the aza-Henry reaction.⁹⁵

Xiao and co-workers have reported an intramolecular variant of these iminium trapping reactions, in which a pendent nitrogen nucleophile adds to the iminium to generate tetrahydroimidazoles.⁹⁶ Using Ru(bpy)₃²⁺ as the photocatalyst and oxygen as the stoichiometric oxidant, diamine **136** is converted to iminium ion **137**, which upon cyclization yields the product tetrahydroimidazole **138** (Scheme 31). The *cis* diastereomer may be obtained with high selectivity if the reaction is performed for an extended period of time, presumably due to postreaction epimerization at the aminal carbon. These authors have subsequently shown that this strategy may be extended to the synthesis of *N,O*-acetals via the attack of pendent alcohol nucleophiles on photoredox-generated iminium ions.⁹⁷

The ability of an amine to readily undergo single-electron oxidation thus enables the development of a wide range of α -functionalization reactions. Using this general reaction mechanism, one might conceive of developing similar α -functionalization reactions with amides. However, a critical problem in this regard is the significantly higher reduction potential of an amide relative to that of an amine ($E_{1/2}^{\text{red}} = +2.3$ V vs SCE for *N,N*-dimethylformamide⁹⁸ as compared to $E_{1/2}^{\text{red}} = +0.7$ V vs SCE for *N,N*-dimethylaniline);⁹⁹ amides therefore cannot be oxidized by any commonly employed visible light photocatalyst.

Stephenson has reported a solution to this problem by performing the direct abstraction of a hydrogen atom from the α -position of amides.¹⁰⁰ Using persulfate (**139**) as an oxidative quencher for $^*\text{Ru}(\text{bpy})_3^{2+}$ generates 1 equiv of sulfate and 1 equiv of the sulfate radical anion (**140**) (Scheme 32). This sulfate radical anion is proposed to directly abstract a hydrogen atom from the α -position of *N,N*-dimethylformamide (DMF, **141**), giving rise to α -amido radical **142**. This species may then be oxidized by $\text{Ru}(\text{bpy})_3^{3+}$ to the *N*-acyliminium species **143**. Addition of a nucleophile furnishes the α -functionalized product **144**. This direct hydrogen abstraction mechanism thus circumvents the problem of amide oxidation by generating an intermediate, **142**, which is much easier to oxidize than the parent amide. In their report, Stephenson and co-workers intercept *N*-acyliminium ions derived from several amides with a range of Friedel–Crafts nucleophiles, such as anisole derivatives and indoles, to achieve an α -arylation of amides.

As we have seen thus far, photoredox catalysis has only rarely been applied to the development of catalytic enantioselective reactions, with efforts such as Ohkubo's use of a chiral photocatalyst proving largely unsuccessful (section 4.3). A powerful strategy that has recently emerged for performing asymmetric catalysis, however, is the merger of photoredox catalysis with a second catalytic activation mode. Taking this approach, DiRocco and Rovis merged photoredox catalysis with *N*-heterocyclic carbene (NHC) catalysis to perform an asymmetric α -acylation of amines.¹⁰¹ In these reactions, a chiral NHC catalyst serves to generate a chiral acyl anion equivalent for addition into iminium ions generated via photoredox catalysis; in this way, a tertiary amine such as *N*-phenyltetrahydroisoquinoline (**122**) may be reacted with a simple aldehyde such as *n*-butanal (**145**) to provide the α -acylated amine **146** (Scheme 33). In the photoredox cycle, oxidative quenching of $^*\text{Ru}(\text{bpy})_3^{2+}$ by *meta*-dinitrobenzene (*m*-DNB, **147**, $E_{1/2}^{\text{red}} = -0.90$ V vs SCE)²¹ generates $\text{Ru}(\text{bpy})_3^{3+}$ and the arene radical anion **148**. $\text{Ru}(\text{bpy})_3^{3+}$ oxidizes the amine to its radical cation, which after loss of a proton and an electron yields the key iminium ion **124**. Simultaneously, the amino-indanol-derived *N*-heterocyclic carbene catalyst **149** reacts with *n*-butanal to form the nucleophilic Breslow intermediate **150**. Attack of **150** on the iminium **124** forges the C–C bond, with the chiral information on the NHC backbone controlling approach of the iminium and thus the configuration at the newly formed stereocenter. The adduct **151** then suffers elimination of the product α -acylamine **146**, regenerating the carbene catalyst. A range of aliphatic aldehydes could be reacted under these conditions to give α -acylamine products with high enantioselectivity. Remarkably, the two activation modes of photoredox catalysis and NHC catalysis act in concert without deleterious interactions between the respective catalysts, such as oxidative degradation of the Breslow intermediate by the photocatalyst.

4.5. Azomethine Ylide [3 + 2] Cycloadditions

Iminium ions generated via photoredox catalysis have additionally been harnessed to perform azomethine ylide [3 + 2] cycloadditions.¹⁰² Xiao and co-workers coupled this reaction with an oxidative aromatization sequence to convert tetrahydroisoquinolines to polycyclic adducts such as **152** (Scheme 34). In this transformation, tetrahydroisoquinoline **153** undergoes single-electron oxidation by $^*\text{Ru}(\text{bpy})_3^{2+}$ to give radical cation **154**. Hydrogen atom abstraction, presumably by superoxide generated during catalyst turnover,

then furnishes iminium **155**. Deprotonation adjacent to nitrogen forms the azomethine ylide **156**, which may engage a host of electron-deficient alkenes in [3 + 2] cycloaddition reactions. Thus, cycloaddition with *N*-phenylmaleimide (**157**) furnishes the pyrrolidine-containing adduct **158**. In initial studies on this reaction, this product was formed as a mixture with dihydropyrroloisoquinoline **152**, the product of oxidative aromatization. In their optimized conditions, Xiao and coworkers add *N*-bromosuccinimide to convert the product mixture exclusively to the oxidized [3 + 2] adduct **152**. Other dipolarophiles amenable to this reaction include β -nitrostyrenes, acrylates, and alkynes.

4.6. Cyclizations of Aminium Radical Cations

As the previous sections have demonstrated, the most common approach to the oxidative functionalization of amines involves a net two-electron oxidation of the amine to the corresponding iminium ion. Alternatively, however, aminium radical cations themselves may be engaged in bond-forming reactions. Zheng has utilized such an approach in a synthesis of indoles from styrenyl anilines.¹⁰³ The strongly oxidizing photocatalyst Ru(bpz)²⁺₃ is capable of oxidizing *N*-*p*-methoxyphenylanilines such as **159** to their radical cations (**160**, Scheme 35). Cyclization of the aminium radical cation onto the pendent olefin, followed by deprotonation of the resulting ammonium ion, yields benzylic radical **161**.¹⁰⁴ A second single-electron oxidation provides the benzylic carbocation **162**, which upon loss of a proton is converted to the product indole **163**. The *p*-methoxyphenyl group is required for reactivity, presumably to render the amine sufficiently electron-rich to undergo oxidation, and oxygen from air serves as the terminal oxidant for this net oxidative process.

5. REDOX NEUTRAL REACTIONS

In the reactions described thus far, the overall reductive or oxidative nature of the transformation necessitates the use of a stoichiometric quantity of a molecule that can serve as a source or reservoir of electrons, respectively. In contrast to these reaction types, much recent work in photoredox catalysis has focused on redox neutral reactions. In these reactions, the substrate or substrates undergo both a single-electron oxidation and a single-electron reduction at disparate points in the reaction mechanism. As a result, there is no net oxidation state change between starting materials and products, and no stoichiometric external components are required to turn over the photocatalytic cycle.

5.1. Atom Transfer Radical Addition

The redox neutral approach is perhaps best exemplified by atom transfer radical addition (ATRA) reactions. In this generic reaction type, an atom transfer reagent formally undergoes σ bond cleavage and addition across a π bond of an alkene or alkyne, in the process forming two new σ bonds.¹⁰⁵ In practice, this transformation is commonly accomplished using haloalkanes as the atom transfer reagents and transition metals as catalysts: the metal first abstracts a halogen atom X from the haloalkane Y–X (Scheme 36). This gives a radical Y•, which adds to the unsaturated substrate **164**. The resulting radical **165** then abstracts the halogen atom from the metal catalyst, completing the atom transfer reaction and regenerating the metal catalyst.

While most transition metal-based ATRA reactions proceed via inner sphere halogen atom abstraction, visible light photoredox catalysis has been applied to the development of ATRA reactions proceeding via outer sphere electron transfer. In an early contribution, Barton and co-workers in 1994 reported that $\text{Ru}(\text{bpy})_3^{2+}$ catalyzes the atom transfer radical addition of *Se*-phenyl *p*-tolueneselenosulfonate (**166**) to a range of vinyl ethers, producing β -phenylselenosulfones in high yields.¹⁰⁶

The mechanism of this ATRA reaction is believed to proceed via single-electron reduction of *Se*-phenyl *p*-tolueneselenosulfonate (**166**) by the photoexcited species $^*\text{Ru}(\text{bpy})_3^{2+}$, which induces fragmentation to give phenylselenolate (**167**) and sulfonyl radical **168** (Scheme 37). Addition of **168** to the vinyl ether (**169**) proceeds selectively to give α -alkoxyalkyl radical **170**. This species is then postulated to react via a radical propagation mechanism, in which a phenylselenium group is abstracted from another equivalent of **166**, providing the β -phenylselenosulfone product **171** and regenerating sulfonyl radical **168**. The photocatalytic cycle is likely turned over via the oxidation of phenylselenolate to phenylselenyl radical (**172**), which dimerizes to form diphenyl diselenide; the formation of only 1 mol of diphenyl diselenide for every 50 mol of product **171** was taken as evidence for a radical propagation mechanism.

More recently, Stephenson and co-workers accomplished the addition of a broad range of atom transfer reagents to olefins via photoredox catalysis.¹⁰⁷ Using $\text{Ru}(\text{bpy})_3^{2+}$ as the photocatalyst, ATRA reactions could be performed using α -halocarbonyls such as diethyl 2-bromomalonate (**173**) and ethyl bromodifluoroacetate (**174**) and haloalkanes such as trifluoromethyl iodide and perfluoroalkyl iodides (Scheme 38). The reactions are amenable to addition across a range of terminal alkenes, as well as cyclic internal alkenes and terminal alkynes.

As in Barton's selenosulfonation reaction, photoexcited $^*\text{Ru}(\text{bpy})_3^{2+}$ likely serves to reduce the haloalkane or α -halocarbonyl substrate **175** by a single electron, generating an electrophilic radical **176**, which undergoes addition to an alkene (Scheme 39). At this stage, one of two reaction pathways may be accessible. The radical addition adduct **177** may abstract a halogen atom from another equivalent of reagent **175** in a radical propagation step to give the ATRA product **178** and regenerate radical **176**. Alternatively, single-electron oxidation of adduct **177** by $\text{Ru}(\text{bpy})_3^{3+}$ may provide carbocation **179** ($E_{1/2}^{\text{red}} = +0.47$ V vs SCE for the 2-propyl radical),¹⁰⁸ which may be trapped by the halogen anion nucleophile in what is termed a radical–polar crossover pathway. These reactions stand in contrast to the reductive radical cyclizations performed by Stephenson's group (vide supra), in which the radical addition product **177** abstracts a hydrogen atom from an amine radical cation to give the product of net reduction. Thus, the lack of a good hydrogen atom source in these reactions enables the ATRA reaction to proceed.

In interrogating the mechanism of this ATRA reaction, evidence was found to support both the radical–polar crossover and the radical propagation pathways. When 4-penten-1-ol (**180**) was used as a substrate in the reaction, the expected ATRA product **181** was obtained along with tetrahydrofuran **182** (Scheme 39A). Resubjection of **181** to the reaction conditions or to refluxing toluene did not provide **182**, demonstrating that **182** does not arise from $\text{S}_{\text{N}}2$

displacement of the bromide. Instead, **182** must arise from trapping of the carbocation **179** by the pendent alcohol, implicating a radical–polar crossover mechanism. On the other hand, experiments conducted using ethyl bromoacetate (**183**) provide evidence for the radical chain propagation pathway. Ethyl bromoacetate itself is not a competent partner in the ATRA reaction, presumably because it cannot undergo single-electron reduction by the photocatalysts being employed; however, if it were present in the reaction alongside a functional substrate, products of **183** incorporation might be observed if a radical chain propagation mechanism were viable. This is indeed the case; when combined with diethyl 2-bromomalonate (**173**), an equal mixture of products arising from ATRA of **173** and **183** is obtained (Scheme 39B). These mechanistic experiments indicate that both the radical–polar crossover and the radical chain propagation pathways are accessible in the photoredox ATRA reaction; the extent to which one pathway is favored over the other likely depends on the nature of the substrates being employed. Finally, photoredox ATRA reactions have also been achieved using the copper photocatalyst $\text{Cu}(\text{dap})_2^+$ (see section 3.2).¹⁰⁹ The photoexcited species $^*\text{Cu}(\text{dap})_2^+$ is sufficiently reducing ($E_{1/2}^{\text{II}^*/\text{I}} = -1.43 \text{ V vs SCE}$) to donate an electron to a range of polyhalomethanes and acyl halides, initiating addition across alkenes via the typical atom transfer mechanism.¹¹⁰

5.2. Photoredox Organocatalysis

As we have noted, radical intermediates generated via photoredox catalysis have only rarely been harnessed to perform enantioselective bond-forming transformations. In 2008, our lab reported the merger of photoredox catalysis with enamine organocatalysis to perform the enantioselective α -alkylation of aldehydes.¹² Enamine catalysis is a general activation mode in which the formation of an enamine from a secondary amine and a carbonyl compound activates the α -position of the carbonyl toward a range of electrophilic functionalization reactions; our lab has extensively investigated the use of chiral secondary amine imidazolidinone catalysts to achieve enantioselective α -functionalization reactions of aldehydes and ketones.¹¹¹ A particularly challenging reaction in this area is the intermolecular α -alkylation of aldehydes, which has yet to be solved in a general sense.

As demonstrated in the atom transfer radical addition chemistry, electrophilic radicals readily undergo addition to simple olefins. Recognizing this, Nicewicz and MacMillan anticipated that inherently electron-rich enamines might couple with electron-deficient radicals generated via photoredox catalysis. If the enamine were derived from a chiral imidazolidinone catalyst, the chiral substituents on the catalyst might control the facial approach of the radical and provide a means of achieving enantioinduction. These concepts were successfully executed: a dual catalyst system composed of $\text{Ru}(\text{bpy})_3^{2+}$ and imidazolidinone **184** was found capable of performing the alkylation of an aldehyde **185** with an electron-deficient alkyl bromide **186** to provide α -alkylated product **187** in good yield and high enantiomeric excess (Scheme 40).

This transformation proceeds via the merger of a photoredox catalytic cycle and an organocatalytic cycle (Scheme 41). Initiation of the reaction requires quenching of the photo-catalyst excited-state $^*\text{Ru}(\text{bpy})_3^{2+}$ by a sacrificial amount of enamine **188** to provide the strongly reducing $\text{Ru}(\text{bpy})_3^+$ (not shown). This species may then transfer an electron to

the alkyl bromide **186**, inducing fragmentation to afford bromide and the electron-deficient radical **189**. Meanwhile, condensation of aldehyde **185** with the imidazolidinone organocatalyst **184** furnishes chiral enamine **188**. Addition of the electrophilic radical to the accessible *Si* face of the enamine forges the C–C bond and generates the α -amino radical **190**. The two catalytic cycles then intersect with the single-electron oxidation of **190** by $^*\text{Ru}(\text{bpy})_3^{2+}$ to yield $\text{Ru}(\text{bpy})_3^+$ and the iminium **191**. Hydrolysis of the iminium releases the α -alkylated product **187** and regenerates the organocatalyst. Photoredox catalysis thus serves not only to generate the reactive radical species but also to perform a key oxidation in the organocatalytic cycle.

This reaction was found amenable to the alkylation of aldehydes with a range of α -bromocarbonyls, including α -bromomalonates, ketones, and esters. Aldehydes having a range of functional groups, as well as substitution at the β -position, were well tolerated. The proposed reductive quenching cycle is supported by Stern–Volmer studies indicating that the α -bromocarbonyl substrates do not quench the photoexcited species $^*\text{Ru}(\text{bpy})_3^{2+}$. As in the previously discussed α -acylation of amines, this dual catalytic approach highlights the utility of combining photoredox catalysis with a second catalytic activation mode for the achievement of enantioselective transformations.

This general approach, termed photoredox organocatalysis, has been extended to the α -trifluoromethylation and α -perfluoroalkylation of aldehydes.¹¹² Methods for the asymmetric installation of trifluoromethyl groups are desirable as this group is widely employed in medicinal chemistry for its ability to modulate the binding affinity, lipophilicity, and metabolic stability of drug candidates.¹¹³ It was found that trifluoromethyl iodide (or the corresponding perfluoroalkyl iodide) may serve as a source of the electrophilic trifluoromethyl radical **192** upon single-electron reduction (Scheme 42). Analogous to the photocatalytic cycle operative in the α -alkylation reaction, reductive quenching of the optimal iridium photocatalyst $\text{Ir}(\text{ppy})_2(\text{dtbbpy})^+$ generates an Ir(II) species, $\text{Ir}(\text{ppy})_2(\text{dtbbpy})$. This intermediate is sufficiently reducing ($E_{1/2}^{\text{III/II}} = -1.51$ V vs SCE)⁵⁸ to donate an electron to CF_3I ($E_{1/2}^{\text{red}} = -1.22$ V vs SCE).¹¹⁴ Mesolysis provides the trifluoromethyl radical, which adds with high facial selectivity to the chiral enamine derived from imidazolidinone **184**, providing access to a range of α -trifluoromethyl aldehydes **193**.

Another previously elusive transformation that has been enabled by photoredox organocatalysis is the α -benzylation of aldehydes.¹¹⁵ As in the α -alkylation and α -trifluoromethylation reactions, it was envisioned that benzyl radicals generated via single-electron reduction of benzyl halides might undergo addition to facially biased enamines. It was anticipated that electron-deficient benzyl halides would be ideal substrates for this reaction, as the installation of electron-withdrawing groups on the arene would both facilitate single-electron reduction of the benzyl halide and render the resulting benzyl radical more electrophilic, promoting coupling with nucleophilic enamines.

In executing this reaction, it was found that electron-deficient benzyl halides could be induced to undergo coupling using the iridium photocatalyst *fac*- $\text{Ir}(\text{ppy})_3$ (see section 3.2) and imidazolidinone organocatalyst **194** to give α -benzyl aldehyde products (Scheme 43). Upon photoexcitation, the strongly reducing excited-state $^*\text{Ir}(\text{ppy})$ ($E_{1/2}^{\text{IV/*III}} = -1.73$ V vs

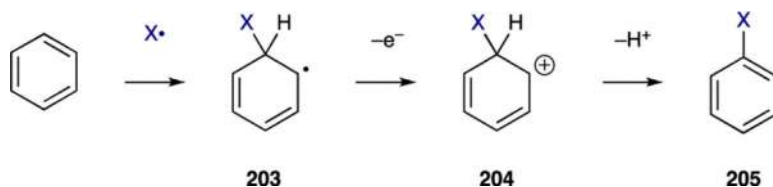
SCE)³⁸ is capable of reducing a benzyl halide **195** to its corresponding benzyl radical **196**. Addition of this radical to the chiral enamine **197** provides α -amino radical **198**, which is oxidized by the intermediate Ir(IV) species ($E_{1/2}^{\text{IV/III}} = +0.77$ V vs SCE). Hydrolysis of the resulting iminium **199** then releases α -benzyl aldehyde **200**. The benzylation reaction thus proceeds via an oxidative quenching cycle, in contrast to the reductive quenching cycles operative in the α -alkylation and α -trifluoromethylation reactions.

The reaction was found to require highly electron-deficient benzyl halides, with substrates bearing both a nitro group and a second electron-withdrawing group undergoing coupling in good yield. The reaction was also amenable to the incorporation of a range of electron-deficient heteroaromatics such as pyridines, pyrazines, pyrimidines, quinolines, and benzimidazoles, moieties that feature prominently in many medicinal agents. Interestingly, the reactivity of certain heteroaryl substrates was significantly improved when the substrate was used as its hydrobromide salt, presumably because protonation of the heterocycle lowers its reduction potential.

The photoredox organocatalysis strategy has also been performed using organic photocatalysts by Zeitler and coworkers.¹¹⁶ Specifically, the xanthene dye eosin Y was employed in concert with imidazolidinone **184** to catalyze the α -alkylation of octanal (**201**) with diethyl bromomalonate (**173**) to give the adduct **202** in good yield and enantiomeric excess (Scheme 44). Eosin Y (EY) absorbs light in the visible region ($\lambda_{\text{max}} = 539$ nm) to give a photoexcited singlet state, $^1\text{EY}^*$, which undergoes intersystem crossing to form the long-lived triplet state $^3\text{EY}^*$. This photoexcited state undergoes reductive quenching, analogously to $\text{Ru}(\text{bpy})_3^{2+}$, oxidizing the intermediate α -amino radical **190** to its corresponding iminium **191** ($^3\text{EY}^*$ is a strong oxidant, $E_{1/2}(^3\text{EY}^*/\text{EY}^{\bullet-}) = +0.83$ V vs SCE). In the process, the photocatalyst is reduced to the eosin Y radical anion ($\text{EY}^{\bullet-}$). This highly reducing species ($E_{1/2}(\text{EY}/\text{EY}^{\bullet-}) = -1.06$ V vs SCE) is then capable of performing the single-electron reduction of the alkyl bromide **186**. This generates the electrophilic α -carbonyl radical **189** and regenerates the ground-state EY species. The organocatalytic cycle proceeds as described in Scheme 41. In yet another variant of this reaction, the α -alkylation of aldehydes has been performed via semiconductor catalysis; König and co-workers have identified surface-modified titanium dioxide and the heterogeneous material PbBiO_2Br as efficient catalysts for this reaction under visible light irradiation.¹¹⁷ These examples demonstrate that reactions developed using one class of visible light photocatalysts are amenable to catalysis via another.

5.3. Radical Additions to Arenes

A great number of photoredox reactions have been developed for the direct functionalization of aromatic rings. In this generic reaction manifold, addition of a radical to an arene first generates a dienyl radical **203** (eq 5). This adduct may readily undergo single-electron oxidation to provide dienyl cation **204**, which upon deprotonation gives the substituted arene product **205**. This approach enables the direct installment of functional groups in place of simple aryl C–H bonds.



(5)

5.3.1. Arylation of Arenes: Diazonium Salts—One of the earliest examples of photoredox catalysis in organic synthesis falls into this general reaction category. In 1984, Cano-Yelo and Deronzier reported that $\text{Ru}(\text{bpy})_3^{2+}$ catalyzes the Pschorr reaction, the intramolecular coupling of an aryldiazonium salt with an unsubstituted arene.¹¹⁸ Single-electron reduction of aryl diazonium salts is very facile ($E_{1/2}^{\text{red}} = -0.1$ V vs SCE for phenyldiazonium tetrafluoroborate) and occurs with concomitant loss of dinitrogen to give aryl radicals.⁷⁰ Thus, upon exposure of aryldiazonium salt **206** to $\text{Ru}(\text{bpy})_3^{2+}$ and visible light, single-electron reduction provides aryl radical **207** (Scheme 45). Intramolecular radical addition to the pendent arene gives adduct radical **208**, which may be oxidized by $\text{Ru}(\text{bpy})_3^{3+}$ to provide carbocation **209**. Deprotonation restores aromaticity and gives the phenanthrene product **210**.

The ability to generate aryl radicals via the single-electron reduction of aryldiazonium salts has been exploited recently by König and co-workers to achieve a Meerwein-type arylation of heteroarenes.^{119,120} The organic photocatalyst eosin Y (vide supra) was found to be a suitable catalyst for this reaction; upon photoexcitation, it is proposed to reduce the aryldiazonium salt to the phenyl radical **211** (Scheme 46). This aryl radical adds to furan (**212**) at the 2-position to provide radical adduct **213**, which is oxidized to oxocarbenium ion **214**, either by the eosin Y radical cation or by another equivalent of diazonium salt in a chain propagation mechanism. Deprotonation provides the 2-arylfuran product **215**. The reaction was found to proceed most efficiently with electron-poor diazonium salts, although electron-rich substrates (such as 4-methoxyphenyldiazonium tetrafluoroborate) couple in moderate yields. In addition to furan, the heteroarene may be a thiophene or *N*-Boc pyrrole.

In these arylation reactions, photoredox catalysis serves to generate aryl radicals that then add directly to organic substrates. Alternative chemical reactions may be accessed if the aryl radical undergoes addition to a metal. Taking this approach, Sanford and co-workers merged photoredox catalysis with high-valent palladium catalysis to perform C–H arylation reactions with diazonium salts.¹²¹ Previous work from the Sanford group demonstrated that a variety of Lewis basic directing groups ligate palladium(II) and facilitate the activation of proximal C–H bonds. Thus, 2-phenylpyridine (**216**) undergoes C–H activation to provide palladacycle **217** (Scheme 47). This intermediate may be intercepted by a range of two-electron oxidants, which oxidize the Pd(II) species to Pd(IV) complex **218**. Reductive elimination between the aryl group and another ligand on the metal then gives the C–H functionalized product **219**. This reaction manifold has been employed to develop a wide range of C–O, C–S, C–X, C–N, and C–C bond-forming reactions.¹²² In one application of

this chemistry, Sanford has introduced the use of diaryliodonium salts (such as **220**) as the two-electron oxidant to perform a C–H arylation reaction, enabling a wide range of substituted aryl rings to be installed at a C–H bond proximal to a directing group.¹²³

A drawback of these arylation reactions, however, is the requirement for elevated temperatures (typically 100 °C). Prompted by mechanistic studies implicating oxidative addition of the diaryliodonium as the rate-determining step,¹²⁴ Sanford and co-workers hypothesized that the use of a more reactive arylating reagent could enable the development of a room temperature C–H arylation reaction. It was further postulated that an aryl radical might serve as a suitably reactive arylating agent.

In the successful execution of these ideas, high-valent palladium catalysis was merged with photoredox catalysis; upon visible light irradiation of a mixture of 2-arylpyridine **221**, phenyldiazonium salt **222**, palladium(II) acetate, and Ru(bpy)₃²⁺ at room temperature, the C–H arylation product **223** is obtained in good yield (Scheme 48). According to the mechanism proposed for this reaction, the photoexcited species *Ru(bpy)₃²⁺ reduces phenyldiazonium salt **222** to the phenyl radical **211**. Simultaneously, C–H activation of 2-arylpyridine **221** generates Pd(II) intermediate **224**. The aryl radical is postulated to add to this species, oxidizing the metal by one electron to generate Pd(III) intermediate **225**. At this point, the two catalytic cycles merge, with the highly oxidizing Ru(bpy)₃³⁺ removing an electron from **225**, giving the Pd(IV) species **226**. Reductive elimination from this high-valent palladium complex generates the biphenyl product **223** and, following C–H activation of another molecule of **221**, regenerates Pd(II) complex **224**.

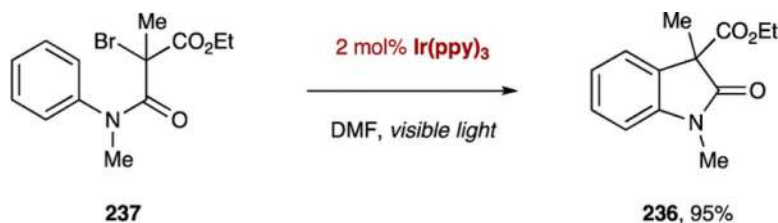
The reaction was found to tolerate substitution on both rings of the 2-phenylpyridine substrate. In addition to pyridine, amides, pyrazoles, pyrimidines, and oximes could be employed as directing groups. A diverse range of substituted aryldiazonium salts readily undergo reaction, as demonstrated in the arylation of *N*-phenylpyrrolidinone. Most significantly, this reaction provides a striking example of the utility of single-electron processes in transition metal chemistry. While the monocatalytic C–H arylation with diaryliodonium salts proceeds via a single two-electron oxidation event, and suffers from the requirement for elevated reaction temperatures, the multicatalytic C–H arylation with diazonium salts proceeds via two sequential one-electron oxidation events. In this case, the lower energy barriers to the single-electron processes enable the dramatic lowering in reaction temperature.

5.3.2. Alkylation of Arenes—In addition to aryldiazonium salts, a range of other radical precursors may be employed in arene functionalization reactions. Stephenson and co-workers have shown that malonyl radicals, generated by the single-electron reduction of 2-bromomalonates, undergo efficient addition to electron-rich heterocycles.¹²⁵ Key to the success of this reaction is the use of 4-methoxy-*N,N*-diphenylaniline (**227**) as a reductive quencher for the photocatalyst. Oxidation of triarylamine **227** by *Ru(bpy)₃²⁺ furnishes aminium radical cation **228** and Ru(bpy)₃³⁺, which reduces diethyl 2-bromomalonate (**173**) to malonyl radical **229** (Scheme 49). When amine reductants having α -hydrogens are employed, **229** may abstract a hydrogen atom (H[•]) from the amine radical cation to give the product of reductive dehalogenation. As radical cation **228** lacks α -hydrogens, however,

malonyl radical **229** instead engages in coupling, adding to the 2-position of indoles to give benzylic radical adduct **230**. Oxidation of **230**, either by $^*\text{Ru}(\text{bpy})_3^{2+}$ or by bromomalonate **173**, followed by deprotonation gives the 2-alkylated indole **231**. This reaction was demonstrated to be effective for alkylation at the 2-position of indole, pyrrole, azaindole, and furan ring systems. If the 2-position of indole is blocked, alkylation proceeds efficiently at the 3-position. The reaction may also be carried out intramolecularly when the heterocycle bears a tethered bromomalonate moiety.

Stephenson has applied the photoredox indole alkylation reaction to the total synthesis of (+)-gliocladin C, a natural product having a C3–C3' linked indole/pyrroloindoline core (Scheme 50).¹²⁶ Previous work in the Stephenson group on reductive dehalogenation reactions demonstrated that bromopyrroloindolines such as **232** undergo single-electron reduction to give tertiary benzylic radicals (vide supra). It was proposed that the key C3–C3' bond of gliocladin C could be formed via addition of this radical to indole. Because of the preference for radical addition at the 2-position of indole, however, indole-2-carboxaldehyde (**233**) was employed to block the 2-position and direct reactivity toward the desired C3–C3' bond construction. This approach proved successful, and bromopyrroloindoline **232** was converted in high yield to C3–C3' coupled product **234**. Subsequent decarbonylation with Wilkinson's catalyst provided deformylated indole **235**, which was carried forward to gliocladin C. In total, gliocladin C was synthesized in 10 steps from commercial starting materials in 30% overall yield.

In related work, Yu and co-workers have reported the synthesis of oxindoles such as **236** from 2-bromoanilides via intramolecular radical cyclization (eq 6).¹²⁷ Highest yields were obtained using the photocatalyst $\text{Ir}(\text{ppy})_3$; the photoexcited species $^*\text{Ir}(\text{ppy})_3$ is sufficiently reducing to donate an electron directly to 2-bromoanilide **237**, and a stoichiometric reductant is not required.



(6)

5.3.3. Trifluoromethylation of Arenes—A particularly desirable arene functionalization reaction is the direct trifluoromethylation of arene C–H bonds, due to the utility of this group in medicinal chemistry. Our group has recently accomplished this reaction under photoredox conditions using trifluoromethanesulfonyl chloride (triflyl chloride) as a precursor to the trifluoromethyl radical.¹²⁸ The reaction proceeds first via single-electron reduction of triflyl chloride (**238**, $E_{1/2}^{\text{red}} = -0.18 \text{ V vs SCE}$) by the photocatalyst, in this case $\text{Ru}(\text{phen})_3^{2+}$ (phen = phenanthroline, $E_{1/2}^{\text{III/*II}} = -0.87 \text{ V vs SCE}$ for $^*\text{Ru}(\text{phen})_3^{2+}$)¹²⁹ (Scheme 51 and Figure 4). Reduction induces fragmentation of triflyl chloride to give the trifluoromethyl radical, sulfur dioxide, and chloride. Addition of the

trifluoromethyl radical to the arene **239** gives the dienyl radical **240**, which may be oxidized by $\text{Ru}(\text{phen})_3^{3+}$ to the dienyl cation **241**. Deprotonation then delivers trifluoromethylated product **242**. A range of five- and six-membered arenes and heteroarenes may be efficiently and selectively functionalized using this protocol.

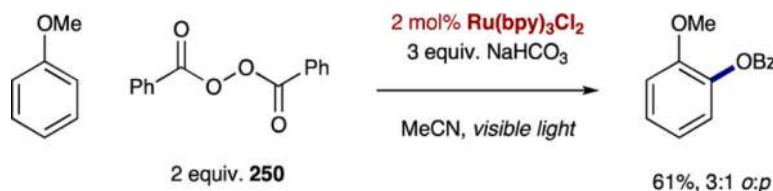
Trifluoromethylation of pyrroles, indoles, furans, and thiophenes proceeds selectively at the 2-position, and a thiazole was shown to react selectively at the 5-position. For the trifluoromethylation of six-membered rings, the optimal photocatalyst was found to be $\text{Ir}(\text{Fppy})_3$ (Fppy = 2-(2,4-difluorophenyl)pyridine). This catalyst enables the efficient trifluoromethylation of a range of simple benzene derivatives, as well as nitrogen-containing heterocycles such as pyridines, pyrazines, and pyrimidines.

A striking feature of this reaction is its amenability to the functionalization of complex molecules such as pharmaceutical agents. This was demonstrated by exposing the cholesterol-lowering statin Lipitor to the arene trifluoromethylation conditions; a mixture of three monotrifluoromethylated Lipitor derivatives is obtained (Scheme 52). This result highlights the potential utility of this reaction in rapidly diversifying late-stage drug candidates. Cho and co-workers have additionally reported an analogous photoredox-catalyzed arene trifluoromethylation using trifluoromethyl iodide as the source of the trifluoromethyl radical.¹³⁰ The reaction was shown to be amenable to the trifluoromethylation of a range of five-membered heterocycles.

In a mechanistically distinct contribution, Ye and Sanford have reported the trifluoromethylation of arylboronic acids by applying their strategy of merging photoredox catalysis with transition metal catalysis.¹³¹ These authors recognized that copper has been found to catalyze the trifluoromethylation of boronic acids, with the active “ $\text{Cu}-\text{CF}_3$ ” species in these systems being derived from either nucleophilic “ CF_3^- ” sources such as the Ruppert–Prakash reagent¹³² or electrophilic “ CF_3^+ ” sources such as *S*-(trifluoromethyl)thiophenium salts¹³³ and Togni's reagent.¹³⁴ Postulating that the trifluoromethyl radical might be used to generate a copper– CF_3 complex, they explored visible light photoredox conditions for the generation of $^{\bullet}\text{CF}_3$ in conjunction with copper catalyst systems. This approach proved fruitful, with phenylboronic acid (**243**) undergoing conversion to trifluoromethylbenzene (**244**) upon exposure to conditions employing $\text{Ru}(\text{bpy})_3^{2+}$ as the photo-catalyst, trifluoromethyl iodide (**245**) as the $^{\bullet}\text{CF}_3$ source, copper(I) acetate, and visible light (Scheme 53). The reaction gives only trace product in the absence of a copper catalyst or when the conditions for photoredox C–H trifluoromethylation are employed, demonstrating the intermediacy of a copper– CF_3 species. The reaction is therefore proposed to proceed first via single-electron oxidation of the copper(I) species **246** ($E_{1/2}^{\text{red}} = -0.08$ V vs SCE for $\text{Cu}(\text{I})$) by $^*\text{Ru}(\text{bpy})_3^{2+}$ to give a copper(II) species **247** and $\text{Ru}(\text{bpy})_3^+$. As previously described, $\text{Ru}(\text{bpy})_3^+$ is capable of donating an electron to trifluoromethyl iodide to generate the trifluoromethyl radical (**192**) and regenerate ground-state $\text{Ru}(\text{bpy})_3^{2+}$. Addition of $^{\bullet}\text{CF}_3$ to the copper(II) species **247** oxidizes the metal by a single electron to give the high-valent trifluoromethyl–copper(III) species **248**. Transmetalation of phenylboronic acid (**243**) may then proceed to give aryl–copper(III) intermediate **249**, which may undergo reductive elimination to forge the aryl– CF_3 bond and regenerate the copper(I) species. The authors alternatively suggest that the order of

trifluoromethyl radical addition and transmetalation may be reversed, with transmetalation between **247** and **243** giving rise to a copper(II)–aryl species, which may be converted to copper(III) species **249** upon addition of the CF₃ radical. As in the photoredox- and palladium-catalyzed C–H arylation using aryldiazonium salts, a key feature of this reaction is the intermediacy of a high-valent metal species; while the arylation reaction proceeds via a putative Pd(IV) intermediate, in the trifluoromethylation reaction reductive elimination proceeds from a high-valent Cu(III) species. Also common to both reactions is the manner in which these high-valent species are accessed; one single-electron oxidation is performed by the photocatalyst, while the second single-electron oxidation occurs upon addition of the radical. In each reaction, the photocatalyst thus serves not only to generate the desired radical but also plays an integral part in the transition metal catalytic cycle. This dual catalytic system was found to successfully trifluoromethylate both electron-rich and electron-deficient arylboronic acids, as well as transform boronic acids derived from heteroarenes such as pyridine and quinoline.

5.3.4. Oxygenation of Arenes—A final arene functionalization reaction enabled by photoredox catalysis is the benzoyloxylation of arenes reported by Li, which proceeds via the intermediacy of benzoyloxy radicals (eq 7).¹³⁵ In this protocol, single-electron reduction of benzoyl peroxide (**250**) induces mesolysis to give 1 equiv of benzoate and 1 equiv of the benzoyloxy radical (*OBz). Addition of the benzoyloxy radical to the arene followed by oxidation and rearomatization via deprotonation yields the oxygenated arene product. This reaction was found to require electron-rich arenes and was successfully applied to the functionalization of a range of anisole derivatives.¹³⁶



(7)

5.4. Radical Additions to Other π Nucleophiles

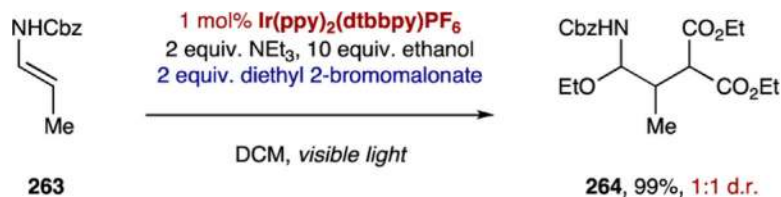
Electron-deficient radicals have been employed to functionalize a wide range of electron-rich π systems beyond enamines and arene rings. Aryldiazonium salts, for instance, have been employed to develop a photoredox arylation of styrenes.¹³⁷ Upon reductive fragmentation of the aryldiazonium salt with Ru(bpy)₃²⁺, the phenyl radical undergoes addition to the β -position of styrene to provide benzylic radical **251**, which is oxidized and deprotonated to give stilbene (**26**) as a mixture of olefin isomers (Scheme 54). Aryl radicals may also add to enol acetates to afford α -aryl ketones.¹³⁸ These reactions proceed via the intermediacy of α -acetoxy radicals such as **252**, which upon single-electron oxidation and loss of acetate yields α -aryl ketone **253** (Scheme 54).¹³⁹

In a recent contribution from our lab, we described the synthesis of α -trifluoromethyl ketones, esters, and amides via radical addition to the corresponding enolsilanes, silylketene

acetals, and silylketene *N,O*-acetals.¹⁴⁰ Reductive quenching of $^*\text{Ru}(\text{bpy})_3^{2+}$ followed by reduction of trifluoromethyl iodide by $\text{Ru}(\text{bpy})_3^+$ generates the trifluoromethyl radical (**192**), which adds to the electron-rich enolsilane **254** to provide α -silyloxy radical **255** (Scheme 55). Single-electron oxidation of **255** by $^*\text{Ru}(\text{bpy})_3^{2+}$ generates silyloxocarbenium **256**, and hydrolysis of **256** provides the α -trifluoromethyl carbonyl product **257**. The reaction was found to be applicable to the trifluoromethylation of a range of aromatic and aliphatic enolsilanes. Surprisingly, when silylketene acetals and *N,O*-acetals were employed as substrates in the reaction, good yields of the products were obtained in the absence of a photocatalyst; these reactions may proceed via a photoinduced charge-transfer complex.¹⁴¹ Additionally, it was demonstrated that the direct α -trifluoromethylation of ketones, esters, and amides could be carried out in a one-pot procedure, in which the enolsilane or silylketene acetal is generated in situ and exposed without purification to the photoredox conditions. These conditions were also found to be amenable to the introduction of perfluoroalkyl groups.

Using styrenes as π -nucleophilic partners for coupling with trifluoromethyl radicals, Akita and co-workers have developed an oxytrifluoromethylation reaction proceeding via a radical–polar crossover mechanism.¹⁴² These authors make use of Umemoto's reagent (**258**) as a source of the trifluoromethyl radical; this species ($E_{1/2}^{\text{red}} = -0.37 \text{ V}$ vs SCE) is proposed to undergo single-electron reduction by $^*\text{Ir}(\text{ppy})_3$ to yield dibenzothiophene and the trifluoromethyl radical (Scheme 56). Addition of trifluoromethyl radical to styrene (**259**) gives a benzylic radical (**260**), which may be oxidized by the intermediate $\text{Ir}^{\text{IV}}(\text{ppy})_3$ to the benzylic carbocation **261**. When methanol is employed as a cosolvent, this carbocation is converted to the product methyl ether **262**. In addition to alcohols, water and carboxylic acids may also be employed as nucleophiles to deliver the products of hydroxytrifluoromethylation and carboxytrifluoromethylation, respectively. This protocol was applied to a range of styrenes, with substrates such as *trans*-stilbene and indene undergoing oxytrifluoromethylation with moderate to good levels of diastereoselectivity.

Masson has employed a similar radical–polar crossover mechanism to achieve the tandem alkylation/nucleophilic trapping of enamides and enecarbamates.¹⁴³ In this three-component coupling, malonyl radical addition to enecarbamate **263** provides an α -amido radical, which upon oxidation to the *N*-acyliminium ion and trapping by ethanol provides the adduct **264** (eq 8).¹⁴⁴



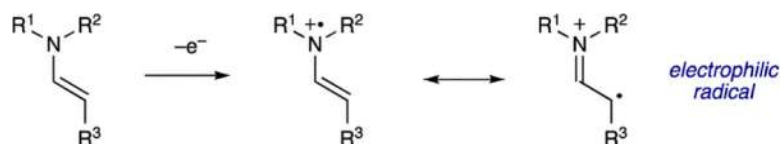
(8)

Finally, the copper photocatalyst $\text{Cu}(\text{dap})_2^+$ has been employed to achieve the allylation of α -halocarbonyls with allylstannanes.¹⁰⁹ Photoexcitation of $\text{Cu}(\text{dap})_2^+$ generates an excited

species, which reduces the α -chloroketone **265** to give α -carbonyl radical **266** (Scheme 57). Addition of this radical to allyltributyltin (**267**), with concurrent release of stannyl radical **268**, provides the allylated product **269**. Single-electron reduction of the stannyl radical by $\text{Cu}(\text{dap})_2^{2+}$ then closes the photocatalytic cycle.

5.5. Reactions of Enamine Radical Cations

The electrophilic radicals discussed thus far are typically generated by single-electron reduction and fragmentation of the corresponding halide. A unique approach to forming an electrophilic radical, however, is single-electron oxidation of an enamine. The resulting enamine radical cation possesses significant spin density on the carbon β to nitrogen and may also be considered as an α -iminium radical.¹⁴⁵ This species thus reacts as an electrophilic radical at the β -position of the enamine (eq 9).¹⁴⁶ While the reactions in this section are net oxidative, rather than redox neutral, we consider them here to place them in the context of related chemistry of enamines and similar radical additions to π systems.



(9)

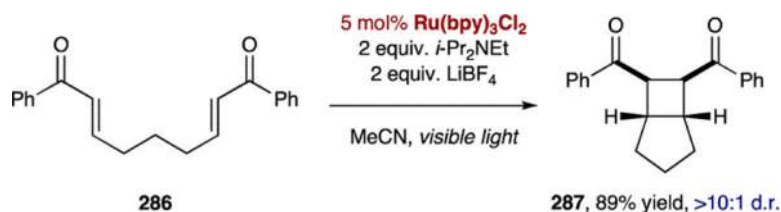
Akita and co-workers employed $\text{Ru}(\text{bpy})_3^{2+}$ to generate this enamine radical cation and demonstrated that it adds to enolsilanes in a net oxidative transformation to provide 1,4-diketone products.¹⁴⁷ Duroquinone is employed in this reaction as a stoichiometric oxidant, and increased yields are observed using lithium tetrafluoroborate as an additive, presumably because lithium coordination lowers the reduction potential of the quinone. Thus, lithium-complexed duroquinone (**270**) is proposed to oxidatively quench $^*\text{Ru}(\text{bpy})_3^{2+}$, giving **271**, which may be reduced by another electron to afford hydroquinone **272** (Scheme 58). The oxidant $\text{Ru}(\text{bpy})_3^{3+}$ then removes an electron from morpholine enamine **273**, generating the enamine radical cation **274**. Coupling with enolsilane **275** provides the α -silyloxy radical **276**, which upon loss of another electron and silyl group cleavage furnishes ketone **277**. Hydrolysis of the iminium ultimately provides the 1,4-diketone product **278**. The reaction tolerates electron-donating and weakly electron-withdrawing substitution on the phenyl ring of the enolsilane. As both the enamine **273** and the duroquinone quench the photocatalyst, the photocatalyst may also be engaged in a reductive quenching cycle.

Koike and Akita have also made use of enamine radical cations to perform an α -oxyamination of aldehydes.¹⁴⁸ Condensation of hydrocinnamaldehyde (**279**) with morpholine (**280**) generates enamine **281** (Scheme 59). Single-electron oxidation of **281** by $^*\text{Ru}(\text{bpy})_3^{2+}$ generates the enamine radical cation **282**. This species is proposed to undergo radical-radical coupling with 2,2,6,6-tetramethylpiperidine-1-oxyl (TEMPO, **283**), providing iminium **284**, hydrolysis of which generates α -oxyamination product **285** and regenerates the amine catalyst. The stoichiometric oxidant operative in this process is likely adventitious oxygen.¹⁴⁹

5.6. [2 + 2] Cycloadditions

As these reactions of enamine radical cations demonstrate, photoredox catalysis may be employed to access stable radical cations and radical anions that do not undergo fragmentation to give neutral radicals. Often, these radical ions possess reactivity that is inherently unique from that of their native oxidation state, and these species may be harnessed to access exotic transformations.

A prime example of this reaction type is the cycloaddition chemistry developed by Yoon and co-workers. Inspired by reports indicating that single-electron reduction of certain bis(enone) substrates initiates [2 + 2] cycloaddition reactions,¹⁵⁰ Yoon demonstrated that Ru(bpy)₃Cl₂ catalyzes the transformation of bis(enone) **286** to cyclobutane-containing adduct **287** in high yield and with good diastereoselectivity (eq 10).¹¹ Hünig's base is required for reactivity, suggesting that the first step in the photocatalytic



(10)

cycle is reductive quenching of $^*\text{Ru(bpy)}_3^{2+}$ by the amine (Scheme 60). The lithium cation is also essential, and likely functions as a Lewis acid to activate the enone toward one-electron reduction by Ru(bpy)_3^+ . The resulting lithium-bound radical anion **288** then undergoes [2 + 2] cycloaddition, resulting in the ketyl radical **289**, which is oxidized to give cyclobutane adduct **287**. This oxidation may conceivably be performed by the photoexcited catalyst $^*\text{Ru(bpy)}_3^{2+}$, the amine radical cation, or another equivalent of lithium-bound bis(enone). The organic substrate thus undergoes no net change in oxidation state: it accepts an electron, undergoes bond rearrangement, and then donates an electron to an acceptor to complete the cycle. Various substituted aryl and heteroaryl bis(enone) substrates were found to perform well in the reaction, but symmetrical aliphatic enones and enoates do not cyclize, likely because they fail to undergo reduction. As long as one aryl enone is present, however, unsymmetrical substrates having a tethered aliphatic enone or enoate may be employed. While the intramolecular cyclizations give rise predominantly to the *meso cis*-dione products, the cycloadditions may also be performed in an intermolecular manner to give as the major product the *trans*-dione.

Yoon and co-workers subsequently sought to extend this chemistry to crossed intermolecular [2 + 2] cycloadditions. It was anticipated that the inherent challenge of homodimerization could be overcome if only one of the two reaction partners were an aryl enone and thus capable of undergoing reduction. In addition, it was conceived that the enone radical anion would react less readily with another equivalent of itself than it would with Michael acceptors lacking substituents at the β -position. In the event, aryl enone **290** was found to react with 2.5 equiv of methyl vinyl ketone (**291**) to give the crossed cyclobutane

product **292** in good yield and diastereoselectivity (Scheme 61).¹⁵¹ Aryl enones having a variety of alkyl groups at the β -position could be employed, and acrylate esters and thioesters could also function as the Michael acceptor. A thioester acceptor having a methyl group at the α -position was even found to give moderate yield in the reaction, providing access to cyclobutane **293** bearing a quaternary carbon center.

Recognizing that the requirement for an aryl enone coupling partner places limitations on the scope of available products, Yoon recently introduced α,β -unsaturated 2-imidazolyl ketones such as **294** as substrates for the photoredox [2 + 2] cycloaddition (Scheme 62).¹⁵² The *N*-methylimidazol-2-yl group functions as an auxiliary that enables reduction of the enone, allowing such ketones to perform in a range of inter- and intramolecular [2 + 2] cycloadditions. Following the photoredox reaction, *N*-alkylation of the product **295** followed by treatment with a nucleophile provides access to carboxylic acid, ester, thioester, and amide products. The imidazolyl group, termed a “redox auxiliary”, thus enables access to a range of cyclobutane adducts that cannot be formed directly in the [2 + 2] reaction.

A key feature of these [2 + 2] cycloadditions is the requirement for a lithium cation to act as a Lewis acid and lower the reduction potential of the aryl enone substrate. Yoon speculated that Brønsted acids could similarly activate these substrates toward reduction by protonating the enone. When various acids were examined as additives in the reaction, however, very different reactivity was observed: instead of giving [2 + 2] cycloaddition products, the products of net reductive cyclization were obtained (Scheme 63).¹⁵³ In particular, when dione **286** was treated with Ru(bpy)₃²⁺, Hünig's base, and 5 equiv of formic acid, cyclopentane **296** is obtained as the exclusive product. The reaction presumably proceeds via reduction of protonated dione **297** to give the neutral β -ketoradical **298**. In contrast to the lithium-bound radical anion **288**, which undergoes [2 + 2] cycloaddition, this species undergoes 5-*exo*-trig cyclization to give α -carbonyl radical **299** solely as the *trans* diastereomer. Abstraction of a hydrogen atom from the amine radical cation then delivers the product **296**.

Using these conditions, a range of aryl enones could be cyclized to give the *trans*-substituted cyclopentane products. Heteroatoms could be employed in the tether between the reacting enones, and the tether length could be extended to give access to six-membered rings. Interestingly, aliphatic enones, which are unreactive in the lithium-promoted [2 + 2] cycloadditions, efficiently undergo cycloaddition using the photocatalyst Ir(ppy)₂(dtbbpy)PF₆. A number of acceptors that are unreactive with aryl enone-derived radicals, such as styrenes and vinyl nitriles, were additionally found to be reactive with the aliphatic enone-derived radicals. Similar reductive intramolecular cyclization reactions have been accomplished using 9,10-dicyanoanthracene as a visible light photocatalyst and triphenylphosphine as the stoichiometric reductant.¹⁵⁴

Similarly unanticipated reactivity was uncovered when chalcones were exposed to the conditions for photoredox cycloaddition. Instead of affording [2 + 2] adducts, *trans*-chalcone (**300**) is converted to cyclopentanol **301** (Scheme 64).¹⁵⁵ Employing samarium(III) triflate as a Lewis acid, single-electron reduction of **300** proceeds to give samarium-bound radical anion **302**. Competition experiments with methyl vinyl ketone suggest that radical

anion **302** does not add to a molecule of neutral **300**, but rather undergoes radical–radical coupling with another equivalent of **302** to give dienolate **303**. Protonation of one of the enolates followed by an intra-molecular aldol addition provides the cyclopentanol product **301**.

In these reductive cyclization reactions as well as the related [2 + 2] cycloadditions, reductive quenching of $\text{Ru}(\text{bpy})_3^{2+}$ serves to generate $\text{Ru}(\text{bpy})_3^+$, which reduces an electron-poor organic substrate to initiate the cyclization. In addition to radical anions, however, radical cations are also known to undergo cycloaddition reactions.¹⁵⁶ To engage electron-rich bis(styrenes) in [2 + 2] cycloadditions, Yoon and co-workers employed an oxidative quenching cycle to generate $\text{Ru}(\text{bpy})_3^{3+}$.¹⁵⁷ Specifically, oxidative quenching of $\text{Ru}(\text{bpy})_3^{2+}$ by the electron acceptor methyl viologen (MV^{2+}) generates the strongly oxidizing $\text{Ru}(\text{bpy})_3^{3+}$ (Scheme 65). This species is capable of oxidizing the electron-rich styrene **304** ($E_{1/2}^{\text{red}} = +1.2$ V vs SCE for *trans*-anethole)¹⁵⁸ to its radical cation **305**, which was found to undergo [2 + 2] cycloaddition followed by single-electron reduction to give cyclobutane-containing adduct **306**. As the reaction is redox neutral with respect to the substrate, it may be conducted with a substoichiometric amount (15 mol %) of methyl viologen. The substituted cyclobutane adducts are formed predominantly as the *cis*-isomers. As a requirement for the oxidation step, one of the styrenes on the substrate must bear an electron-donating group at the para or ortho position. The second styrene partner, however, may bear electron-donating as well as -withdrawing groups.

Yoon subsequently disclosed an intermolecular variant of this reaction, achieving crossed [2 + 2] cycloadditions between electron-rich styrenes and a variety of acceptor olefins.¹⁵⁹ Critical to the success of this reaction was the use of the photocatalyst ruthenium(II) tris(bipyrimidine), or $\text{Ru}(\text{bpm})_3^{2+}$ (Scheme 66).¹⁶⁰ In initial experiments, $\text{Ru}(\text{bpy})_3^{2+}$ was found incapable of promoting the dimerization of *trans*-anethole in the absence of an oxidative quenching cycle, while the strongly oxidizing tris(bipyrazyl) analogue $\text{Ru}(\text{bpz})_3^{2+}$ (see section 3.4) was found to give moderate yields of the adduct **307**. Unfortunately, $\text{Ru}(\text{bpz})_3^{2+}$ ($E_{1/2}^{*\text{III}} = +1.45$ V vs SCE) was also found to oxidize the product **307** ($E_{1/2}^{\text{red}} = +1.27$ V vs SCE), leading to cycloreversion and preventing the isolation of **307** in high yields. The photocatalyst $\text{Ru}(\text{bpm})_3^{2+}$ occupies a middle ground between $\text{Ru}(\text{bpy})_3^{2+}$ and $\text{Ru}(\text{bpz})_3^{2+}$; it is proposed that its photoexcited state ($E_{1/2}^{*\text{III}} = +0.99$ V vs SCE)¹⁶¹ may oxidize *trans*-anethole but may not remove an electron from the product cyclobutane **307**. Using $\text{Ru}(\text{bpm})_3^{2+}$, electron-rich styrenes could be engaged in crossed [2 + 2] cycloadditions in high yield with a range of electronically diverse acceptor styrenes as well as vinyl ethers and allyl silanes.

5.7. [4 + 2] and [2 + 2 + 2] Cycloadditions

The cycloaddition chemistry of radical anions and radical cations is not limited to [2 + 2] cycloadditions, and with the proper choice of substrates [4 + 2] cycloadditions may be induced. Yoon observed [4 + 2] adducts in the course of studies on the bis(enone) [2 + 2] cycloaddition reaction. While bis(enones) tethered by a three-carbon linker give exclusively [2 + 2] cycloadducts upon treatment with $\text{Ru}(\text{bpy})_3^{2+}$, Hünig's base, and LiBF_4 , bis(enones) tethered by a four-carbon linker (as in **308**) give dihydropyrans, the products of hetero-

Diels–Alder cycloaddition (Scheme 67).¹⁶² As in the radical anion [2 + 2] cycloaddition, binding of the Lewis acidic lithium ion to the enone enables this species to accept an electron to give **309**. This initiates radical cyclization to give radical anion **310**. This step proceeds to give the *trans*-cyclohexane, thus rendering [2 + 2] cycloaddition highly disfavored as it would require formation of a highly strained *trans* [4.2.0] ring system. Instead, formation of a carbon–oxygen bond proceeds to give ketyl radical **311**, which is oxidized to give the dihydropyran **312**. Interestingly, high regioselectivity is observed for the cyclization of unsymmetrical bis(enones), presumably driven by formation of the more stable ketyl radical.

In addition to this radical anion hetero-Diels–Alder reaction, radical cations generated via photoredox catalysis have been found to react with dienes to give Diels–Alder adducts. Specifically, upon oxidation of *trans*-anethole (**313**), radical cation **314** was found to react with isoprene (**315**) in a [4 + 2] cycloaddition to provide cyclohexene Diels–Alder adduct **316** (Scheme 68).¹⁶³ Although Ru(bpy)₃²⁺ is a competent catalyst for this reaction, Yoon and co-workers observed higher efficiencies for the [4 + 2] cycloaddition using the more oxidizing analog Ru(bpz)₃²⁺. In contrast to Ru(bpy)₃²⁺, which must be oxidized to its Ru(bpy)₃³⁺ oxidation state before it can oxidize electron-rich styrenes such as *trans*-anethole ($E_{1/2}^{\text{red}} = +1.2$ V vs SCE),¹⁵⁸ Ru(bpz)₃²⁺ is capable of performing this oxidation directly from its photoexcited state ($E_{1/2}^{*\text{III}} = +1.45$ V vs SCE⁵⁵ for *Ru(bpz)₃²⁺ as compared to $E_{1/2}^{*\text{III}} = +0.77$ vs SCE²¹ for *Ru(bpy)₃²⁺). Following oxidation, radical cation **314** reacts with isoprene to give radical cation adduct **317**, which must be reduced, either by Ru(bpz)₃⁺ or by another equivalent of styrene **313**. It was found that the highest yields were obtained when the reaction was run under air, presumably because oxygen helps to turn over the photoredox catalyst and regenerate Ru(bpz)₃²⁺. As in the related radical cation [2 + 2] cycloaddition, electron-donating groups are required on the styrene. A variety of substituted dienes are tolerated in the reaction, and when the potential exists for endo and exo diastereomers, the endo product is preferred. Cyclic styrenes can also be employed, providing access to bicyclic products. Yoon and co-workers have subsequently reported an intra-molecular variant of this reaction.¹⁶⁴

Strikingly, these radical ion Diels–Alder reactions are orthogonal in scope to classic thermal Diels–Alder reactions, in which one component (typically the diene) is electron-rich and the other component (typically the dienophile) is electron-poor. In the radical anion Diels–Alder, two electronically mismatched enones are induced to react via reduction of one enone to an electron-rich radical anion. Similarly, in the radical cation Diels–Alder, single-electron oxidation of the dienophile renders this component electron-poor, enabling a [4 + 2] reaction between two substrates that in their native oxidation states are electronically mismatched.

Yoon and co-workers demonstrated the utility of their photoredox radical cation Diels–Alder cycloaddition in a total synthesis of the natural product heitziamide A.¹⁶³ Exposure of styrene **318** and myrcene (**319**) to the photoredox conditions afforded cyclohexene **320** in 80% yield (Scheme 69). Deprotection of the silyl group, oxidation, and amide coupling completed the rapid synthesis of heitziamide A. Along with Stephenson's synthesis of gliocladin C, this represents one of the first applications of photoredox catalysis with transition metal complexes toward the synthesis of a natural product.

The strongly oxidizing $\text{Ru}(\text{bpz})_3^{2+}$ catalyst was also found to be uniquely effective at catalyzing the [2 + 2] cycloaddition of bis(styrenes) with molecular oxygen to give endoperoxide products (Scheme 70).¹⁶⁵ When the reaction of bis(styrene) **321** with $\text{Ru}(\text{bpz})_3^{2+}$ is performed under four atmospheres of oxygen, generation of radical cation **322** is followed by reaction with triplet oxygen to give the six-membered radical cation **323**. Reduction of this radical cation, either by $\text{Ru}(\text{bpz})_3^+$ or another equivalent of styrene **321**, affords endoperoxide **324**. A pathway involving reaction of singlet oxygen with the bis(styrene) is disfavored due to the failure of tetraphenylporphyrin, a known photosensitizer for the generation of singlet oxygen, to provide any endoperoxide product. As in the [2 + 2] bis(styrene) cycloaddition, one of the styrenes must bear an electron-donating group, but a variety of substitution is tolerated on the second styrene ring.

5.8. [3 + 2] Cycloadditions: Cyclopropane Ring-Opening

Photoredox catalysis has also been applied to the development of [3 + 2] cycloadditions by making use of the radical ring-opening of cyclopropanes. As is well-known from studies on cyclopropanes as radical clocks,¹⁶⁶ the generation of a cyclopropylcarbinyl radical induces homolytic cleavage of a carbon–carbon bond in the ring; in this way, a cyclopropane ring may serve as a surrogate for a reactive three-carbon fragment.

Yoon and co-workers employed this strategy to add the three-carbon unit of a cyclopropyl ketone across olefins in an intramolecular [3 + 2] cycloaddition.¹⁶⁷ Cyclopropyl ketone **325** was found to undergo reduction by $\text{Ru}(\text{bpy})_3^+$ (generated by reductive quenching of $^*\text{Ru}(\text{bpy})_3^{2+}$), and fragmentation of the resulting cyclopropyl ketyl radical **326** gives distonic radical anion **327** (Scheme 71).¹⁶⁸ This key intermediate undergoes sequential radical additions to the tethered enoate to afford ketyl radical **328**. Oxidation provides the bicyclic product **329**. Interestingly, the lithium Lewis acids employed in the [2 + 2] cycloaddition chemistry were not competent at promoting the reduction of **325**, and the stronger Lewis acid $\text{La}(\text{OTf})_3$ was required. Tetramethylenediamine (TMEDA) was additionally found to be superior to Hünig's base as a reductive quencher of $^*\text{Ru}(\text{bpy})_3^{2+}$. In addition to enoates, tethered enones and styrenes may be employed in the [3 + 2] cycloaddition. Remarkably, a cyclic aliphatic olefin may be employed to give tricyclic adduct **330**, and addition across tethered alkynes may be carried out to provide products such as **331**. An intermolecular reaction of cyclopropyl phenyl ketone with methacrylonitrile was possible, affording cyclopentane **332**.

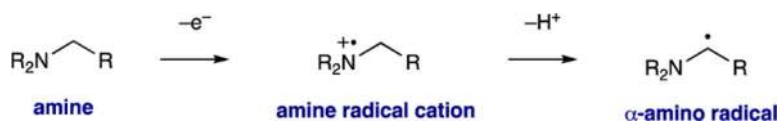
A similar approach has been used to engage cyclopropylamines in cycloaddition reactions. Zheng and co-workers found that $\text{Ru}(\text{bpz})_3^{2+}$ mediates the intermolecular [3 + 2] cycloaddition of secondary and tertiary cyclopropylamines with styrenes (Scheme 72).¹⁶⁹ Upon single-electron oxidation of cyclopropylamine **333**, the cyclopropyl ring fragments to give the distonic radical cation **334**. Addition of this radical to the β -position of styrene produces a benzylic radical, which adds to the iminium ion to afford radical cation **335**. Single-electron reduction by $\text{Ru}(\text{bpz})_3^+$ generates the cyclopentane product **336** as a 1:1 mixture of diastereomers and completes the photocatalytic cycle. The reaction requires an aryl group on the amine, but substitution on the aryl ring is well tolerated, with even very electron-deficient 4-trifluoromethylphenyl and 3-pyridyl groups tolerated. Styrenes bearing electron-

donating and electron-withdrawing groups may be employed, and tertiary amines may be used to provide bicyclic adducts.

These cycloaddition reactions highlight the simplicity of redox neutral transformations: in this case, one electron is added to the substrate, it undergoes a transformation, and then the electron is removed. The “native state” substrates are unreactive with each other, but simply adjusting their oxidation level by one electron enables a reaction to proceed.

5.9. Radical Conjugate Addition Reactions

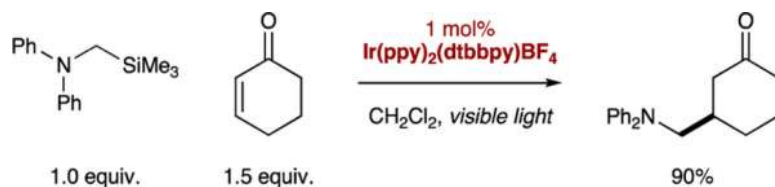
Zheng's [3 + 2] cycloaddition makes use of the inherent propensity of the cyclopropylamine radical cation to undergo fragmentation. As described in section 4.4, a more general reactivity mode of amine radical cations is deprotonation at the α -position to give α -amino radicals (eq 11).¹⁷⁰ Although these species often serve as intermediates on the path to iminium ions, they may also be employed as reactive intermediates in their own right to perform unique transformations. Strikingly, while iminium ions are potent electrophiles, α -amino radicals are potent nucleophiles. The inherent reactivity at the amine α -position may thus be reversed simply by adjusting the oxidation state. As highly nucleophilic radicals, α -amino radicals will



(11)

undergo conjugate addition to a variety of Michael acceptors. Pandey and Reiser have shown that *N*-phenyltetrahydroquino-line (**124**) reductively quenches the photoexcited species $^*\text{Ir}(\text{ppy})_2(\text{dtbbpy})^+$ to give $\text{Ir}^{\text{II}}(\text{ppy})_2(\text{dtbbpy})$ and the amine radical cation **125** (Scheme 73).¹⁷¹ Deprotonation at the benzylic position of **125** provides α -amino radical **337**, which adds to methyl vinyl ketone to give α -carbonyl radical **338**. Reduction of this species by $\text{Ir}^{\text{II}}(\text{ppy})(\text{dtbbpy})$ completes the photocatalytic cycle and upon protonation provides the conjugate addition product **339**. In addition to methyl vinyl ketone, a variety of α,β -unsaturated aldehydes, ketones, and esters may be employed. Nishibayashi and co-workers have additionally reported the conjugate addition of α -amino radicals generated by photoredox catalysis to alkylidene malonates.¹⁷²

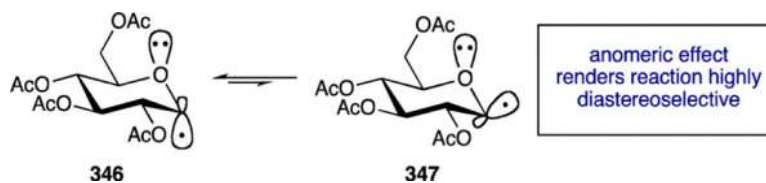
Conjugate additions of α -amino radicals have also been performed using α -silylamines, which upon single-electron oxidation undergo α -desilylation in preference to α -deprotonation.¹⁷³ The α -amino radicals thus generated were found to add to a range of enones (eq 12). The organic photocatalyst 9,10-dicyanoanthracene has also been extensively employed to promote conjugate addition reactions of α -amino radicals.¹⁷⁴



(12)

Analogous to α -amino radicals, carbon-centered α -alkoxy radicals possess a singly occupied molecular orbital (SOMO) adjacent to an oxygen atom, and are similarly stabilized by donation into the SOMO from an adjacent filled p orbital. However, whereas α -amino radicals are commonly generated by single-electron oxidation of the heteroatom followed by α -deprotonation, α -alkoxy radicals are difficult to generate in this way due to the high oxidation potential of ethers ($E_{1/2}^{\text{red}} = +3.1$ V for dimethylether).¹⁷⁵ Taking an alternative approach, Gagné and co-workers employed photoredox catalysis to generate α -alkoxy radicals via the single-electron reduction of α -glycosyl bromides, and they demonstrated that these species may undergo conjugate addition reactions.^{176,177} Under their conditions, reductive quenching of $^*\text{Ru}(\text{bpy})_3^{2+}$ by Hünig's base generates $\text{Ru}(\text{bpy})_3^+$, which is sufficiently reducing to donate an electron to α -glucosyl bromide **340** ($E_{1/2}^{\text{red}} = -1.27$ V vs SCE),¹⁷⁸ thereby generating α -alkoxy radical **341** (Scheme 74). Addition of this nucleophilic radical to methyl acrylate provides α -carbonyl radical **342**, which must accept an electron and a proton to give the conjugate addition product **343**. In the course of studies on this reaction, Gagné and co-workers observed a significant amount of double addition product, arising from addition of **342** to another equivalent of methyl acrylate. They found that generation of this product could be suppressed, and yields of the desired C-glycoside adduct **343** improved, by adding Hantzsch ester as a hydrogen atom source. Thus, radical **342** may be converted to product **343** either by abstracting a hydrogen atom from Hantzsch ester, abstracting a hydrogen atom from the Hünig's base radical cation, or undergoing reduction followed by protonation. In addition to methyl acrylate, a range of enones, enals, styrenes, and vinyl nitriles are all suitable Michael acceptors. Galactosyl and mannosyl bromides were also suitable substrates, providing access to C-glycosides **344** and **345**, respectively.

In all of these reactions, the product C-glycosides are formed exclusively as the α -anomers. This very high diastereoselectivity has been explained as arising from an anomeric effect. The pyramidal glycosyl radical may orient itself in one of two ways, shown as **346** and **347** (eq 13). In **346**, the lone pair on the endocyclic oxygen is in plane with the SOMO on the adjacent carbon and stabilizes this orientation via donation into the half-empty orbital.¹⁷⁹ In **347**, the SOMO is oriented out of plane of the lone pair on oxygen, and no such donation may occur, resulting in **346** being favored. Furthermore, donation into the SOMO renders glycosyl radical **346** more nucleophilic than **347**.¹⁸⁰ This combination of greater stability and nucleophilicity likely accounts for the excellent selectivities observed.



(13)

Photoredox radical conjugate addition reactions have found use in complex settings, with Overman employing such a reaction as a key step in the total synthesis of (–)-aplyviolene.¹⁸¹ Instead of an α -amino or α -alkoxy radical, however, the reactive species is a tertiary carbon-centered radical generated via single-electron reduction of an *N*-(acyloxy)phthalimide (see section 3). Under conditions similar to those employed by Gagne, the intermediate $\text{Ru}(\text{bpy})_3^+$ reduces *N*-(acyloxy)-phthalimide **348**, initiating fragmentation to yield tertiary radical **349** (Scheme 75). Conjugate addition of **349** to α -chlorocyclopentenone **350** proceeds to give an adduct α -carbonyl radical, which accepts a proton and an electron to give conjugate addition product **351** as a single diastereomer. Subsequent steps convert this α -chloroketone to the target (–)-aplyviolene. Notable in this example is the success of a radical strategy in forging the highly congested bond between adjacent quaternary and tertiary carbon stereocenters. Because glycosyl bromides and *N*-(acyloxy)phthalimides must undergo single-electron reduction to generate the reactive radicals, these reactions are net reductive, unlike the redox neutral conjugate addition reactions of α -amino radicals.

5.10. α -Arylation of Amines

In addition to their use as nucleophiles in conjugate addition reactions, α -amino radicals have also been exploited to perform the direct α -arylation of amines. We have recently reported that upon exposure to the photocatalyst $\text{Ir}(\text{ppy})_3$ and visible light, simple amines such as *N*-phenylpyrrolidine (**352**) react with benzonitriles such as 1,4-dicyanobenzene (**353**) to give benzylic amine products, where the α -position of the amine has undergone C–C bond formation with the ipso position of the benzonitrile, displacing cyanide as a leaving group (Scheme 76).^{182,183} The iridium photocatalyst $\text{Ir}(\text{ppy})_3$ undergoes photoexcitation to generate the strongly reducing $^*\text{Ir}(\text{ppy})_3$ ($E_{1/2}^{\text{IV}/*III} = -1.73$ V vs SCE).³⁸ This species is capable of reducing 1,4-dicyanobenzene ($E_{1/2}^{\text{red}} = -1.6$ V vs SCE)¹⁸⁴ to its radical anion (**354**) and in the process is oxidized to $\text{Ir}^{\text{IV}}(\text{ppy})_3$. This species acts as an oxidant ($E_{1/2}^{\text{IV}/III} = +0.77$ V vs SCE) to accept an electron from *N*-phenylpyrrolidine, completing the photocatalytic cycle and generating the amine radical cation **355**. Deprotonation of the radical cation by a base provides the α -amino radical **356**. At this point, it is postulated that the arene radical anion and the α -amino radical undergo radical–radical coupling to forge the C–C bond and generate adduct **357**. Aromatization via expulsion of cyanide then provides the benzylic amine product **358**.

This reaction was found to be applicable to the functionalization of a wide range of *N*-aryl amine substrates (Scheme 77A). In addition to *N*-phenylpyrrolidine, heterocyclic amines

such as *N*-phenylmorpholine and acyclic amines such as *N,N*-diethylaniline may be employed. Substitution on the aryl ring is tolerated, and an amine bearing the common *para*-methoxyphenyl (PMP) protecting group reacts in high yield. In examining the arene scope, it was found that benzonitriles bearing a second electron-withdrawing group are required, presumably so that the arene is sufficiently electron-deficient to undergo single-electron reduction. Thus, benzonitriles bearing esters and amides at the *para* position were found to be suitable substrates (Scheme 77B). Heteroaromatics such as 4-cyanopyridine, which are inherently electron-deficient, may also be employed. For certain five-membered heterocycles, a chloride substituent may function as the leaving group, enabling the installation of benzoxazole, *N*-Boc benzimidazole, and caffeine at the α -position of amines in good yield (Scheme 77C).

5.11. Hydrothiolation

Yoon has employed photoredox catalysis to achieve the anti-Markovnikov hydrothiolation of alkenes (or thiol–ene reaction).¹⁸⁵ The strongly oxidizing catalyst $\text{Ru}(\text{bpz})_3^{2+}$ is required for the success of this reaction and is proposed to oxidize the thiol **359** ($E_{1/2}^{\text{red}} = +0.83$ V vs SCE for benzyl mercaptan) to give the thiol radical cation **360** (Scheme 78).¹⁸⁶ Single-electron oxidation strongly acidifies the S–H bond ($\text{p}K_{\text{a}} = 2.4$ for the benzyl mercaptan radical cation), and deprotonation generates the electrophilic thiyl radical **361**. Addition of this species to the alkene proceeds in an anti-Markovnikov manner to give the more stable radical **362**. This adduct may abstract a hydrogen atom from another equivalent of thiol, providing the product thioether **363** and generating another molecule of thiyl radical **361**. Using this protocol, the hydrothiolation of a variety of styrenes, simple alkenes, and alkynes could be performed.¹⁸⁷

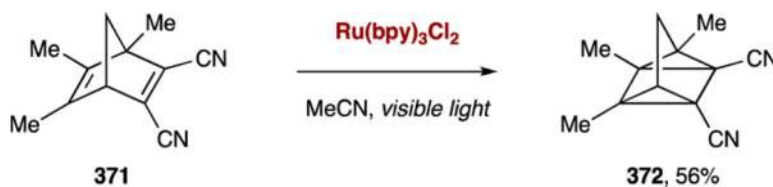
5.12. Generation of the Vilsmeier–Haack Reagent

A final application of redox-neutral photoredox catalysis is the generation of the Vilsmeier–Haack reagent (**364**), a species commonly used to perform formylation and nucleophilic displacement reactions. Stephenson and co-workers found that when tetrabromomethane was employed as a stoichiometric oxidant for $\text{Ru}(\text{bpy})_3^{2+}$ in *N,N*-dimethylformamide (DMF), alcohols are efficiently transformed into their corresponding bromides.¹⁸⁸ The reaction is believed to proceed first via single-electron reduction of tetrabromomethane to the tribromomethyl radical (**365**) (Scheme 79). Addition of this radical to a molecule of DMF furnishes stabilized radical **366**, which may be oxidized by $\text{Ru}(\text{bpy})_3^{3+}$ to give imidinium ion **367**. Attack of bromide ion on this species generates the Vilsmeier–Haack reagent (**364**) as well as COBr_2 , itself a reagent that reacts with DMF to give **364**. When an alcohol such as **368** is present, it may add either to the Vilsmeier–Haack reagent **364** or to its precursor **367**. The resulting imidinium **369** is then attacked by bromide in an $\text{S}_{\text{N}}2$ fashion, displacing DMF as a leaving group and generating alkyl bromide product **370**. This approach has subsequently been extended to the synthesis of symmetric anhydrides from the corresponding carboxylic acids.¹⁸⁹

6. ENERGY TRANSFER REACTIONS

The photoredox chemistry presented thus far relies on the ability of photoexcited catalysts (either organic or metal-based) to engage in electron transfer with organic molecules. A second, fundamental pathway for decay of photoexcited states, however, is energy transfer. Using $\text{Ru}(\text{bpy})_3^{2+}$ as an example, irradiation of this species excites the complex from its ground singlet state (S_0) to its lowest singlet excited state (S_1) (Scheme 80). Intersystem crossing (ISC) generates the long-lived lowest-energy triplet state (T_1). This triplet excited state of $\text{Ru}(\text{bpy})_3^{2+}$ may engage in electron transfer, but it may also engage in a process termed triplet–triplet energy transfer (TTET). In this process, decay of $^*\text{Ru}(\text{bpy})_3^{2+}$ from its triplet state to its ground singlet state promotes another molecule **A** from its ground singlet state S_0 to its lowest-energy triplet state T_1 .

Triplet–triplet energy transfer from visible light photo-catalysts such as $\text{Ru}(\text{bpy})_3^{2+}$ has thus far been employed to achieve only a handful of organic transformations. In an early example, this pathway has been used to convert the substituted norbornadiene **371** to quadricyclene **372** (eq 14).¹⁹⁰ Triplet–triplet energy transfer from $^*\text{Ru}(\text{bpy})_3^{2+}$ to the norbornadiene **371** promotes this species to its triplet state, which then undergoes bond rearrangement to give **372**. Electron-transfer pathways are not possible in this transformation, as the oxidation ($E_{1/2}^{+1/0} = +1.82$ V vs SCE) and reduction potentials ($E_{1/2}^{0/-1} = -1.39$ V vs SCE) of **371** indicate that reductive or oxidative quenching of $^*\text{Ru}(\text{bpy})_3^{2+}$ would both be severely disfavored. Furthermore, direct photoexcitation of **371** with UV light promotes the isomerization, suggesting that generation of an excited state, and not a different oxidation state, is the key to achieving reactivity. Similar reactions accomplished via triplet–triplet energy transfer from $\text{Ru}(\text{bpy})_3^{2+}$ and its analogues include the isomerization of *trans*-stilbene to *cis*-stilbene¹⁹¹ and the dimerization of anthracene.¹⁹²



(14)

Recently, Yoon has exploited triplet–triplet energy transfer to perform the [2 + 2] styrene cycloadditions that are a focus of work in his laboratory.¹⁹³ As discussed in section 5.6, these reactions have been accomplished under an electron-transfer manifold, but require that the styrene be sufficiently electron-rich (typically methoxy-substituted) to undergo single-electron oxidation to the corresponding radical cation. This limitation stimulated an attempt to perform these [2 + 2] cycloadditions via an energy transfer manifold. Toward this end, the iridium photocatalyst $\text{Ir}[\text{dF}(\text{CF}_3)\text{ppy}]_2(\text{dtbbpy})^+$ (see section 4.2) was identified as a potential energy transfer catalyst. This complex possesses an excited-state triplet energy of 61 kcal/mol,⁷⁷ suggesting that it may be capable of energy transfer to styrenes, which have triplet energies of approximately 60 kcal/mol.¹⁹⁴ Indeed, this catalyst was found to promote the [2 + 2] cycloaddition of electron-neutral styrene **373** to give cyclo-butane **374** in high

yield (Scheme 81). This reaction is not thought to proceed via electron transfer, as the iridium catalyst ($E_{1/2}^{*III/II} = +1.21$ V vs SCE)⁷⁷ is not sufficiently oxidizing to remove an electron from **373** ($E_{1/2}^{red} = +1.42$ V vs SCE). Also consistent with an energy transfer mechanism, catalysts that are more strongly oxidizing than Ir[dF(CF₃)ppy](dtbbpy)⁺, but that possess lower triplet state energies (E_T), such as Ru(bpy)₃²⁺ ($E_T = 46.8$ kcal/mol) and Ru(bpz)₃²⁺ ($E_T = 47.4$ kcal/mol),² do not catalyze the formation of **374**. In striking contrast with the electron-transfer-mediated [2 + 2] styrene cycloadditions, even highly electron-deficient systems such as a 4-nitrostyrene and a 2-pyridylstyrene efficiently undergo cycloaddition. Nonconjugated alkenes, however, are inert under these conditions, which may be rationalized on the basis of their higher triplet state energies. The cyclization of electron-rich styrene **375** additionally illustrates how electron and energy transfer pathways may provide access to orthogonal reactivity. When an electron-transfer pathway is employed, styrene **375** reacts via its radical cation to give the [4 + 2] adduct **376**. In contrast, Ir[dF(CF₃)ppy]₂(dtbbpy)⁺ promotes cyclization of **375** via an energy transfer pathway and provides cyclobutane **377** as the exclusive product.¹⁹⁵

Other approaches to utilizing energy transfer pathways have merged photocatalysis with transition metal catalysis.¹⁹⁶ Osawa and co-workers have introduced the ruthenium polypyridyl complex **378** as a “light-harvesting” ligand for transition metal catalysis (Scheme 82).¹⁹⁷ The Ru(bpy)₃²⁺ analogue, which they term **Pru**, bears a phenanthroline ligand with a diphenylphosphine group at the 3-position. This phosphine may then act as a ligand for transition metals, effectively forming a bridge between the photoactive ruthenium complex and the nonphotoactive transition metal. Osawa prepared a bimetallic ensemble by reacting **Pru**(PF₆)₂ with the ruthenium complex [CpRu(CH₃CN)₂(CO)]PF₆ (Cp = cyclopentadiene). The phosphine ligand displaces a molecule of acetonitrile, providing the bimetallic complex [CpRu(CH₃CN)(CO)(**Pru**)](PF₆)₃ (**379**). It was found that this complex is capable of catalyzing the trans to cis isomerization of 4-cyanostilbene, which is proposed to proceed via an intermediate complex **380** in which the nitrile of the stilbene substrate has replaced acetonitrile as a ligand on the metal. At this point, triplet–triplet energy transfer from the **Pru** ligand to the stilbene substrate (via the bridging ruthenium complex) is postulated to promote the isomerization event. High concentrations of acetonitrile strongly suppress trans to cis isomerization, presumably by occupying the coordination site at ruthenium where the substrate must bind; this suggests that the isomerization is promoted intramolecularly via complex **380** and not via intermolecular energy transfer from **Pru** to *trans*-4-cyano-stilbene.

Rather than link the photocatalyst to a metal center via a chelating phosphine ligand, Inagaki and co-workers have introduced bimetallic complexes in which a 2,2'-bipyrimidine ligand coordinates both a photoactive ruthenium center and a catalytically active palladium center.¹⁹⁸ Crucially, the presence of a second metal does not dramatically alter the photophysical properties of the ruthenium complex; like the mononuclear Ru(bpy)₃²⁺, these bimetallic species possess a MLCT band in the visible region. Remarkably, the binuclear Ru–Pd complex **381** has been identified as an efficient catalyst for the selective dimerization of α -methylstyrene (**382**, Scheme 83). In the presence of 2 mol % of the binuclear photocatalyst and visible light, the product 2,4-diphenyl-4-methyl-1-pentene (**383**) is

produced in high yield, and the formation of oligomerization and polymerization products is suppressed. The reaction does not proceed when the mononuclear compounds $\text{Ru}(\text{bpy})_3^{2+}$ and $[(\text{bpy})\text{PdMe}(\text{MeCN})]^+$ are used (either alone or as an equimolar mixture); combination of the two metal centers into a single complex is thus critical for reactivity.

The transformation is proposed to proceed first via migratory insertion of α -methylstyrene into the palladium–methyl bond of bimetallic complex **381** (Scheme 84). The alkylpalladium adduct **384** then undergoes β -hydride elimination to expel (*E*)-2-phenyl-2-butene (**385**) and furnish palladium hydride **386**. Migratory insertion of α -methylstyrene into this intermediate provides alkyl palladium species **387**. In support of this mechanism, Inagaki and co-workers were able to isolate the intermediate **387** by treating complex **381** with a large excess of α -methylstyrene. Critically, this intermediate could be formed in the dark, but could only be induced to react further and provide the product **383** upon irradiation with light. It is therefore postulated that photoexcitation at the ruthenium center of **387** promotes migratory insertion of a second equivalent of α -methylstyrene to give alkylpalladium **388**, presumably via energy transfer from the ruthenium center to the palladium center. Subsequent β -hydride elimination generates the product **383** and returns palladium hydride **386**, thus closing the catalytic cycle.¹⁹⁹ Together, these reports suggest that merging photoredox catalysis with the action of transition metal catalysts may provide access to unprecedented reactivity.

7. CONCLUSIONS

Although photoredox catalysis with transition metal complexes has only recently received widespread attention as a tool for synthetic organic chemists, it has already been applied to the development of a wide range of new carbon–carbon bond-forming reactions. The utility of photoredox catalysis arises not from its ability to promote any one kind of bond formation, but rather from its ability to generate a diverse array of reactive intermediates via single-electron transfer. As we have shown, these species include electrophilic α -carbonyl radicals, trifluoromethyl radicals, arene radical cations, iminium ions, and enone radical anions, among others. These intermediates have been used to develop reactions as varied as atom transfer radical additions, arene C–H functionalizations, amine α -functionalizations, and [2 + 2] cycloadditions. Furthermore, photoredox catalysis has been merged with other modes of catalytic activation, such as enamine catalysis and *N*-heterocyclic carbene catalysis, to achieve enantioselective transformations, and has been merged with transition metal catalysis to achieve previously elusive bond constructions.

Photoredox catalysis has also proven to be a valuable tool for the construction of complex molecules, as demonstrated by its application in the total syntheses of gliocladin C, heitziamide A, and aplyviolene, among others. In each of these syntheses, simple, typically inert functionalities in the starting materials are transformed into reactive intermediates upon single-electron oxidation or reduction. Particularly remarkable is the use of radical intermediates to forge congested quaternary carbon centers in the syntheses of gliocladin C and aplyviolene. Additionally, the challenges of performing photoredox catalysis efficiently on large scales have recently been addressed using continuous flow chemistry.²⁰⁰ The diverse applications of this chemistry, as well as the tremendous outpouring of work in the

area that has appeared since 2008, demonstrate that visible light photoredox catalysis has emerged as a powerful tool for the development of new and valuable transformations of organic molecules.

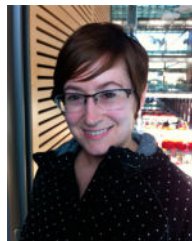
Acknowledgments

Financial support was provided by the NIH General Medical Sciences (Grant NIHGM5 R01 GM103558-01) and gifts from Merck, Amgen, Abbott, and Bristol-Myers Squibb.

Biography



Christopher K. Prier was born in Philadelphia, PA in 1987. He obtained his B.A. degree in Chemistry and Biochemistry in 2009 from the University of Pennsylvania, where he conducted undergraduate research in the laboratory of Professor Madeleine M. Joullie. In the same year, he began his graduate studies at Princeton University under the supervision of Professor David W. C. MacMillan. At Princeton he is engaged in the development of new chemical reactions using visible light photoredox catalysis, with a particular focus on the chemistry of α -amino radicals.



Danica A. Rankic was born in Calgary, Alberta, Canada in 1982. In 2004, she received her B.Sc. in Chemistry with distinction from the University of Calgary. She continued on to graduate studies at the University of Calgary in the laboratory of Professor Brian A. Keay studying the effect of ligand modification in asymmetric catalysis. She completed her Ph.D. in 2010 and then began her postdoctoral studies with Professor David W. C. MacMillan at Princeton University. Her research in the MacMillan group has focused on combining photoredox catalysis with amine catalysis, specifically with an interest in developing novel arylation methods.



David W. C. MacMillan was born in Bellshill, Scotland and received his undergraduate degree in chemistry at the University of Glasgow, where he worked with Dr. Ernie Colvin. In 1990, he left the U.K. to begin his doctoral studies under the direction of Professor Larry Overman at the University of California, Irvine. In 1996, he moved to a postdoctoral position with Professor David Evans at Harvard University, where his studies centered on enantioselective catalysis. He began his independent career at the University of California, Berkeley in July of 1998 before moving to the California Institute of Technology in June of 2000. In 2003, he was promoted to Full Professor at Caltech, before being appointed the Earle C. Anthony Chair of Organic Chemistry in 2004. In 2006, David moved to the east coast of the U.S. to take up a position at Princeton University as the A. Barton Hepburn Chair of Chemistry and Director of the Merck Center for Catalysis at Princeton University. He became the Princeton Chemistry Department Chair in July of 2010, and in July of 2011 became the James S. McDonnell Distinguished University Chair. David was recently inducted into the Fellowship of the Royal Society (2012) and elected to the American Academy of Arts and Sciences (2012). Research in the MacMillan group is centered on chemical synthesis with specific interests in new reaction development, enantioselective organocatalysis, and the rapid construction of molecular complexity.

ABBREVIATIONS

bpm	2,2'-bipyrimidine
bpy	2,2'-bipyridine
bpz	2,2'-bipyrazine
dap	2,9-bis(<i>p</i> -anisyl)-1,10-phenanthroline
dF(CF₃)ppy	2-(2,4-difluorophenyl)-5-trifluoromethylpyridine
dtbbpy	4,4-di- <i>tert</i> -butyl-2,2'-bipyridine
Fppy	2-(2,4-difluorophenyl)pyridine
ISC	intersystem crossing
menbpy	4,4'-dimenthoxycarbonyl-2,2'-bipyridine
MLCT	metal to ligand charge transfer
phen	phenanthroline
ppy	2-phenylpyridine

REFERENCES

1. Kalyanasundaram K. *Coord. Chem. Rev.* 1982; 46:159.
2. Juris A, Balzani V, Barigelletti F, Campagna S, Belser P, von Zelewsky A. *Coord. Chem. Rev.* 1988; 84:85.
3. Juris A, Balzani V, Belser P, von Zelewsky A. *Helv. Chim. Acta.* 1981; 64:2175.
4. a Grätzel M. *Acc. Chem. Res.* 1981; 14:376. b Meyer TJ. *Acc. Chem. Res.* 1989; 22:163.
5. Takeda H, Ishitani O. *Coord. Chem. Rev.* 2010; 254:346.
6. Kalyanasundaram K, Grätzel M. *Coord. Chem. Rev.* 1998; 77:347.
7. a Lowry MS, Bernhard S. *Chem.-Eur. J.* 2006; 12:7970. [PubMed: 16933348] b Ulbricht C, Beyer B, Friebe C, Winter A, Schubert US. *Adv. Mater.* 2009; 21:4418.
8. a Lalevée J, Blanchard N, Tehfe M-A, Morlet-Savary F, Fouassier JP. *Macromolecules.* 2010; 43:10191. b Lalevée J, Peter M, Dumur F, Gimes D, Blanchard N, Tehfe M-A, Morlet-Savary F, Fouassier JP. *Chem.-Eur. J.* 2011; 17:15027. [PubMed: 22124944] c Fors BP, Hawker CJ. *Angew. Chem., Int. Ed.* 2012; 51:8850.
9. Howerton BS, Heidary DK, Glazer EC. *J. Am. Chem. Soc.* 2012; 134:8324. [PubMed: 22553960]
10. a Renaud, P.; Sibi, MP., editors. *Radicals in Organic Synthesis.* Wiley-VCH; Weinheim, Germany: 2001. b Curran DP. *Synthesis.* 1988; 1988:417. c Curran DP. *Synthesis.* 1988; 1988:489.
11. Ischay MA, Anzovino ME, Du J, Yoon TP. *J. Am. Chem. Soc.* 2008; 130:12886. [PubMed: 18767798]
12. Nicewicz DA, MacMillan DWC. *Science.* 2008; 322:77. [PubMed: 18772399]
13. Narayanam JMR, Tucker JW, Stephenson CRJ. *J. Am. Chem. Soc.* 2009; 131:8756. [PubMed: 19552447]
14. Ischay MA, Yoon TP. *Eur. J. Org. Chem.* 2012:3359.
15. For reviews and perspectives on visible light photoredox catalysis: Zeitler K. *Angew. Chem., Int. Ed.* 2009; 48:9785. Yoon TP, Ischay MA, Du J. *Nature Chem.* 2010; 2:527. [PubMed: 20571569] Narayanam JMR, Stephenson CR. *J. Chem. Soc. Rev.* 2011; 40:102. Teply F. *Collect. Czech. Chem. Commun.* 2011; 76:859. Xuan J, Xiao W-J. *Angew. Chem., Int. Ed.* 2012; 51:6828. Shi L, Xia W. *Chem. Soc. Rev.* 2012; 41:7687. [PubMed: 22869017] Wallentin C-J, Nguyen JD, Stephenson CR. *J. Chimia.* 2012; 66:394.
16. For reviews on organic photocatalysis. a Fagnoni M, Dondi D, Ravelli D, Albini A. *Chem. Rev.* 2007; 107:2725. [PubMed: 17530909] b Pandey G. *Top. Curr. Chem.* 1993; 168:175. c Miranda MA, García H. *Chem. Rev.* 1994; 94:1063. d Fukuzumi S, Ohkubo K. *Chem. Sci.* 2013; 4:561.
17. Wang Y, Wang X, Antonietti M. *Angew. Chem., Int. Ed.* 2012; 51:68.
18. Kisch H. *Angew. Chem., Int. Ed.* 2013; 52:812.
19. Campagna S, Puntoriero F, Nastasi F, Bergamini G, Balzani V. *Top. Curr. Chem.* 2007; 280:117.
20. McCusker JK. *Acc. Chem. Res.* 2003; 36:876. [PubMed: 14674779]
21. Bock CR, Connor JA, Gutierrez AR, Meyer TJ, Whitten DG, Sullivan BP, Nagle JK. *J. Am. Chem. Soc.* 1979; 101:4815.
22. Throughout this Review, redox potentials are quoted against the saturated calomel electrode (SCE). In some cases, the referenced potentials have been determined versus different electrodes and have been converted to SCE for the purpose of comparison. For conversion constants, see: Pavlishchuk VV, Addison AW. *Inorg. Chim. Acta.* 2000; 298:97.
23. Tucker JW, Stephenson CRJ. *J. Org. Chem.* 2012; 77:1617. [PubMed: 22283525]
24. Turro, NJ. *Modern Molecular Photochemistry.* Benjamin/Cummings; Menlo Park, CA: 1978.
25. Pac C, Ihama M, Yasuda M, Miyauchi Y, Sakurai H. *J. Am. Chem. Soc.* 1981; 103:6495.
26. Tanner DD, Kharrat A, Oumar-Mahamat H. *Can. J. Chem.* 1990; 68:1662.
27. a Pac C, Miyauchi Y, Ishitani O, Ihama M, Yasuda M, Sakurai H. *J. Org. Chem.* 1984; 49:26. b Ishitani O, Ihama M, Miyauchi Y, Pac C. *J. Chem. Soc., Perkin Trans. 1.* 1985:1527.
28. Additional reports employed this system to achieve the reduction of activated carbonyls: Ishitani O, Pac C, Sakurai H. *J. Org. Chem.* 1983; 48:2941. Ishitani O, Yanagida S, Takamuku S, Pac C. *J. Org. Chem.* 1987; 52:2790.

29. Fukuzumi S, Mochizuki S, Tanaka T. *J. Phys. Chem.* 1990; 94:722.
30. Fukuzumi S, Koumitsu S, Hironaka K, Tanaka T. *J. Am. Chem. Soc.* 1987; 109:305.
31. Tanner DD, Singh HK. *J. Org. Chem.* 1986; 51:5182.
32. Hironaka K, Fukuzumi S, Tanaka T. *J. Chem. Soc., Perkin Trans. 2.* 1984:1705.
33. Kern J-M, Sauvage J-P. *J. Chem. Soc., Chem. Commun.* 1987:546.
34. Lawless JG, Bartak DE, Hawley MD. *J. Am. Chem. Soc.* 1969; 91:7121.
35. Wayner DDM, Dannenberg JJ, Griller D. *Chem. Phys. Lett.* 1986; 131:189.
36. Dinnocenzo JP, Banach TE. *J. Am. Chem. Soc.* 1989; 111:8646.
37. Nguyen JD, D'Amato EM, Narayanam JMR, Stephenson CRJ. *Nature Chem.* 2012; 4:854. [PubMed: 23001000]
38. Flamigni L, Barbieri A, Sabatini C, Ventura B, Barigelletti F. *Top. Curr. Chem.* 2007; 281:143.
39. Howes KR, Bakac A, Espenson JH. *Inorg. Chem.* 1988; 27:3147.
40. This reaction has been applied to the development of a one-pot deoxygenation of alcohols: Nguyen JD, Reiß B, Dai C, Stephenson CR. *J. Chem. Commun.* 2013 ASAP, DOI: 10.1039/C2CC37206A.
41. a Goren Z, Willner I. *J. Am. Chem. Soc.* 1983; 105:7764. b Maidan R, Goren Z, Becker JY, Willner I. *J. Am. Chem. Soc.* 1984; 106:6217. c Willner I, Goren Z, Mandler D, Maidan R, Degani Y. *J. Photochem.* 1985; 28:215.
42. Bockman TM, Kochi JK. *J. Org. Chem.* 1990; 55:4127.
43. The reduction of vicinal dibromides to olefins using Ru(bpy)₃²⁺ alone has been reported: Willner I, Tsfania T, Eichen Y. *J. Org. Chem.* 1990; 55:2656. For a similar reaction, see: Maji T, Karmakar A, Reiser O. *J. Org. Chem.* 2011; 76:736. [PubMed: 21192632]
44. The merger of photoredox and viologen catalysis has also been applied to the reduction of carbonyls: Herance JR, Ferrer B, Bourdelande JL, Marquet J, Garcia H. *Chem.-Eur. J.* 2006; 12:3890. [PubMed: 16521136]
45. Maidan R, Willner I. *J. Am. Chem. Soc.* 1986; 108:1080.
46. a Mandler D, Willner I. *J. Am. Chem. Soc.* 1984; 106:5352. b Mandler D, Willner I. *J. Chem. Soc., Perkin Trans. 2.* 1986:805. c Mandler D, Willner I. *J. Chem. Soc., Chem. Commun.* 1986:851.
47. a Hedstrand DM, Kruizinga WM, Kellogg RM. *Tetrahedron Lett.* 1978; 19:1255. b van Bergen TJ, Hedstrand DM, Kruizinga WH, Kellogg RM. *J. Org. Chem.* 1979; 44:4953.
48. Zhu X-Q, Li H-R, Li Q, Ai T, Lu J-Y, Yang Y, Cheng J-P. *Chem.-Eur. J.* 2003; 9:871. [PubMed: 12584702]
49. Nakamura K, Fujii M, Mekata H, Oka S, Ohno A. *Chem. Lett.* 1986:87.
50. Hirao T, Shiori J, Okahata N. *Bull. Chem. Soc. Jpn.* 2004; 77:1763.
51. Gazi S, Ananthakrishnan R. *Appl. Catal., B.* 2011; 105:317.
52. Chen Y, Kamlet AS, Steinman JB, Liu DR. *Nat. Chem.* 2011; 3:146. [PubMed: 21258388]
53. Willner I, Ford WE, Otvos JW, Calvin M. *Nature.* 1979; 280:823.
54. Zhu M, Zheng N. *Synthesis.* 2011; 14:2223. [PubMed: 23543799]
55. a Crutchley RJ, Lever ABP. *J. Am. Chem. Soc.* 1980; 102:7128. b Haga M-A, Dodsworth ES, Eryavec G, Seymour P, Lever ABP. *Inorg. Chem.* 1985; 24:1901.
56. Photoredox catalysis has also been employed to reduce nitroalkenes to oximes: Tomioka H, Ueda K, Ohi H, Izawa Y. *Chem. Lett.* 1986:1359.
57. Tucker JW, Nguyen JD, Narayanam JMR, Krabbe SW, Stephenson CRJ. *Chem. Commun.* 2010; 46:4985.
58. For the synthesis and photophysical properties of Ir(ppy)₂(dtbbpy)PF₆: Slinker JD, Gorodetsky AA, Lowry MS, Wang J, Parker S, Rohl R, Bernhard S, Malliaras GG. *J. Am. Chem. Soc.* 2004; 126:2763. [PubMed: 14995193]
59. For another report on this reaction type: Kim H, Lee C. *Angew. Chem., Int. Ed.* 2012; 51:12303.
60. Tucker JW, Stephenson CRJ. *Org. Lett.* 2011; 13:5468. [PubMed: 21939250]
61. Larraufie M-H, Pellet R, Fensterbank L, Goddard J-P, Lacôte E, Malacria M, Ollivier C. *Angew. Chem., Int. Ed.* 2011; 50:4463.

62. Hasegawa et al. have also reported the reductive ring-opening of α -ketoepoxides using $\text{Ru}(\text{bpy})_3^{2+}$ and dimethylbenzimidazoles as stoichiometric reductants: Hasegawa E, Takizawa S, Seida T, Yamaguchi A, Yamaguchi N, Chiba N, Takahashi T, Ikeda H, Akiyama K. *Tetrahedron*. 2006; 62:6581.
63. a Guindon Y, Jung G, Guérin B, Ogilvie WW. *Synlett*. 1998:213.b Guindon Y, Guérin B, Chabot C, Mackintosh N, Ogilvie WW. *Synlett*. 1995:449.
64. a Okada K, Okamoto K, Morita N, Okubo K, Oda M. *J. Am. Chem. Soc.* 1991; 113:9401.b Okada K, Okubo K, Morita N, Oda M. *Chem. Lett.* 1993:2021.c Okada K, Okubo K, Morita N, Oda M. *Tetrahedron Lett.* 1992; 33:7377.
65. Edson JB, Spencer LP, Boncella JM. *Org. Lett.* 2011; 13:6156. [PubMed: 22046963]
66. a Sundararajan C, Falvey DE. *J. Am. Chem. Soc.* 2005; 127:8000. [PubMed: 15926809] b Borak JB, Falvey DE. *J. Org. Chem.* 2009; 74:3894. [PubMed: 19361187]
67. Boncella and co-workers have exploited this photoredox deprotection protocol to achieve in situ vesicle formation upon cleavage of long-chain N-methylpicolinium esters: DeClue MS, Monnard P-A, Bailey JA, Maurer SE, Collis GE, Ziock H-J, Rasmussen S, Boncella JM. *J. Am. Chem. Soc.* 2009; 131:931. [PubMed: 19115944]
68. Zlotorzynska M, Sammis GM. *Org. Lett.* 2011; 13:6264. [PubMed: 22060120]
69. Cano-Yelo H, Deronzier A. *Tetrahedron Lett.* 1984; 25:5517.
70. a Allongue P, Delamar M, Desbat B, Fagebaume O, Hitmi R, Pinson J, Savéant J-M. *J. Am. Chem. Soc.* 1997; 119:201.b Galli C. *Chem. Rev.* 1988; 88:765.
71. Su Y, Zhang L, Jiao N. *Org. Lett.* 2011; 13:2168. [PubMed: 21446682]
72. Recupero F, Punta C. *Chem. Rev.* 2007; 107:3800. [PubMed: 17848093]
73. Zou Y-Q, Chen J-R, Liu X-P, Lu L-Q, Davis RL, Jørgensen KA, Xiao W-J. *Angew. Chem., Int. Ed.* 2012; 51:784.
74. Cheng Y, Yang J, Qu Y, Li P. *Org. Lett.* 2012; 14:98. [PubMed: 22146071]
75. a Conrad JC, Kong J, Laforteza BN, MacMillan DWC. *J. Am. Chem. Soc.* 2009; 131:11640. [PubMed: 19639997] b Inamoto K, Hasegawa C, Hiroya K, Doi T. *Org. Lett.* 2008; 10:5147. [PubMed: 18947183] c Joyce LL, Batey RA. *Org. Lett.* 2009; 11:2792. [PubMed: 19476320] d Inamoto K, Hasegawa C, Kawasaki J, Hiroya K, Doi T. *Adv. Synth. Catal.* 2010; 352:2643.
76. Tucker JW, Narayanam JMR, Shah PS, Stephenson CRJ. *Chem. Commun.* 2011; 47:5040.
77. Lowry MS, Goldsmith JJ, Slinker JD, Rohl R, Pascal RA, Malliaras GG, Bernhard S. *Chem. Mater.* 2005; 17:5712.
78. Murayama E, Kohda A, Sato T. *J. Chem. Soc., Perkin Trans. 1*. 1980:947.
79. Lechner R, König B. *Synthesis*. 2010:1712.
80. a Bauer EB. *Chem. Soc. Rev.* 2012; 41:3153. [PubMed: 22306968] b Herrero S, Usón MA. *J. Chem. Educ.* 1995; 72:1065.
81. a Hamada T, Ishida H, Usui S, Watanabe Y, Tsumura K, Ohkubo K. *J. Chem. Soc., Chem. Commun.* 1993:909.b Hamada T, Ishida H, Usui S, Tsumura K, Ohkubo K. *J. Mol. Catal.* 1994; 88:L1.
82. a Fancy DA, Kodadek T. *Proc. Natl. Acad. Sci. U.S.A.* 1999; 96:6020. [PubMed: 10339534] b Kim K, Fancy DA, Carney D, Kodadek T. *J. Am. Chem. Soc.* 1999; 121:11896.c Fancy DA, Denison C, Kim K, Xie Y, Holdeman T, Amini F, Kodadek T. *Chem. Biol.* 2000; 7:697. [PubMed: 10980450] d Amini F, Denison C, Lin H-J, Kuo L, Kodadek T. *Chem. Biol.* 2003; 10:1115. [PubMed: 14652079] e Denison C, Kodadek T. *J. Proteome Res.* 2004; 3:417. [PubMed: 15253422] f Kodadek T, Duroux-Richard I, Bonnafous J-C. *Trends Pharmacol. Sci.* 2005; 26:210. [PubMed: 15808346]
83. Parker VD, Tilset M. *J. Am. Chem. Soc.* 1991; 113:8778.
84. Condie AG, González-Gómez JC, Stephenson CRJ. *J. Am. Chem. Soc.* 2010; 132:1464. [PubMed: 20070079]
85. Vicinal diamines have also been employed as substrates in photoredox aza-Henry reactions; iminium generation occurs upon C–C bond cleavage of the amine radical cation: Cai S, Zhao X, Wang X, Liu Q, Li Z, Wang DZ. *Angew. Chem., Int. Ed.* 2012; 51:8050.
86. Rueping M, Zhu S, Koenigs RM. *Chem. Commun.* 2011; 47:12709.

87. Zhao G, Yang C, Guo L, Sun H, Chen C, Xia W. *Chem. Commun.* 2012; 48:2337.
88. Rueping M, Vila C, Koenigs RM, Poschorny K, Fabry DC. *Chem. Commun.* 2011; 47:2360.
89. Rueping M, Zhu S, Koenigs RM. *Chem. Commun.* 2011; 47:8679.
90. Freeman DB, Furst L, Condie AG, Stephenson CRJ. *Org. Lett.* 2012; 14:94. [PubMed: 22148974]
91. For the α -arylation of α -amino carbonyls: Wang Z-Q, Hu M, Huang X-C, Gong L-B, Xie Y-X, Li J-H. *J. Org. Chem.* 2012; 77:8705. [PubMed: 22985461] Zhu S, Rueping M. *Chem. Commun.* 2012; 48:11960.
92. Rueping M, Koenigs RM, Poschorny K, Fabry DC, Leonori D, Vila C. *Chem.-Eur. J.* 2012; 18:5170. [PubMed: 22431393]
93. a Pan Y, Wang S, Kee CW, Dubuisson E, Yang Y, Loh KP, Tan C-H. *Green Chem.* 2011; 13:3341. b Fu W, Guo W, Zou G, Xu C. *J. Fluorine Chem.* 2012; 140:88.
94. a Hari DP, König B. *Org. Lett.* 2011; 13:3852. [PubMed: 21744842] b Pan Y, Kee CW, Chen L, Tan C-H. *Green Chem.* 2011; 13:2682. c Liu Q, Li Y-N, Zhang H-H, Chen B, Tung C-H, Wu L-Z. *Chem.-Eur. J.* 2012; 18:620. [PubMed: 22162148]
95. Mitkina T, Stanglmair C, Setzer W, Gruber M, Kisch H, König B. *Org. Biomol. Chem.* 2012; 10:3556. [PubMed: 22447128]
96. Xuan J, Cheng Y, An J, Lu L-Q, Zhang X-X, Xiao W-J. *Chem. Commun.* 2011; 47:8337.
97. Xuan J, Feng Z-J, Duan S-W, Xiao W-J. *RSC Adv.* 2012; 2:4065.
98. Hall LR, Iwamoto RT, Hanzlik RP. *J. Org. Chem.* 1989; 54:2446.
99. Seo ET, Nelson RF, Fritsch JM, Marcoux LS, Leedy DW, Adams RN. *J. Am. Chem. Soc.* 1966; 88:3498.
100. Dai C, Meschini F, Narayanam JMR, Stephenson CRJ. *J. Org. Chem.* 2012; 77:4425. [PubMed: 22458307]
101. DiRocco DA, Rovis T. *J. Am. Chem. Soc.* 2012; 134:8094. [PubMed: 22548244]
102. a Zou Y-Q, Lu L-Q, Fu L, Chang N-J, Rong J, Chen J-R, Xiao W-J. *Angew. Chem., Int. Ed.* 2011; 50:7171. b Rueping M, Leonori D, Poisson T. *Chem. Commun.* 2011; 47:9615.
103. Maity S, Zheng N. *Angew. Chem., Int. Ed.* 2012; 51:9562.
104. Cyclization rates of aminium radical cations are known to be significantly greater than those of the corresponding deprotonated aminyl radicals, see Table 4 of: Horner JH, Musa OM, Bouvier A, Newcomb M. *J. Am. Chem. Soc.* 1998; 120:7738.
105. For reviews on atom transfer radical addition: Curran DP. *Synthesis.* 1988; 7:489. Clark AJ. *Chem. Soc. Rev.* 2002; 31:1. [PubMed: 12108978] Pintauer T, Matyjaszewski K. *Chem. Soc. Rev.* 2008; 37:1087. [PubMed: 18497922]
106. Barton DHR, Csiba MA, Jaszberenyi JC. *Tetrahedron Lett.* 1994; 35:2869.
107. a Nguyen JD, Tucker JW, Konieczynska MD, Stephenson CRJ. *J. Am. Chem. Soc.* 2011; 133:4160. [PubMed: 21381734] b Wallentin C-J, Nguyen JD, Finkbeiner P, Stephenson CRJ. *J. Am. Chem. Soc.* 2012; 134:8875. [PubMed: 22486313]
108. Wayner DDM, Houmam A. *Acta Chem. Scand.* 1998; 52:377.
109. Pirtsch M, Paria S, Matsuno T, Isobe H, Reiser O. *Chem.-Eur. J.* 2012; 18:7336. [PubMed: 22581462]
110. For the synthesis of trifluoromethyl alkenes via an ATRA pathway: Iqbal N, Choi S, Kim E, Cho EJ. *J. Org. Chem.* 2012; 77:11383. [PubMed: 23167602]
111. a MacMillan DWC. *Nature.* 2008; 455:304. [PubMed: 18800128] b Mukherjee S, Yang JW, Hoffmann S, List B. *Chem. Rev.* 2007; 107:5471. [PubMed: 18072803]
112. Nagib DA, Scott ME, MacMillan DWC. *J. Am. Chem. Soc.* 2009; 131:10875. [PubMed: 19722670]
113. a Müller K, Faeh C, Diederich F. *Science.* 2007; 317:1881. [PubMed: 17901324] b Purser S, Moore PR, Swallow S, Gouverneur V. *Chem. Soc. Rev.* 2008; 37:320. [PubMed: 18197348] c Hagmann WK. *J. Med. Chem.* 2008; 51:4359. [PubMed: 18570365]
114. Bonesi SM, Erra-Balsells RJ. *Chem. Soc., Perkin Trans. 2.* 2000:1583.
115. Shih H-W, Vander Wal MN, Grange RL, MacMillan DWC. *J. Am. Chem. Soc.* 2010; 132:13600. [PubMed: 20831195]

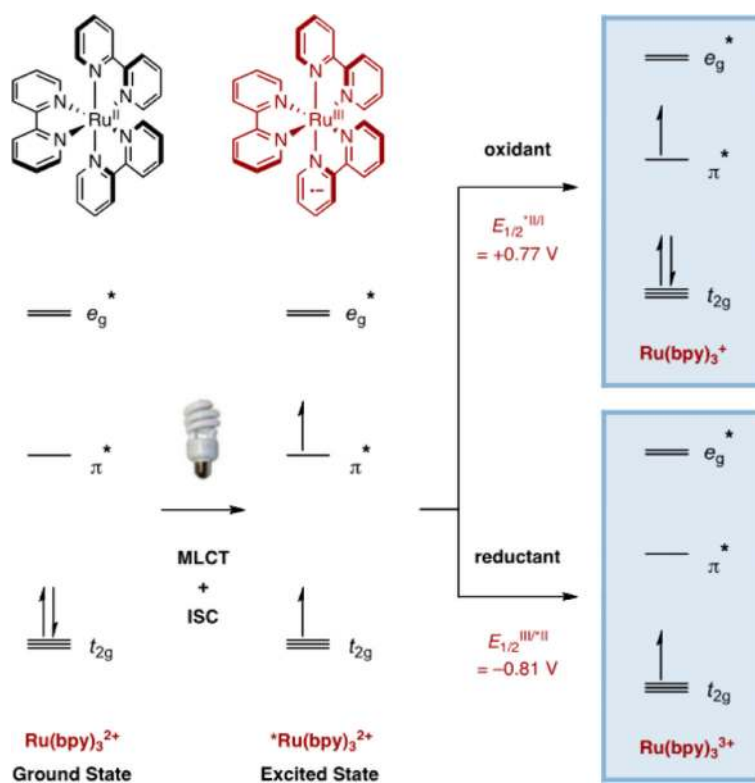
116. Neumann M, Földner S, König B, Zeitler K. *Angew. Chem., Int. Ed.* 2011; 50:951.
117. Cherevatskaya M, Neumann M, Földner S, Harlander C, Kümmel S, Dankesreiter S, Pfitzner A, Zeitler K, König B. *Angew. Chem., Int. Ed.* 2012; 51:4062.
118. a Cano-Yelo H, Deronzier A. *J. Chem. Soc., Perkin Trans. 2.* 1984:1093. b Cano-Yelo H, Deronzier A. *J. Photochem.* 1987; 37:315.
119. Hari DP, Schroll P, König B. *J. Am. Chem. Soc.* 2012; 134:2958. [PubMed: 22296099]
120. For the transition metal-catalyzed Meerwein arylation. a Meerwein H, Büchner E, van Emster K. *J. Prakt. Chem.* 1939; 152:237. b Kochi JK. *J. Am. Chem. Soc.* 1957; 79:2942. c Wetzel A, Pratsch G, Kolb R, Heinrich MR. *Chem.-Eur. J.* 2010; 16:2547. [PubMed: 20066707]
121. Kalyani D, McMurtrey KB, Neufeldt SR, Sanford MS. *J. Am. Chem. Soc.* 2011; 133:18566. [PubMed: 22047138]
122. Lyons TW, Sanford MS. *Chem. Rev.* 2010; 110:1147. [PubMed: 20078038]
123. Kalyani D, Deprez NR, Desai LV, Sanford MS. *J. Am. Chem. Soc.* 2005; 127:7330. [PubMed: 15898779]
124. Deprez NR, Sanford MS. *J. Am. Chem. Soc.* 2009; 131:11234. [PubMed: 19621899]
125. a Tucker JW, Narayanam JMR, Krabbe SW, Stephenson CR. *J. Org. Lett.* 2010; 12:368. b Furst L, Matsuura BS, Narayanam JMR, Tucker JW, Stephenson CR. *J. Org. Lett.* 2010; 12:3104. [PubMed: 20518528]
126. Furst L, Narayanam JMR, Stephenson CR. *Angew. Chem., Int. Ed.* 2011; 50:9655.
127. Ju X, Liang Y, Jia P, Li W, Yu W. *Org. Biomol. Chem.* 2012; 10:498. [PubMed: 22120821]
128. Nagib DA, MacMillan DWC. *Nature.* 2011; 480:224. [PubMed: 22158245]
129. Young RC, Meyer TJ, Whitten DG. *J. Am. Chem. Soc.* 1976; 98:286.
130. Iqbal N, Choi S, Ko E, Cho EJ. *Tetrahedron Lett.* 2012; 53:2005.
131. Ye Y, Sanford MS. *J. Am. Chem. Soc.* 2012; 134:9034. [PubMed: 22624669]
132. a Chu L, Qing F-L. *Org. Lett.* 2010; 12:5060. [PubMed: 20923196] b Senecal TD, Parsons AT, Buchwald SL. *J. Org. Chem.* 2011; 76:1174. [PubMed: 21235259] c Jiang X, Chu L, Qing F-L. *J. Org. Chem.* 2012; 77:1251. [PubMed: 22251059]
133. Xu J, Luo D-F, Xiao B, Liu Z-J, Gong T-J, Fu Y, Liu L. *Chem. Commun.* 2011; 47:4300.
134. Liu T, Shen Q. *Org. Lett.* 2011; 13:2342. [PubMed: 21473568]
135. Rao H, Wang P, Li C-J. *Eur. J. Org. Chem.* 2012:6503.
136. Photoredox catalysis has also been applied to the 3-sulfonylation of N-methylindoles: Chen M, Huang Z-T, Zheng Q-Y. *Chem. Commun.* 2012; 48:11686.
137. Schroll P, Hari DP, König B. *ChemistryOpen.* 2012; 1:130. [PubMed: 24551500]
138. Hering T, Hari DP, König B. *J. Org. Chem.* 2012; 77:10347. [PubMed: 23101908]
139. Eosin Y has been employed in a synthesis of benzothiophenes from o-methylthio-arene diazonium salts and alkynes: Hari DP, Hering T, König B. *Org. Lett.* 2012; 14:5334. [PubMed: 23039199]
140. Pham PV, Nagib DA, MacMillan DWC. *Angew. Chem., Int. Ed.* 2011; 50:6119.
141. a Cho DW, Lee H-Y, Oh SW, Choi JH, Park HJ, Mariano PS, Yoon UC. *J. Org. Chem.* 2008; 73:4539. [PubMed: 18494523] b Fukuzumi S, Fujita M. *J. Org. Chem.* 1993; 58:5405. c Fukuzumi S, Fujita M, Matsubayashi G, Otera J. *Chem. Lett.* 1993:1451. d Fujita M, Fukuzumi S, Matsubayashi G, Otera J. *Bull. Chem. Soc. Jpn.* 1996; 69:1107.
142. Yasu Y, Koike T, Akita M. *Angew. Chem., Int. Ed.* 2012; 51:9567.
143. Courant T, Masson G. *Chem.-Eur. J.* 2012; 18:423. [PubMed: 22161892]
144. For another report on the alkylation of enamides and enecarbamates: Jiang H, Huang C, Guo J, Zeng C, Zhang Y, Yu S. *Chem.-Eur. J.* 2012; 18:15158. [PubMed: 23018775]
145. Um JM, Gutierrez O, Schoenebeck F, Houk KN, MacMillan DWC. *J. Am. Chem. Soc.* 2010; 132:6001. [PubMed: 20387888]
146. a Narasaka K, Okauchi T, Tanaka K, Murakami M. *Chem. Lett.* 1992:2099. b Beeson TD, Mastracchio A, Hong J-B, Ashton K, MacMillan DWC. *Science.* 2007; 316:582. [PubMed: 17395791]
147. Yasu Y, Koike T, Akita M. *Chem. Commun.* 2012; 48:5355.
148. Koike T, Akita M. *Chem. Lett.* 2009; 38:166.

149. A number of similar photoredox α -oxidation reactions have been reported: Liu H, Feng W, Kee CW, Zhao Y, Leow D, Pan Y, Tan C-H. *Green Chem.* 2010; 12:953. Yoon H-S, Ho X-H, Jang J, Lee H-J, Kim S-J, Jang H-Y. *Org. Lett.* 2012; 14:3272. [PubMed: 22681592] Koike T, Yasu Y, Akita M. *Chem. Lett.* 2012; 41:999.
150. a Baik T-G, Luis AL, Wang L-C, Krische MJ. *J. Am. Chem. Soc.* 2001; 123:6716. [PubMed: 11439068] b Wang L-C, Jang H-Y, Roh Y, Lynch V, Schultz AJ, Wang X, Krische MJ. *J. Am. Chem. Soc.* 2002; 124:9448. [PubMed: 12167039] c Roh Y, Jang H-Y, Lynch V, Bauld NL, Krische MJ. *Org. Lett.* 2002; 4:611. [PubMed: 11843604] d Yang J, Felton GAN, Bauld NL, Krische MJ. *J. Am. Chem. Soc.* 2004; 126:1634. [PubMed: 14871085] e Yang J, Cauble DF, Berro AJ, Bauld NL, Krische MJ. *J. Org. Chem.* 2004; 69:7979. [PubMed: 15527279] f Felton GAN, Bauld NL. *Tetrahedron Lett.* 2004; 45:8465. g Felton GAN, Bauld NL. *Tetrahedron.* 2004; 60:10999.
151. Du J, Yoon TP. *J. Am. Chem. Soc.* 2009; 131:14604. [PubMed: 19473018]
152. Tyson EL, Farney EP, Yoon TP. *Org. Lett.* 2012; 14:1110. [PubMed: 22320352]
153. Du J, Espelt LR, Guzei IA, Yoon TP. *Chem. Sci.* 2011; 2:2115. [PubMed: 22121471]
154. a Pandey G, Hajra S. *Angew. Chem., Int. Ed. Engl.* 1994; 33:1169. b Pandey G, Hajra S, Ghorai MK, Kumar KR. *J. Am. Chem. Soc.* 1997; 119:8777.
155. Zhao G, Yang C, Guo L, Sun H, Lin R, Xia W. *J. Org. Chem.* 2012; 77:6302. [PubMed: 22731518]
156. a Bauld NL, Bellville DJ, Harirchian B, Lorenz KT, Pabon RA Jr, Reynolds DW, Wirth DD, Chiou H-S, Marsh BK. *Acc. Chem. Res.* 1987; 20:371. b Bauld NL. *Tetrahedron.* 1989; 45:5307.
157. Ischay MA, Lu Z, Yoon TP. *J. Am. Chem. Soc.* 2010; 132:8572. [PubMed: 20527886]
158. Yueh W, Bauld NL. *J. Phys. Org. Chem.* 1996; 9:529.
159. Ischay MA, Ament MS, Yoon TP. *Chem. Sci.* 2012; 3:2807. [PubMed: 22984640]
160. Hunziker M, Ludi A. *J. Am. Chem. Soc.* 1977; 99:7370.
161. Rillema DP, Allen G, Meyer TJ, Conrad D. *Inorg. Chem.* 1983; 22:1617.
162. Hurtley AE, Cismesia MA, Ischay MA, Yoon TP. *Tetrahedron.* 2011; 67:4442. [PubMed: 21666769]
163. Lin S, Ischay MA, Fry CG, Yoon TP. *J. Am. Chem. Soc.* 2011; 133:19350. [PubMed: 22032252]
164. Lin S, Padilla CE, Ischay MA, Yoon TP. *Tetrahedron Lett.* 2012; 53:3073. [PubMed: 22711942]
165. Parrish JD, Ischay MA, Lu Z, Guo S, Peters NR, Yoon TP. *Org. Lett.* 2012; 14:1640. [PubMed: 22372647]
166. Griller D, Ingold KU. *Acc. Chem. Res.* 1980; 13:317.
167. Lu Z, Shen M, Yoon TP. *J. Am. Chem. Soc.* 2011; 133:1162. [PubMed: 21214249]
168. For reports on the reductive opening of cyclopropyl ketones: Norin T. *Acta Chem. Scand.* 1965; 19:1289. Dauben WG, Deviny EJ. *J. Org. Chem.* 1966; 31:3794. Tanko JM, Drumright RE. *J. Am. Chem. Soc.* 1990; 112:5362.
169. Maity S, Zhu M, Shinabery RS, Zheng N. *Angew. Chem., Int. Ed.* 2012; 51:222.
170. For reviews on the chemistry of α -amino radicals: Chow YL, Danen WC, Nelsen SF, Rosenblatt DH. *Chem. Rev.* 1978; 78:243. Renaud P, Giraud L. *Synthesis.* 1996:913.
171. Kohls P, Jadhav D, Pandey G, Reiser O. *Org. Lett.* 2012; 14:672. [PubMed: 22260623]
172. Miyake Y, Nakajima K, Nishibayashi Y. *J. Am. Chem. Soc.* 2012; 134:3338. [PubMed: 22296639]
173. Miyake Y, Ashida Y, Nakajima K, Nishibayashi Y. *Chem. Commun.* 2012; 48:6966.
174. a Yoon UC, Mariano PS. *Acc. Chem. Res.* 1992; 25:233. b Xu W, Jeon YT, Hasegawa E, Yoon UC, Mariano PS. *J. Am. Chem. Soc.* 1989; 111:406. c Jeon YT, Lee C-P, Mariano PS. *J. Am. Chem. Soc.* 1991; 113:8847. d Xu W, Zhang X-M, Mariano PS. *J. Am. Chem. Soc.* 1991; 113:8863.
175. Albin A, Mella M, Freccero M. *Tetrahedron.* 1994; 50:575.
176. a Andrews RS, Becker JJ, Gagné MR. *Angew. Chem., Int. Ed.* 2010; 49:7274. b Andrews RS, Becker JJ, Gagné MR. *Org. Lett.* 2011; 13:2406. [PubMed: 21473567]

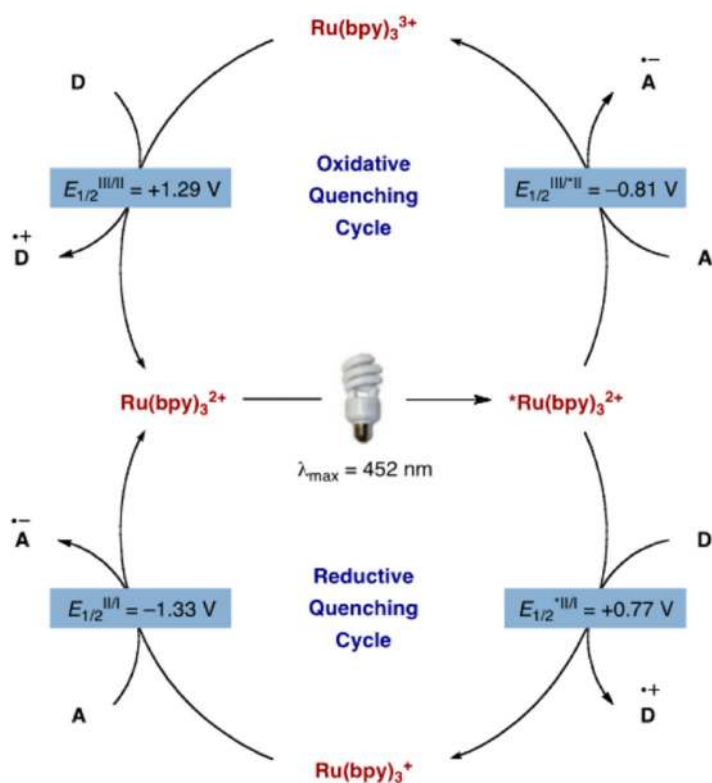
177. For tin hydride-promoted reactions of glycosyl radicals: Giese B, Dupuis J. *Angew. Chem., Int. Ed. Engl.* 1983; 22:622. Adlington RM, Baldwin JE, Basak A, Kozyrod RP. *J. Chem. Soc., Chem. Commun.* 1983:944.
178. Rondinini SB, Mussini PR, Crippa F, Sello G. *Electrochem. Commun.* 2000; 2:491.
179. Gilbert BC, Trenwith M, Dobbs AJ. *J. Chem. Soc., Perkin Trans. 2.* 1974:1772. Malatesta V, Ingold KU. *J. Am. Chem. Soc.* 1981; 103:609. Giese B, Dupuis J. *Tetrahedron Lett.* 1984; 25:1349. For evidence of a boat-like conformation of glycosyl radicals: Dupuis J, Giese B, Rüegge D, Fischer H, Korth H-G, Sustmann R. *Angew. Chem., Int. Ed. Engl.* 1984; 23:896.
180. Giese B, Dupuis J, Haßkerl T, Meixner J. *Tetrahedron Lett.* 1983; 24:703.
181. Schnermann MJ, Overman LE. *Angew. Chem., Int. Ed.* 2012; 51:9576.
182. McNally A, Prier CK, MacMillan DWC. *Science.* 2011; 334:1114. [PubMed: 22116882]
183. For precedent on this reaction type: Ohashi M, Miyake K. *Chem. Lett.* 1977:615. Ohashi M, Miyake K, Tsujimoto K. *Bull. Chem. Soc. Jpn.* 1980; 53:1683. Yamada S, Nakagawa Y, Watabiki O, Suzuki S, Ohashi M. *Chem. Lett.* 1986:361. Hasegawa E, Brumfield MA, Mariano PS. *J. Org. Chem.* 1988; 53:5435.
184. Wakasa M, Sakaguchi Y, Nakamura J, Hayashi H. *J. Phys. Chem.* 1992; 96:9651.
185. Tyson EL, Ament MS, Yoon TP. *J. Org. Chem.* 2012 ASAP. DOI: 10.1021/jo3020825.
186. Bordwell FG, Zhang X-M, Satish AV, Cheng J-P. *J. Am. Chem. Soc.* 1994; 116:6605.
187. Hydroetherification reactions have also been achieved using organic visible light photocatalysis: Hamilton DS, Nicewicz DA. *J. Am. Chem. Soc.* 2012; 134:18577. [PubMed: 23113557]
188. Dai C, Narayanam JMR, Stephenson CRJ. *Nat. Chem.* 2011; 3:140. [PubMed: 21258387]
189. Konieczynska MD, Dai C, Stephenson CRJ. *Org. Biomol. Chem.* 2012; 10:4509. [PubMed: 22573373]
190. Ikezawa H, Kutal C, Yasufuku K, Yamazaki H. *J. Am. Chem. Soc.* 1986; 108:1589.
191. Wrighton M, Markham J. *J. Phys. Chem.* 1973; 77:3042.
192. Islangulov RR, Castellano FN. *Angew. Chem., Int. Ed.* 2006; 45:5957.
193. Lu Z, Yoon TP. *Angew. Chem., Int. Ed.* 2012; 51:10329.
194. Ni T, Caldwell RA, Melton LA. *J. Am. Chem. Soc.* 1989; 111:457.
195. An energy transfer pathway has also been employed to achieve the [2 + 2] cycloaddition of 3-ylideneoxindoles: Zou Y-Q, Duan S-W, Meng X-G, Hu X-G, Gao S, Chen J-R, Xiao W-J. *Tetrahedron.* 2012; 68:6914.
196. Inagaki A, Akita M. *Coord. Chem. Rev.* 2010; 254:1220.
197. Osawa M, Hoshino M, Wakatsuki Y. *Angew. Chem., Int. Ed.* 2001; 40:3472.
198. a Inagaki A, Edure S, Yatsuda S, Akita M. *Chem. Commun.* 2005:5468. b Inagaki A, Yatsuda S, Edure S, Suzuki A, Takahashi T, Akita M. *Inorg. Chem.* 2007; 46:2432. [PubMed: 17328538] c Inagaki A, Nakagawa H, Akita M, Inoue K, Sakai M, Fujii M. *Dalton Trans.* 2008:6709. [PubMed: 19153619] d Murata K, Ito M, Inagaki A, Akita M. *Chem. Lett.* 2010; 39:915. e Nitadori H, Takahashi T, Inagaki A, Akita M. *Inorg. Chem.* 2012; 51:51. [PubMed: 22142429]
199. Ru(bpy)²⁺₃ has also been proposed to accelerate a Sonogashira reaction via energy transfer: Osawa M, Nagai H, Akita M. *Dalton Trans.* 2007:827. [PubMed: 17297509]
200. a Andrews RS, Becker JJ, Gagné MR. *Angew. Chem., Int. Ed.* 2012; 51:4140. b Tucker JW, Zhang Y, Jamison TF, Stephenson CRJ. *Angew. Chem., Int. Ed.* 2012; 51:4144. c Neumann M, Zeitler K. *Org. Lett.* 2012; 14:2658. [PubMed: 22587670] d Bou-Hamdan FR, Seeberger PH. *Chem. Sci.* 2012; 3:1612.



Figure 1.
Ruthenium polypyridyl complexes: versatile visible light photocatalysts.



Scheme 1.
Simplified Molecular Orbital Depiction of $\text{Ru}(\text{bpy})_3^{2+}$ Photochemistry¹



Scheme 2.
Oxidative and Reductive Quenching Cycle of Ru(bpy)_3^{2+}

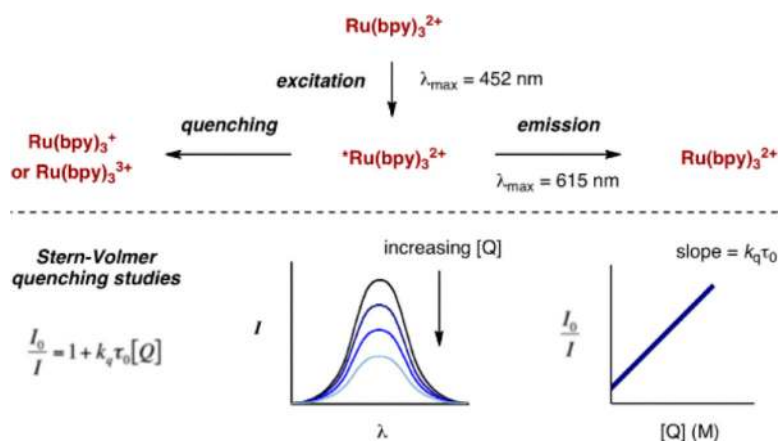
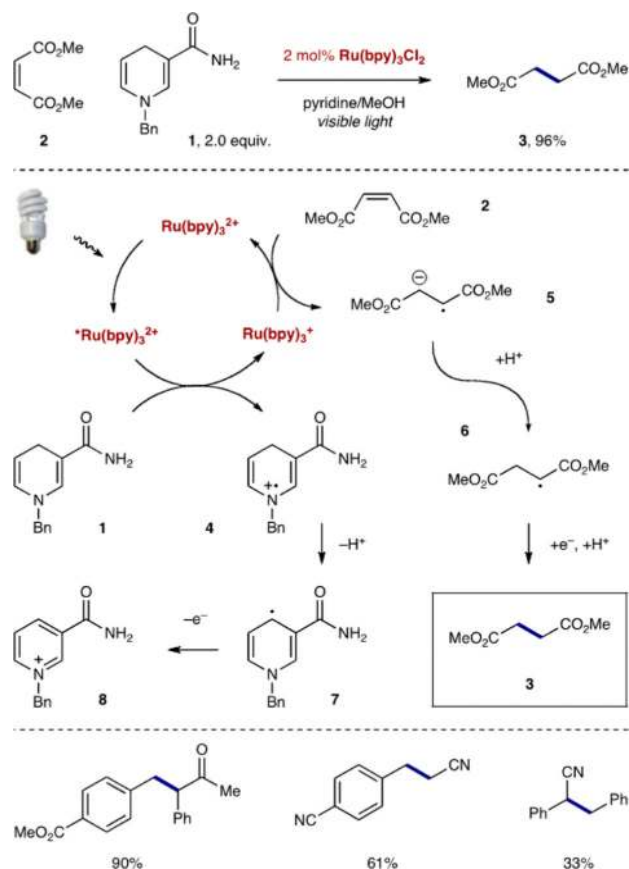
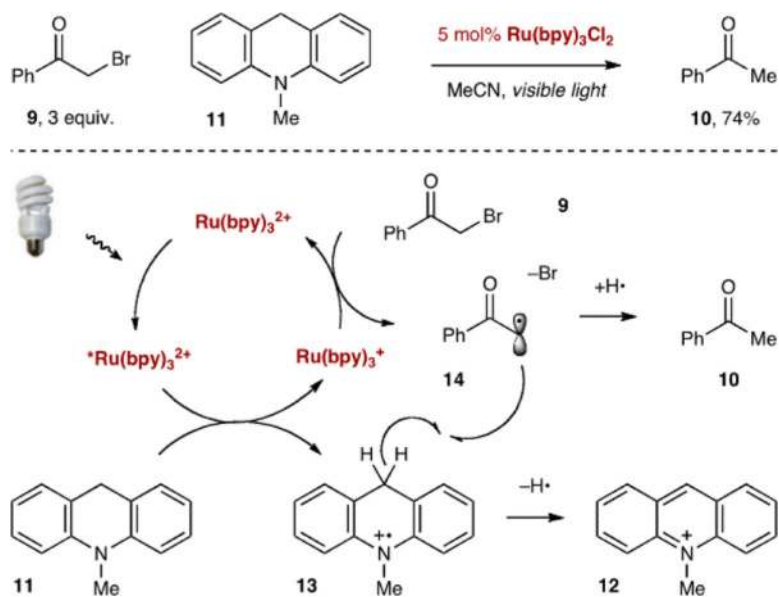


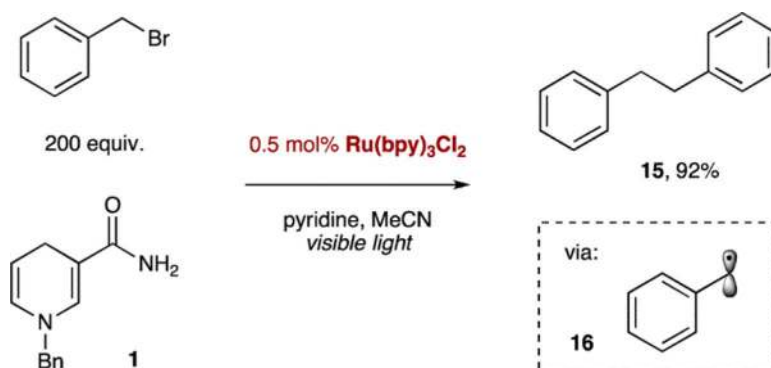
Figure 2.
Fluorescence quenching (Stern–Volmer) studies.



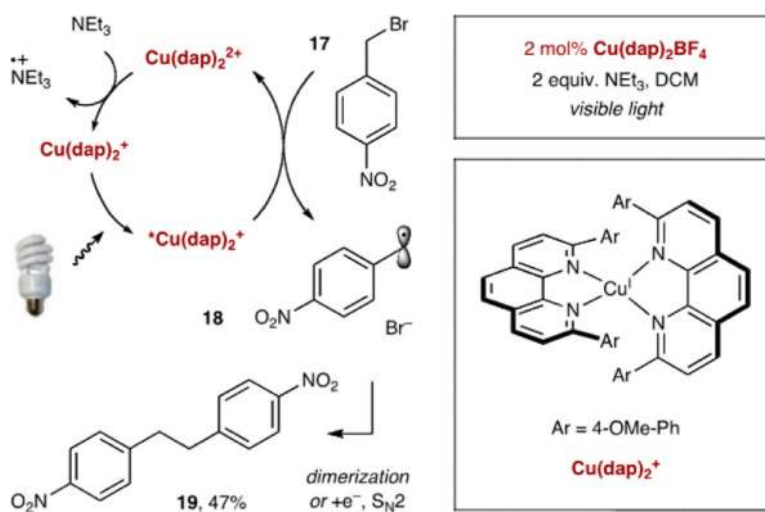
Scheme 3.
Photoredox Reduction of Electron-Deficient Olefins



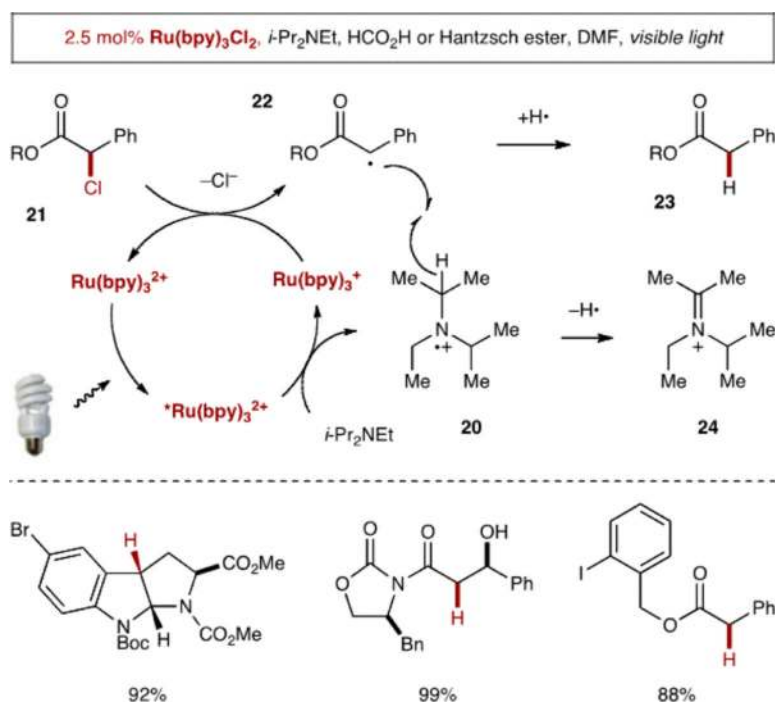
Scheme 4.
Reductive Dehalogenation of Phenacyl Bromides



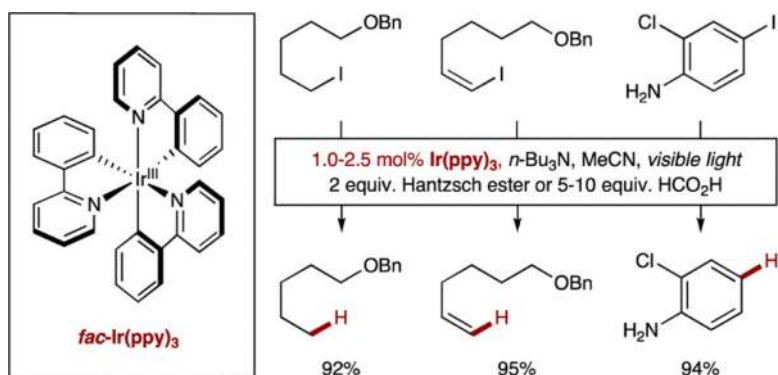
Scheme 5.
Reductive Dimerization of Benzyl Bromide



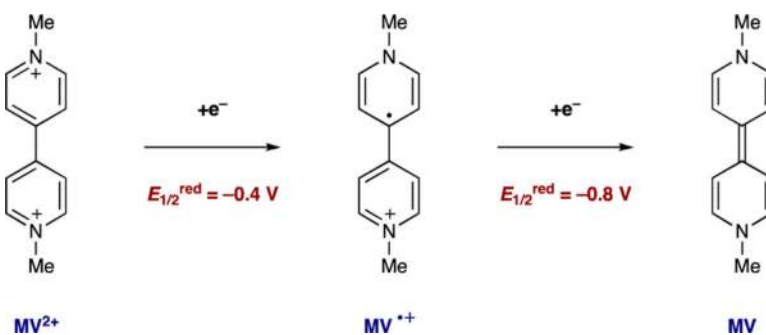
Scheme 6.
Reductive Dimerization of 4-Nitrobenzyl Bromide by Cu(dap)_2^+



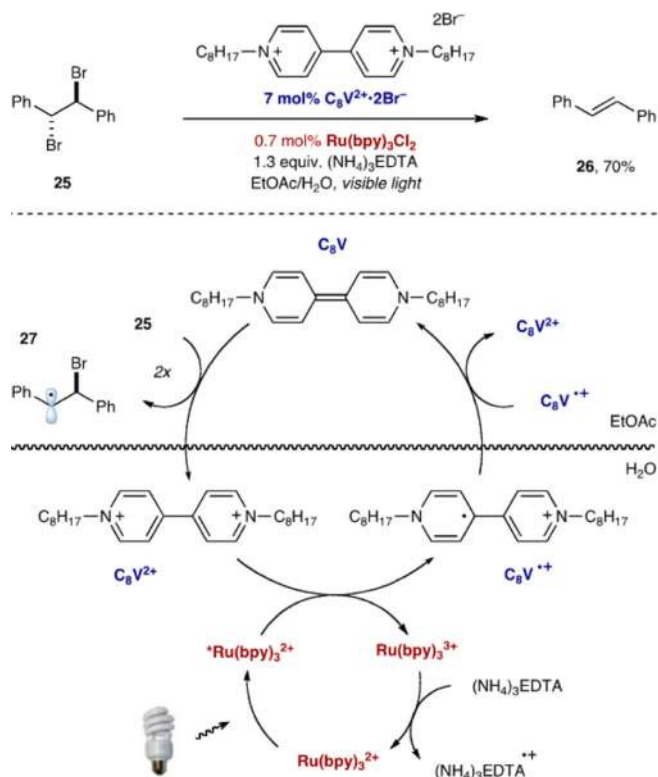
Scheme 7.
Stephenson's Photoredox Reductive Dehalogenation



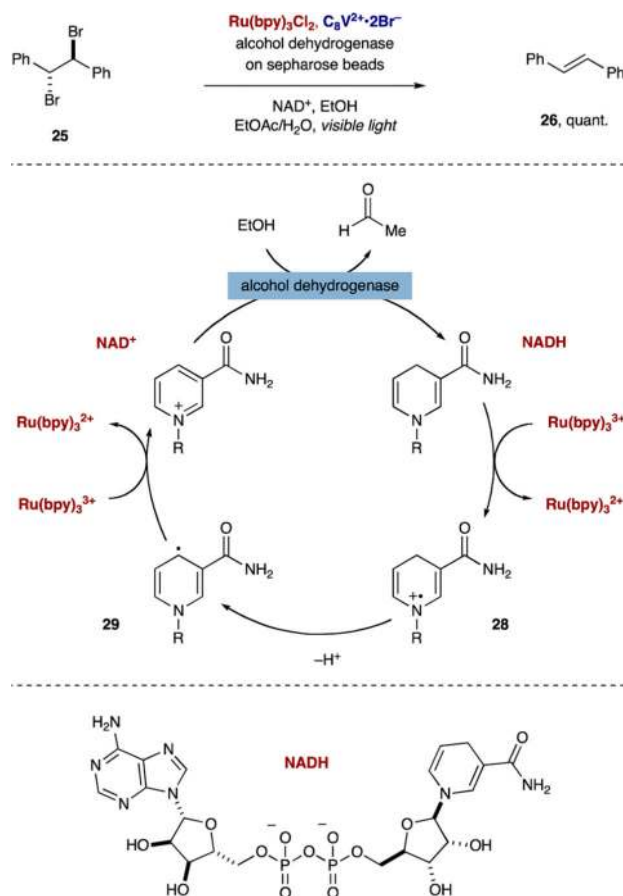
Scheme 8.
Reductive Dehalogenation of Alkyl, Alkenyl, and Aryl Iodides



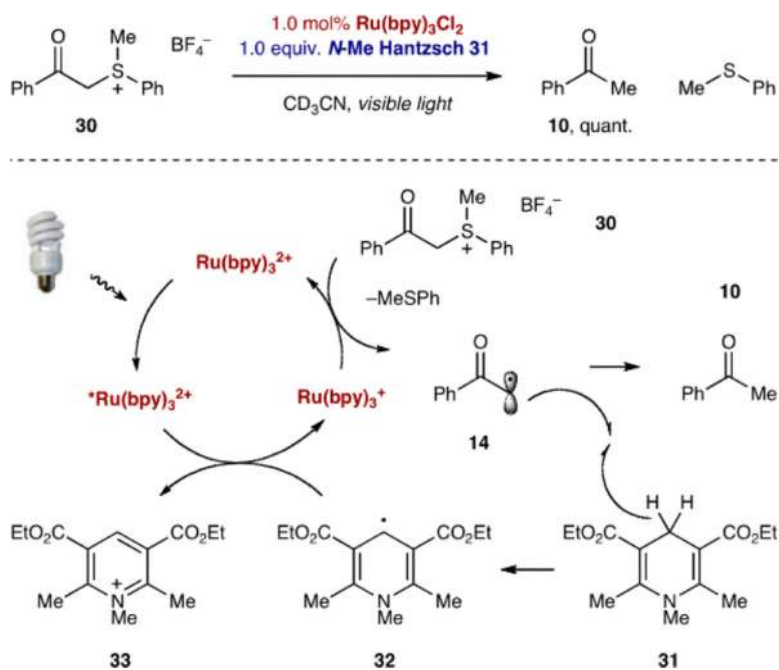
Scheme 9.
Redox Chemistry of Dimethyl Viologen (MV^{2+})

**Scheme 10.**

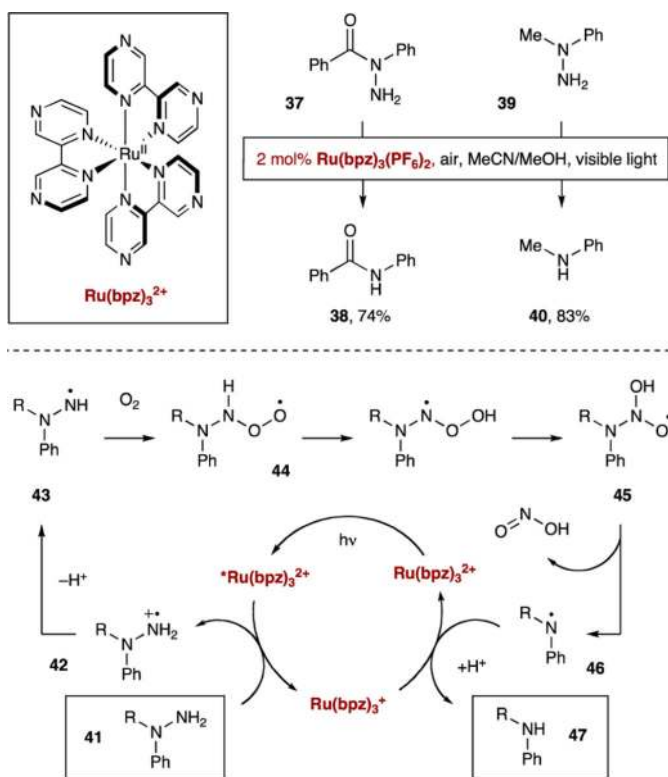
Reduction of vic-Dibromides via Photoredox and Viologen Catalysis in a Biphasic System

**Scheme 11.**

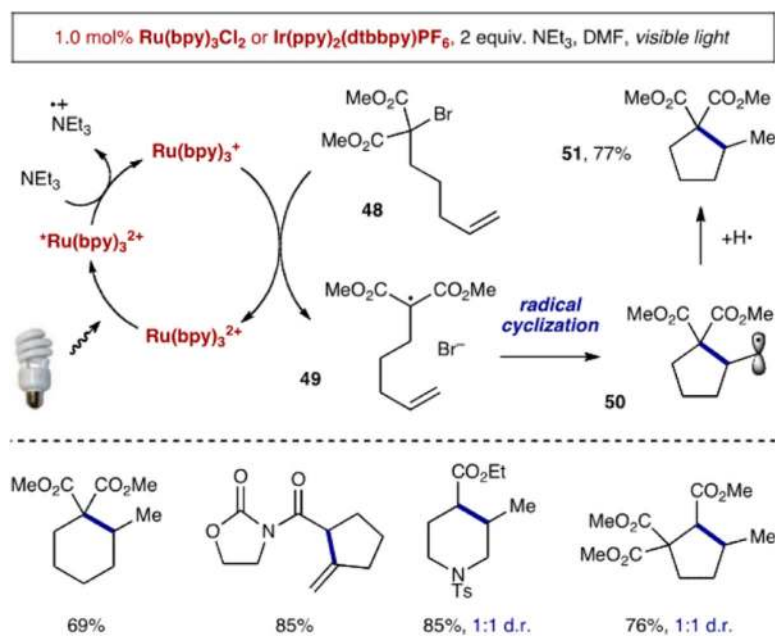
Enzymatic Regeneration of NADH Coupled with the Photoredox Reductive Dehalogenation of vic-Dibromides



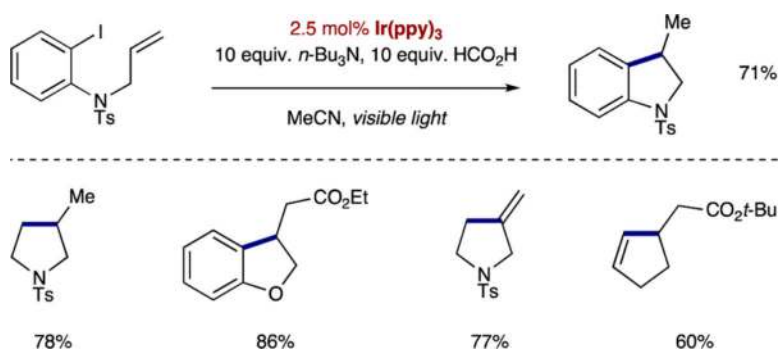
Scheme 12.
Photoredox Reduction of Phenacylsulfonium Salts



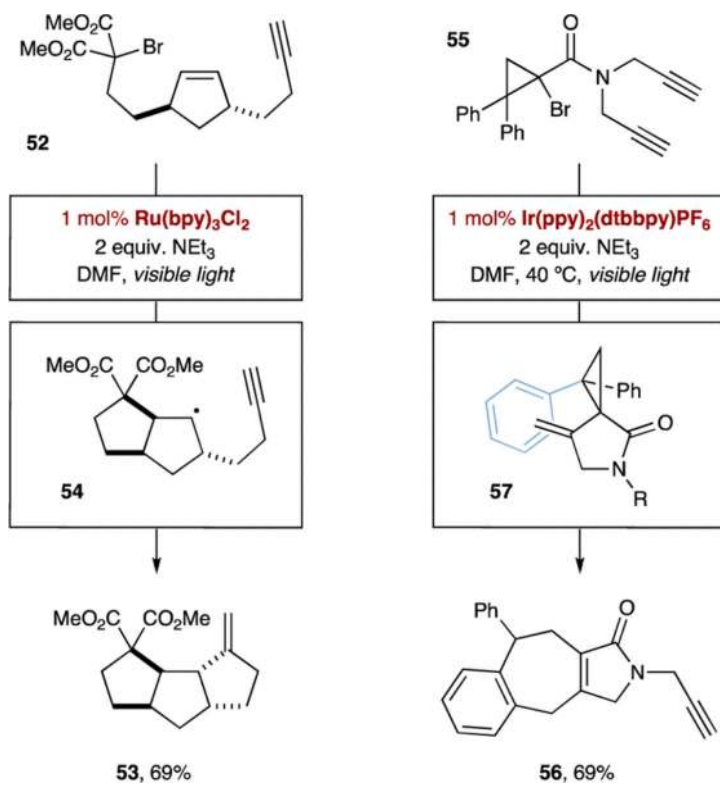
Scheme 13.
Reduction of Hydrazides and Hydrazines Using $\text{Ru}(\text{bpz})_3^{2+}$



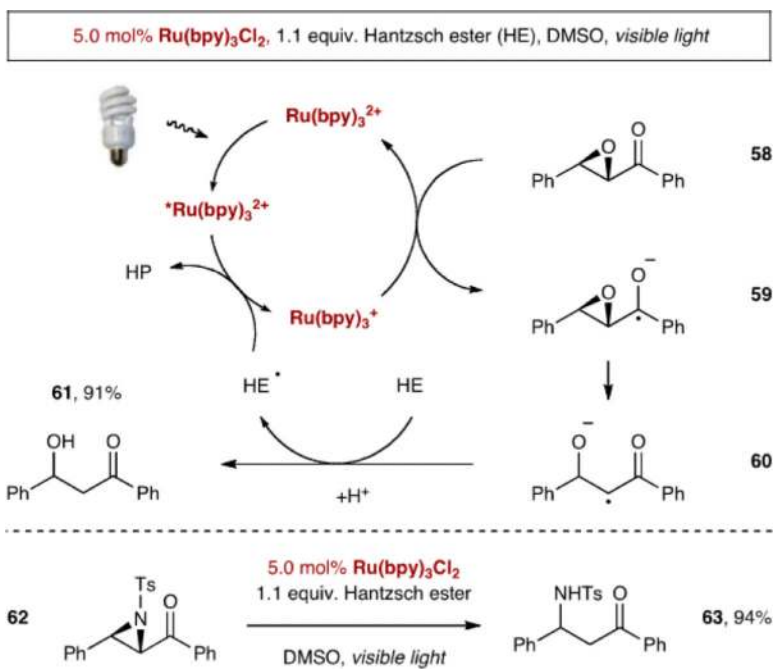
Scheme 14.
Photoredox-Catalyzed Reductive Radical Cyclization

**Scheme 15.**

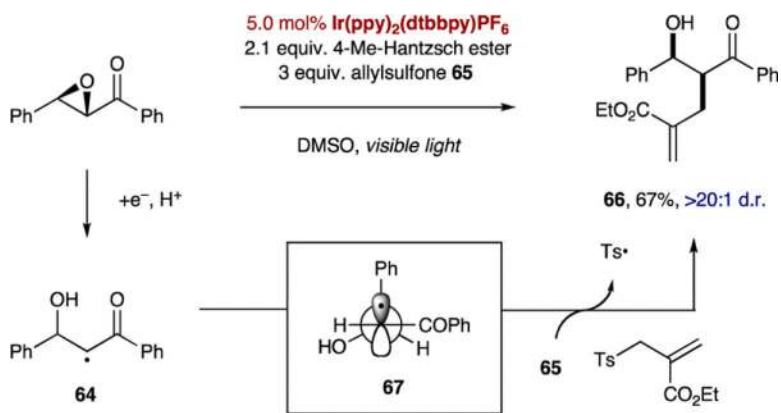
Radical Cyclizations of Alkyl, Alkenyl, and Aryl Iodides



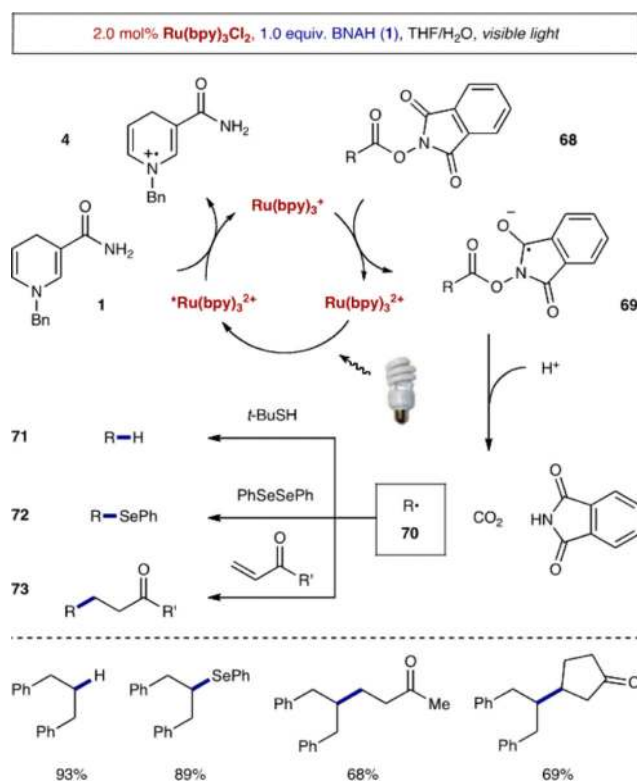
Scheme 16.
Cascade Photoredox Cyclization Reactions

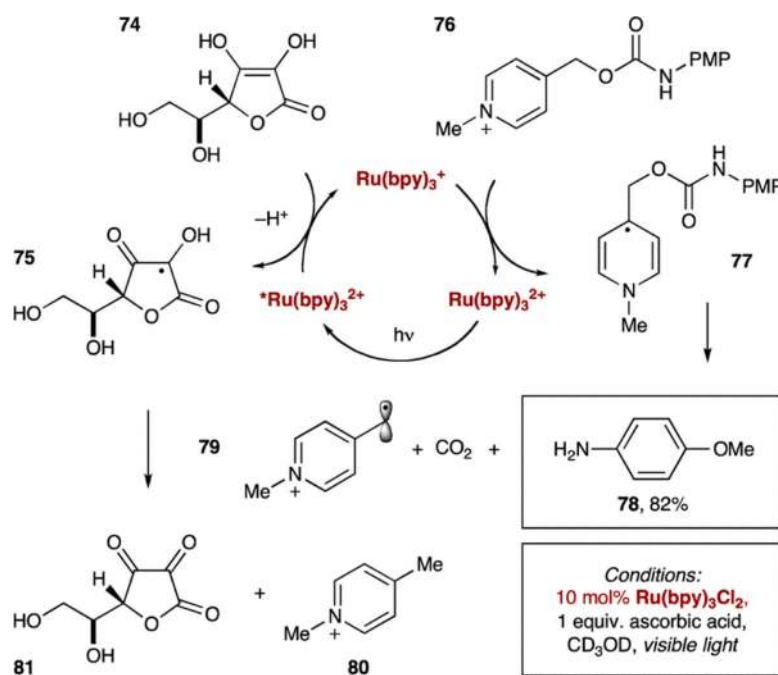


Scheme 17.
Reductive Opening of Epoxides and Aziridines

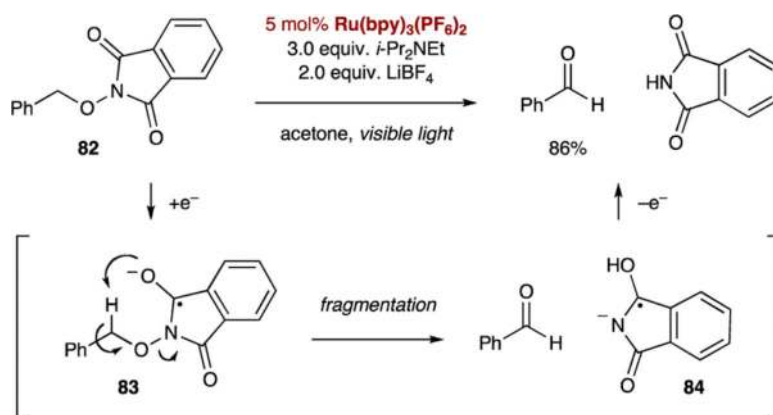


Scheme 18.
Tandem Ring-Opening/Allylation of α -Ketoepoxides

**Scheme 19.***N*-(Acyloxy)phthalimides as Masking Groups for Alkyl Radicals

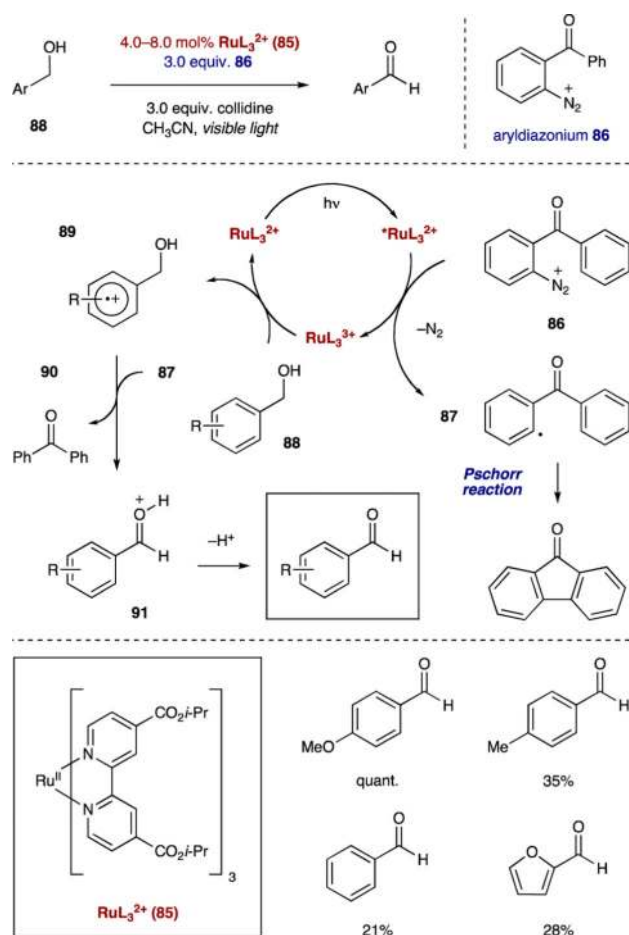


Scheme 20.
Reductive Cleavage of the *N*-Methylpicolinium Group

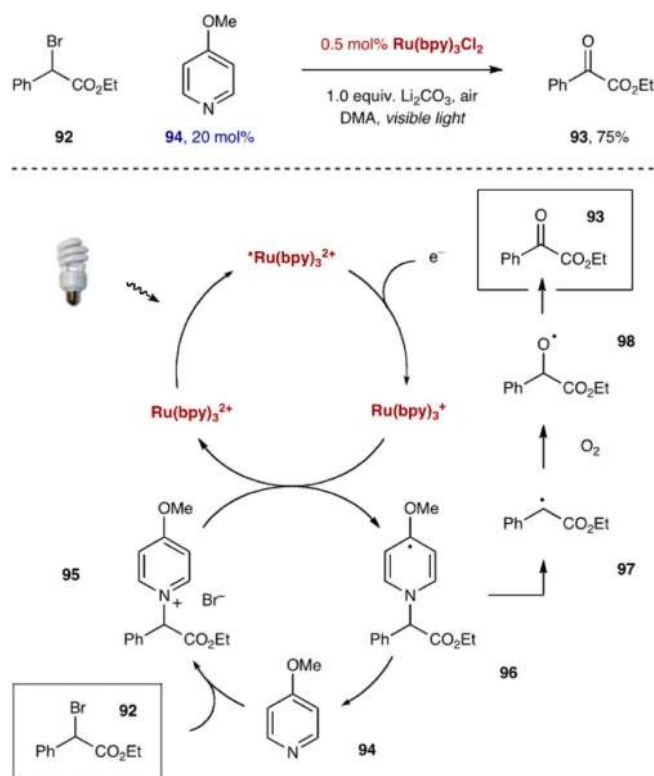


Scheme 21.

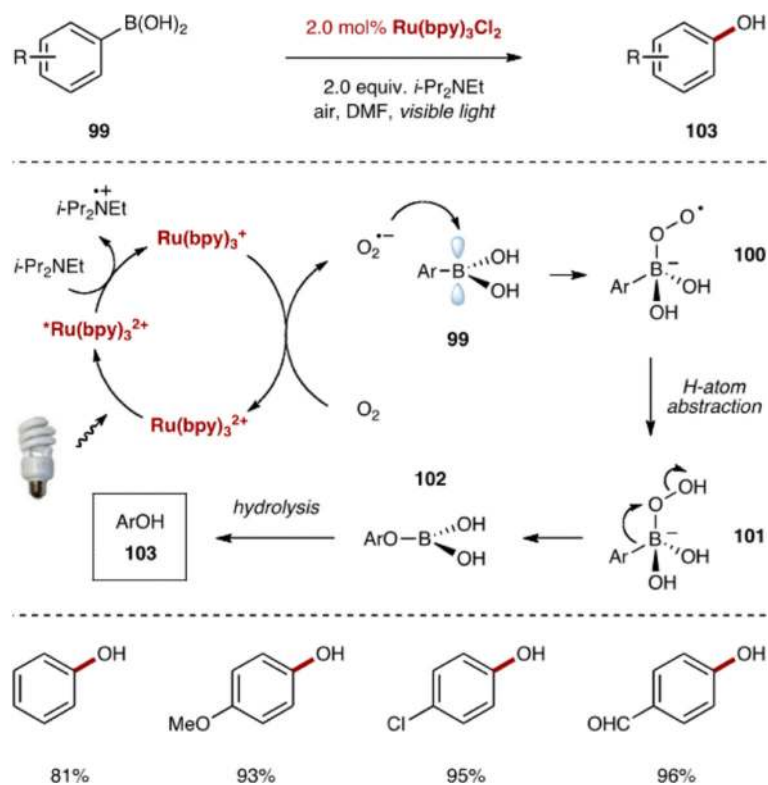
N-Alkoxyphthalimides as Masking Groups for Aldehydes



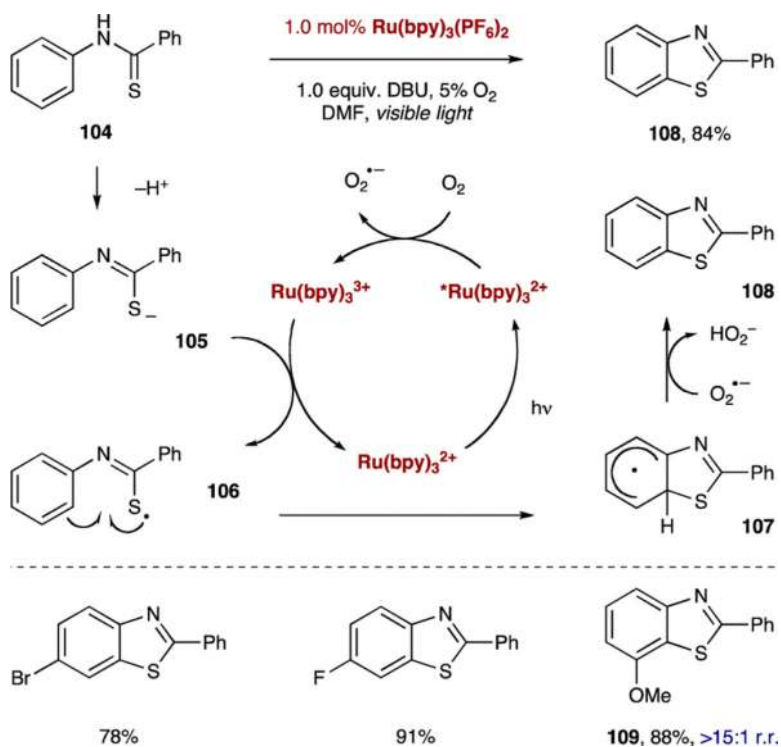
Scheme 22.
Oxidation of Benzylic Alcohols to Aldehydes



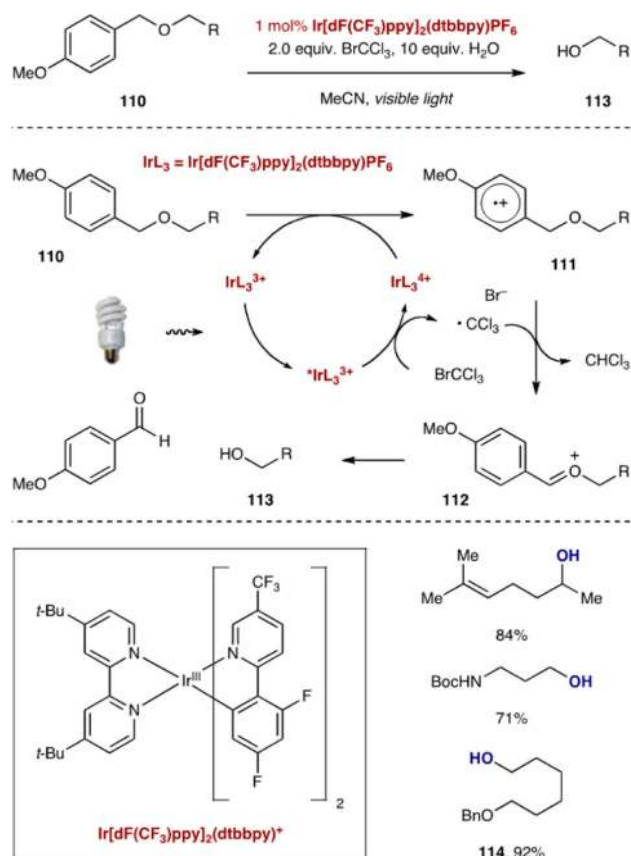
Scheme 23.
Aerobic Oxidation of Benzylic Halides



Scheme 24.
Aerobic Oxidative Hydroxylation of Arylboronic Acids



Scheme 25.
Oxidative Conversion of Thiobenzanilides to Benzothiazoles



Scheme 26.
Oxidative Deprotection of para-Methoxybenzyl Ethers

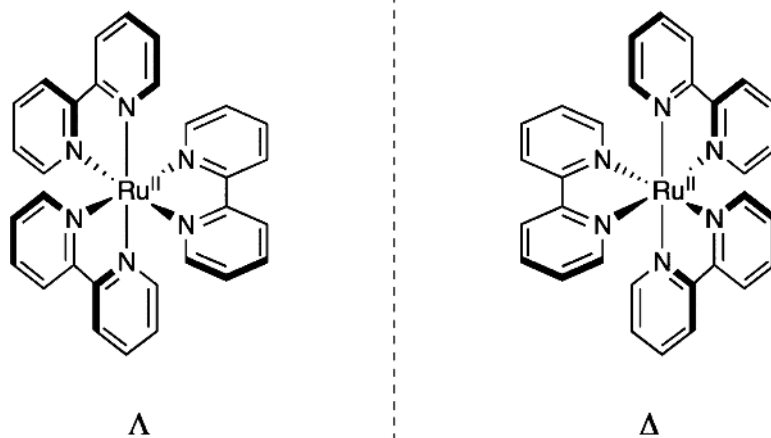
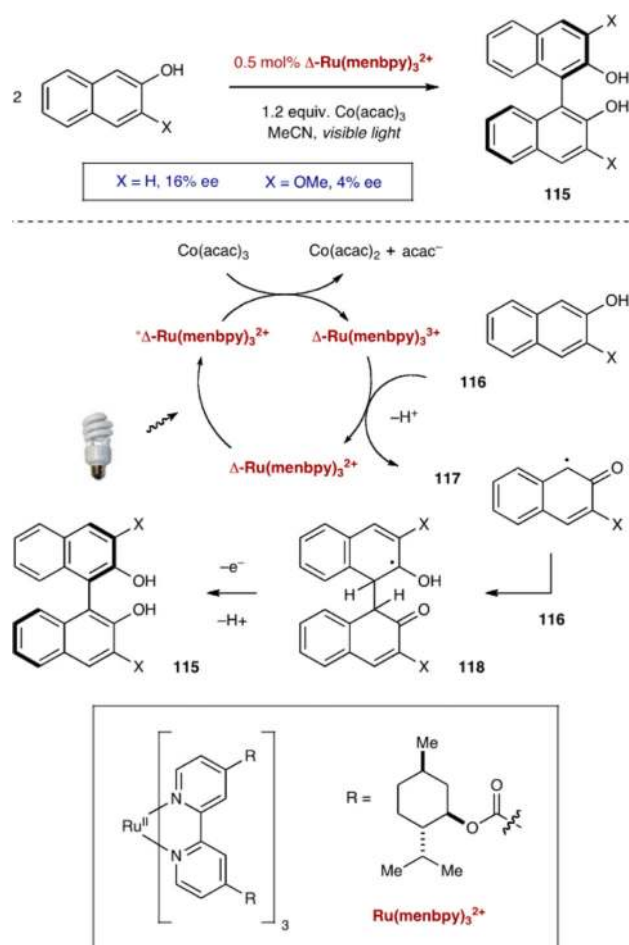
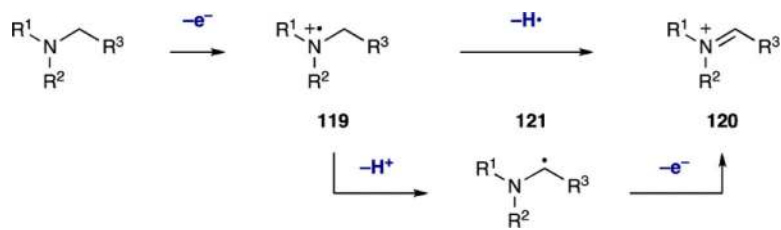


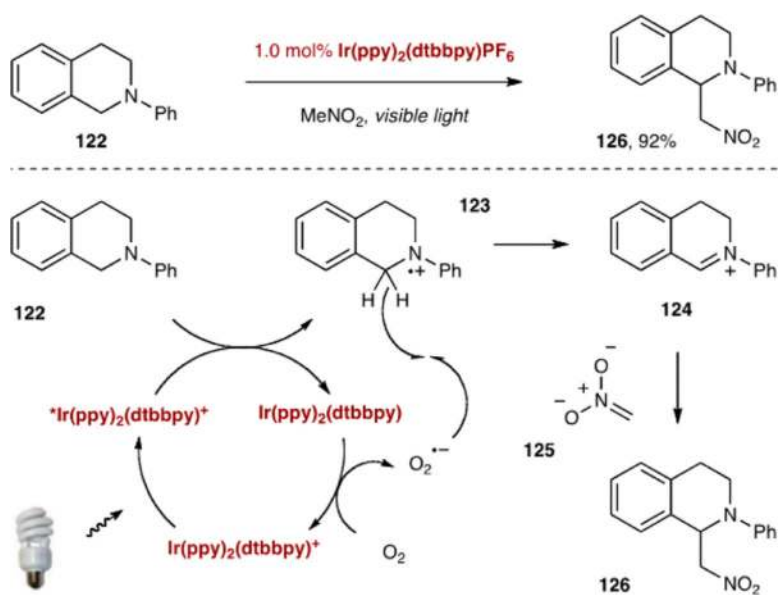
Figure 3.
Enantiomeric forms of $\text{Ru}(\text{bpy})_3^{2+}$.



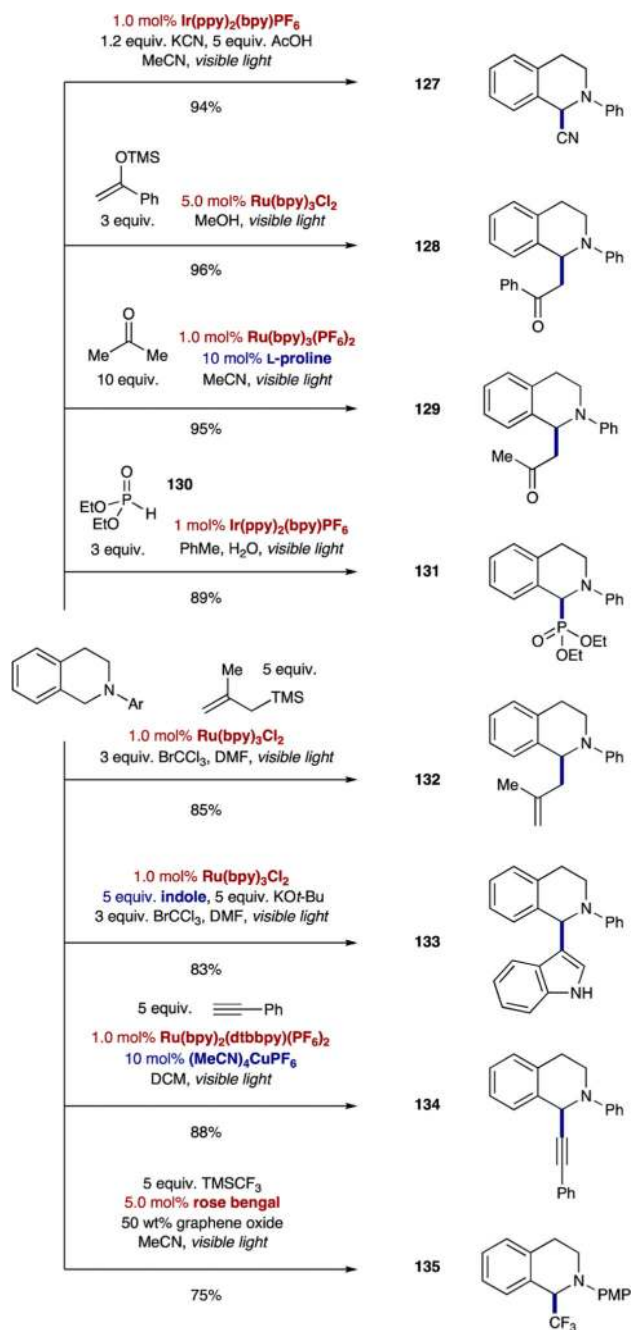
Scheme 27.
Oxidative Biaryl Coupling with a Chiral Photocatalyst



Scheme 28.
Pathways of Amine Oxidation to Iminium Ions

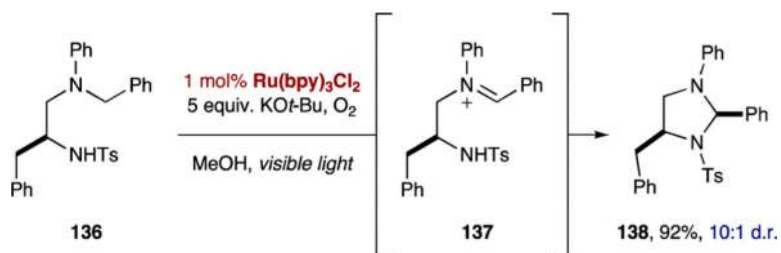


Scheme 29.
 Photoredox aza-Henry Reaction via Iminium Intermediate

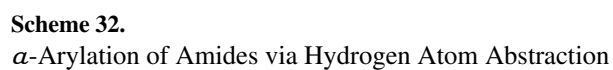


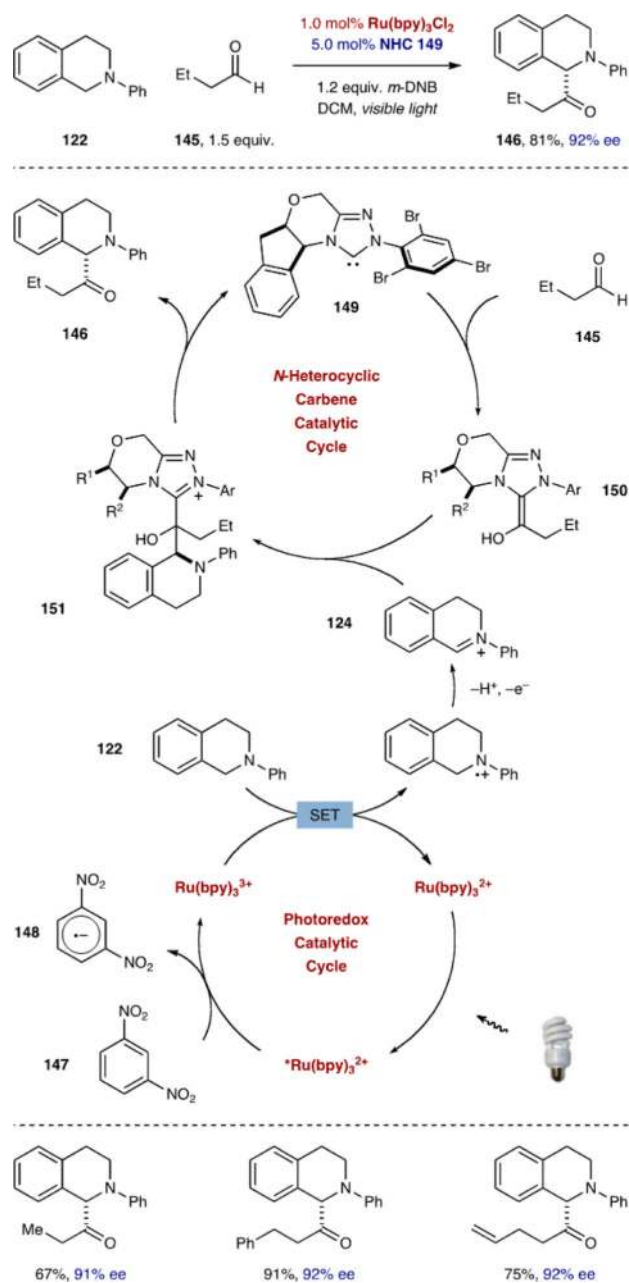
Scheme 30.

Trapping of Photoredox-Generated Iminium Ions with Diverse Nucleophiles

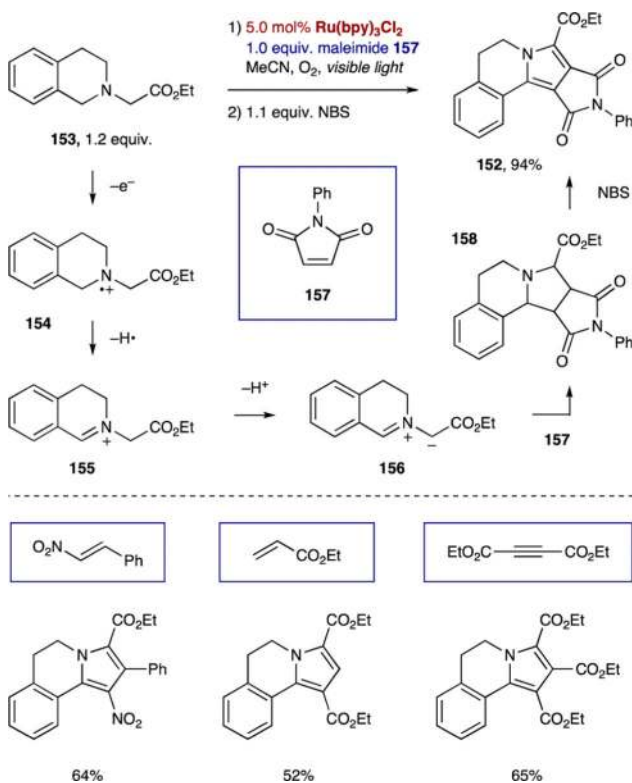
**Scheme 31.**

Synthesis of Tetrahydroimidazoles via Intramolecular Trapping of a Photoredox-Generated Iminium Ion

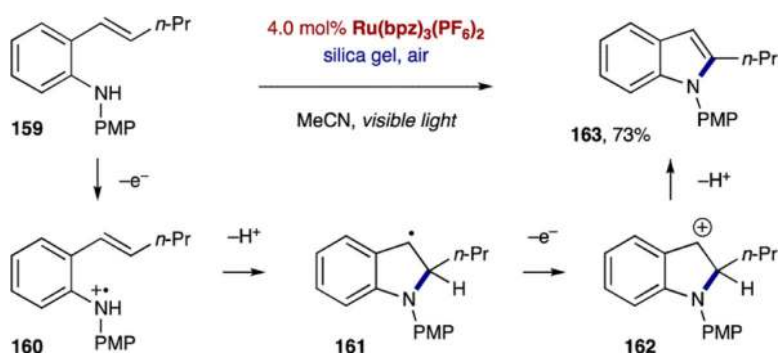


**Scheme 33.**

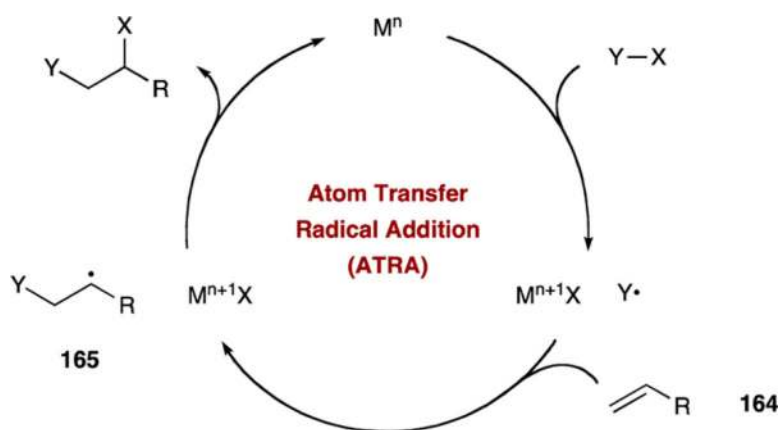
Rois's Merger of Photoredox Catalysis with *N*-Heterocyclic Carbene Catalysis: The α -Acylation of Amines



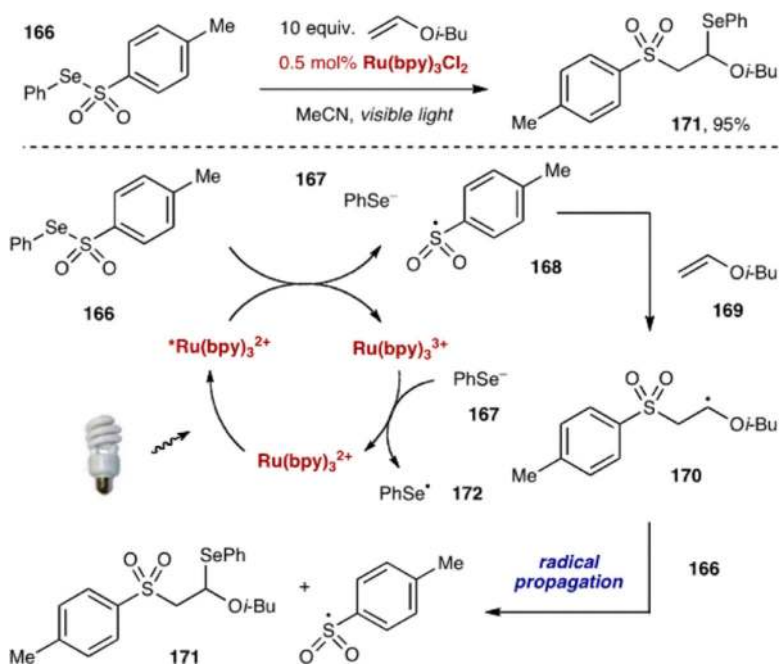
Scheme 34.
Photoredox-Promoted Azomethine Ylide [3 + 2] Cycloadditions



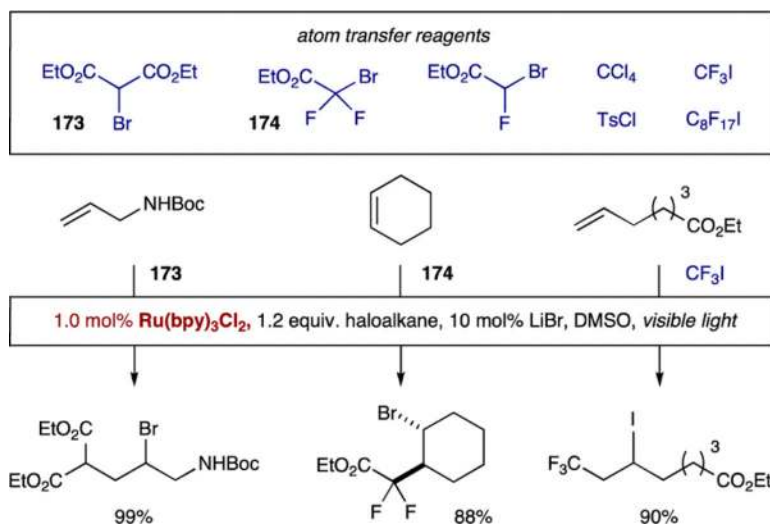
Scheme 35.
Cyclization of Aminium Radical Cations



Scheme 36.
Generic Atom Transfer Radical Addition (ATRA) Cycle

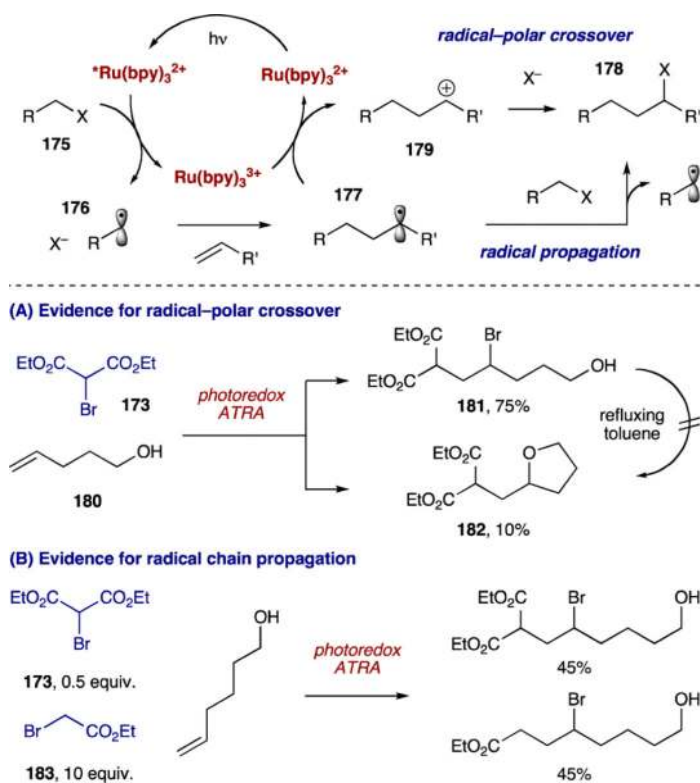
**Scheme 37.**

Atom Transfer Radical Addition of *Se*-Phenyl *p*-Tolueneselenosulfonate to Alkyl Vinyl Ethers

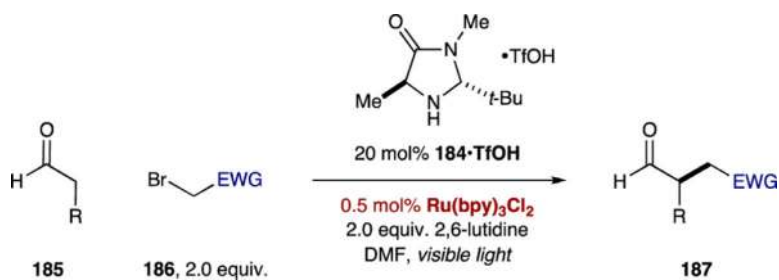


Scheme 38.

Photoredox Atom Transfer Radical Addition (ATRA)

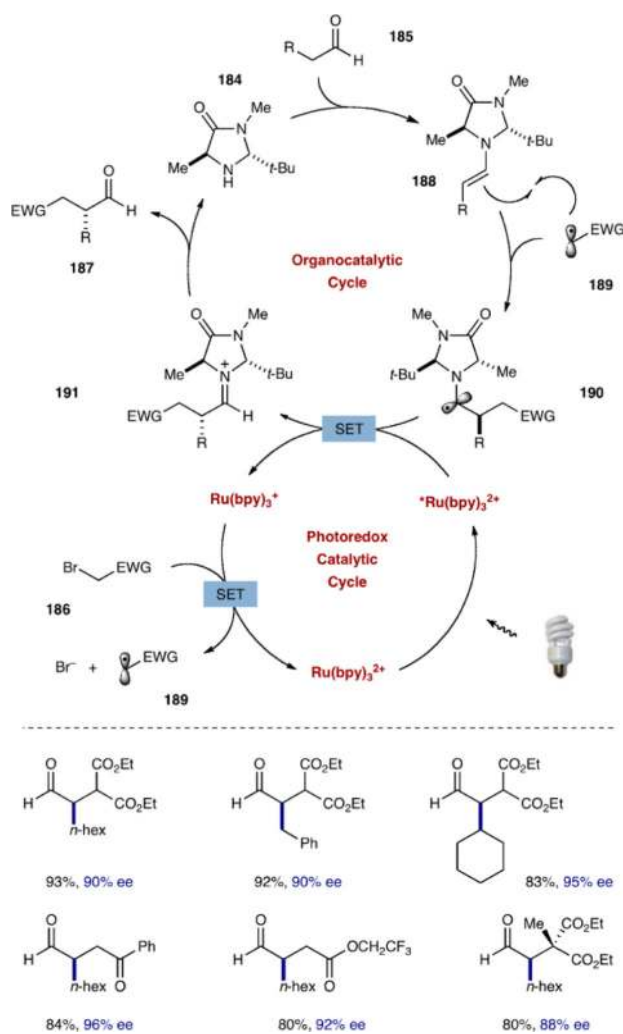


Scheme 39.
Mechanism of the Photoredox ATRA

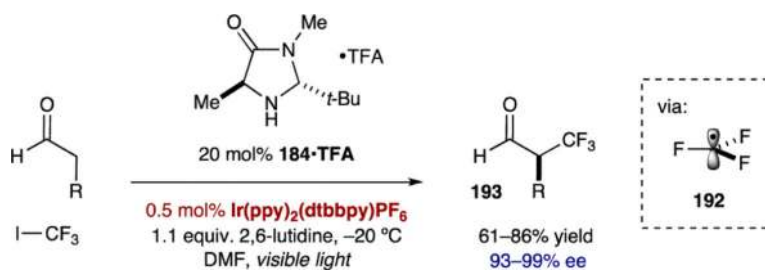


Scheme 40.

Merger of Photoredox Catalysis and Enamine Catalysis: The Asymmetric α -Alkylation of Aldehydes

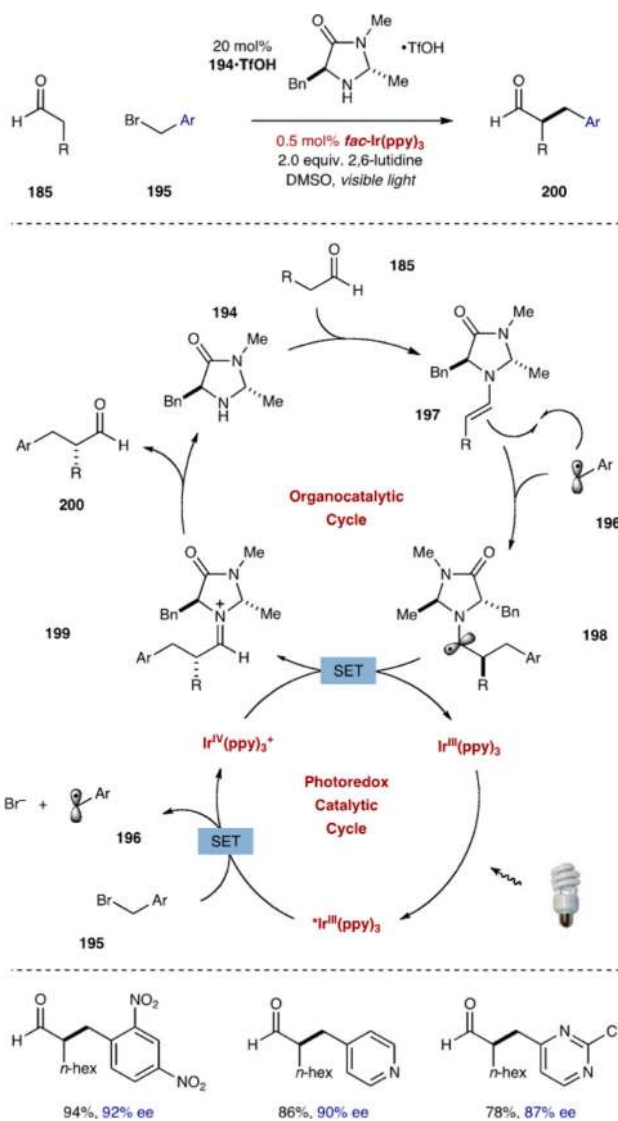


Scheme 41.
Enantioselective α -Alkylation of Aldehydes via Photoredox Organocatalysis

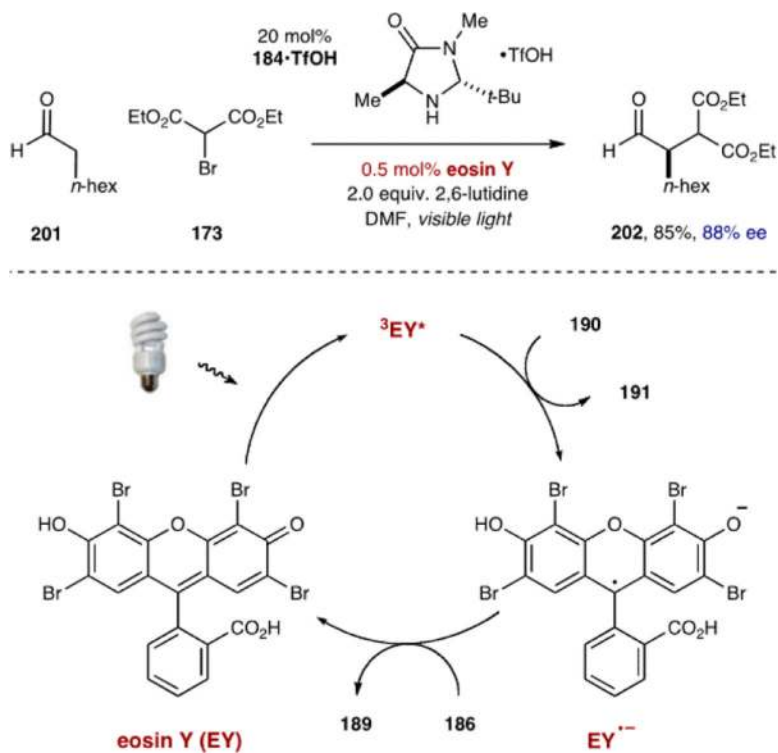


Scheme 42.

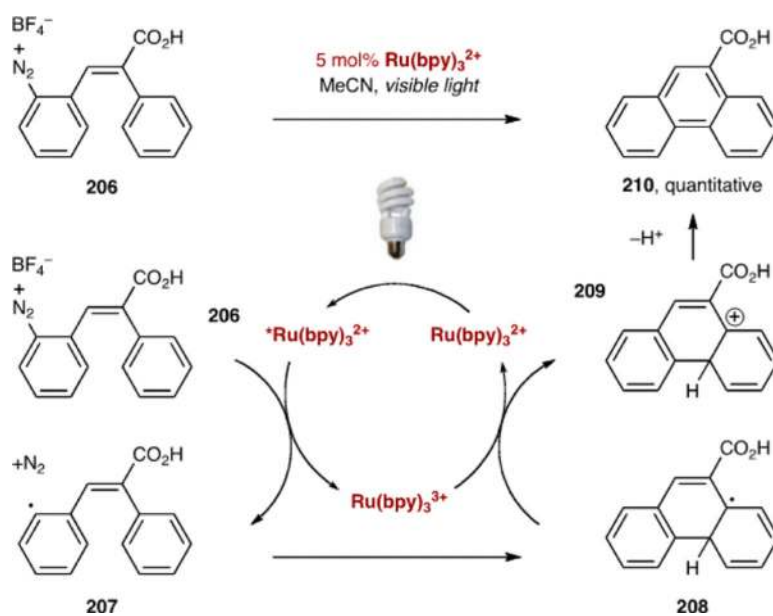
α -Trifluoromethylation of Aldehydes



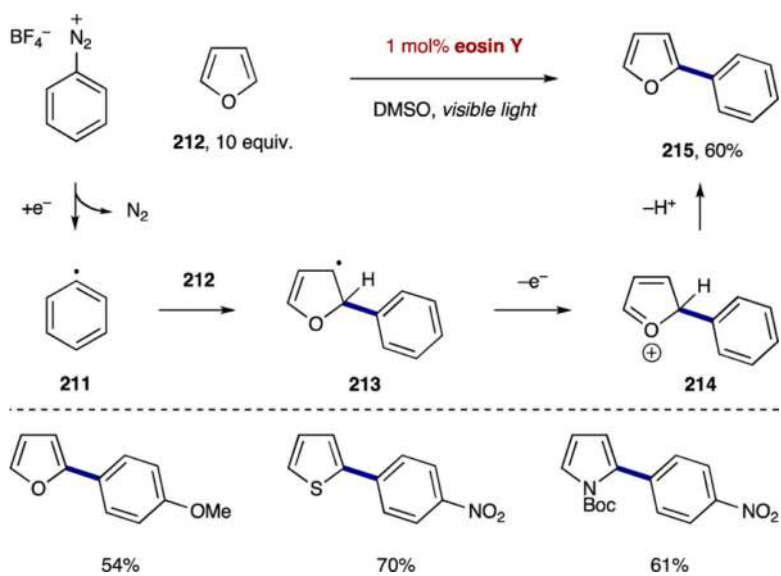
Scheme 43.
 α -Benzylation of Aldehydes via Photoredox Organocatalysis



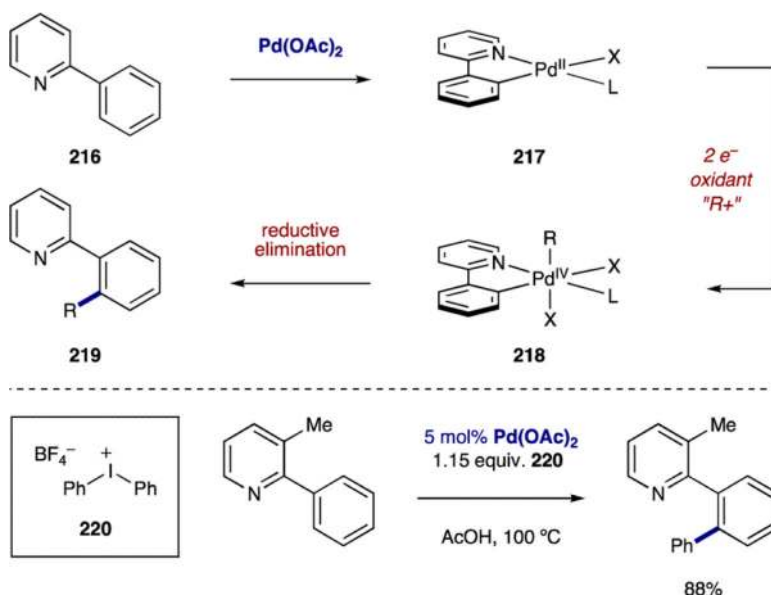
Scheme 44.
Eosin Y-Catalyzed Photoredox Organocatalysis



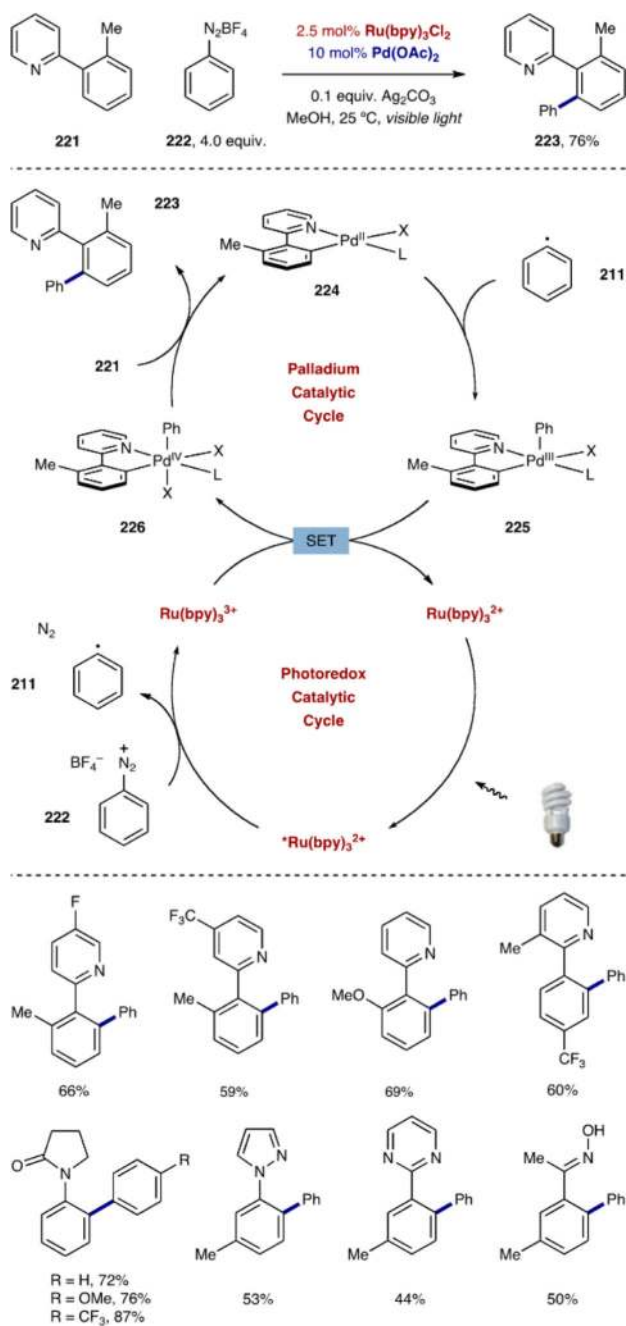
Scheme 45.
Photoredox-Catalyzed Pschorr Reaction



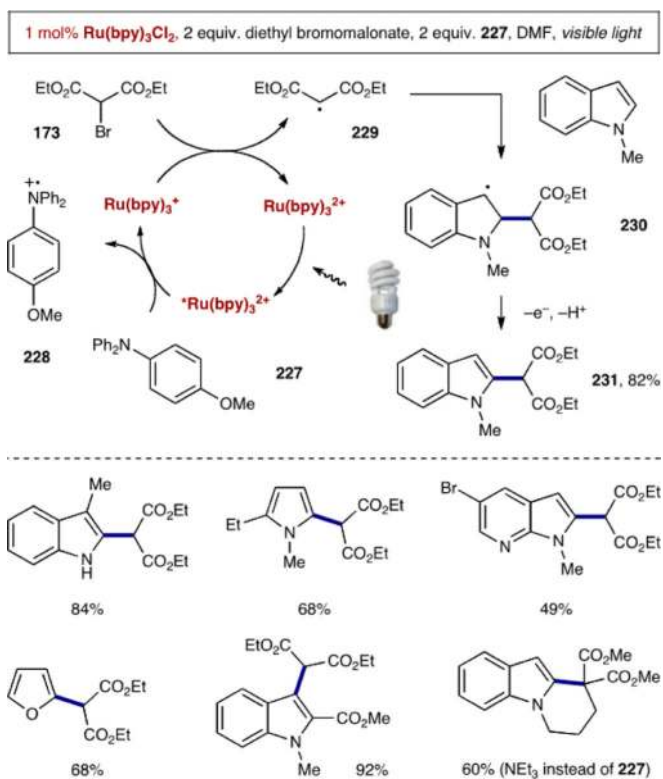
Scheme 46.
Arylation of Heterocycles with Diazonium Salts



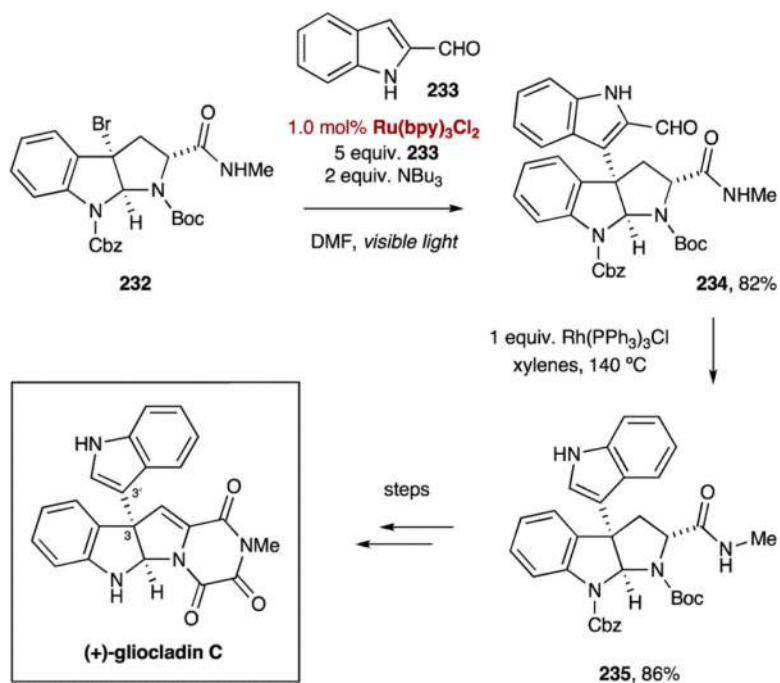
Scheme 47.
Pd-Catalyzed C–H Functionalization and Arylation



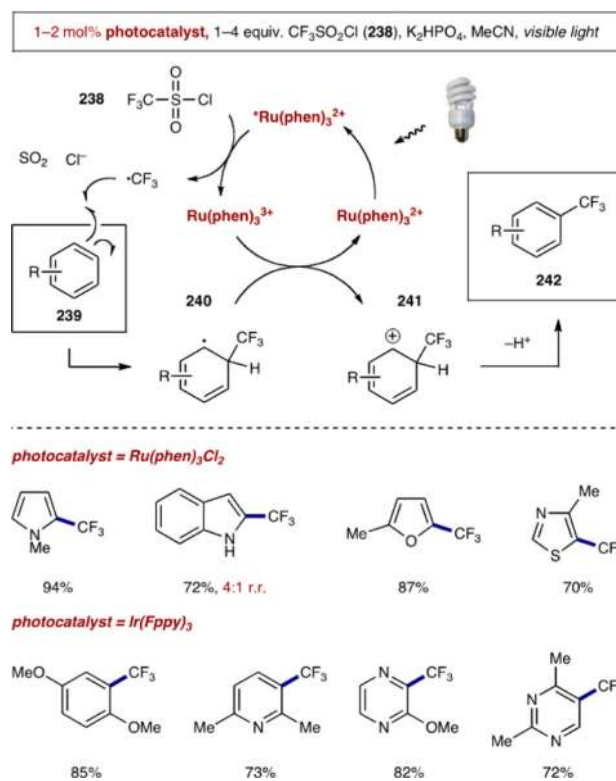
Scheme 48.
Merger of Palladium and Photoredox Catalysis in C–H Arylation with Aryldiazonium Salts



Scheme 49.
Malonyl Radical Additions to Electron-Rich Heterocycles



Scheme 50.
Photoredox Catalysis in the Total Synthesis of Gliocladin C



Scheme 51.
Photoredox Arene and Heteroarene Trifluoromethylation

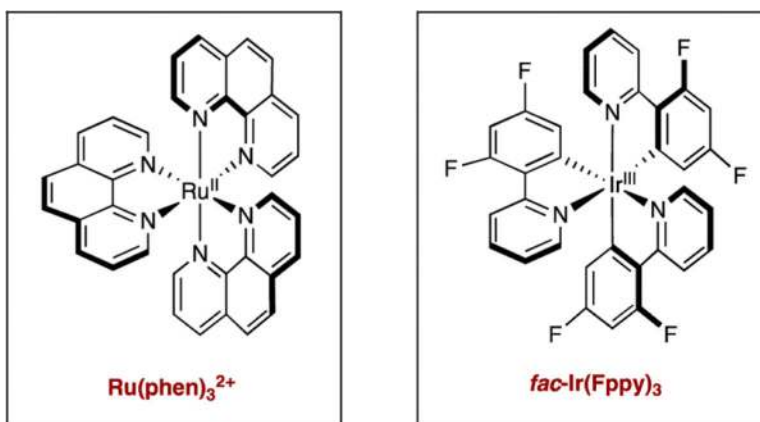
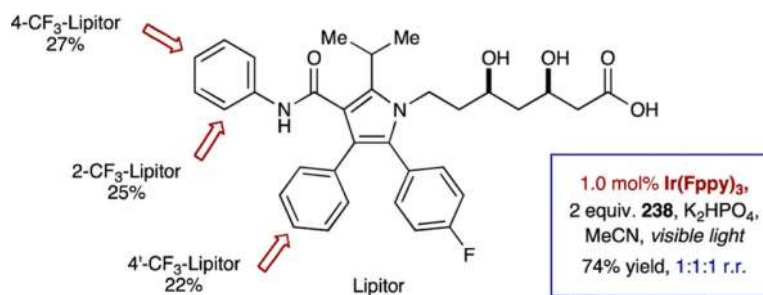
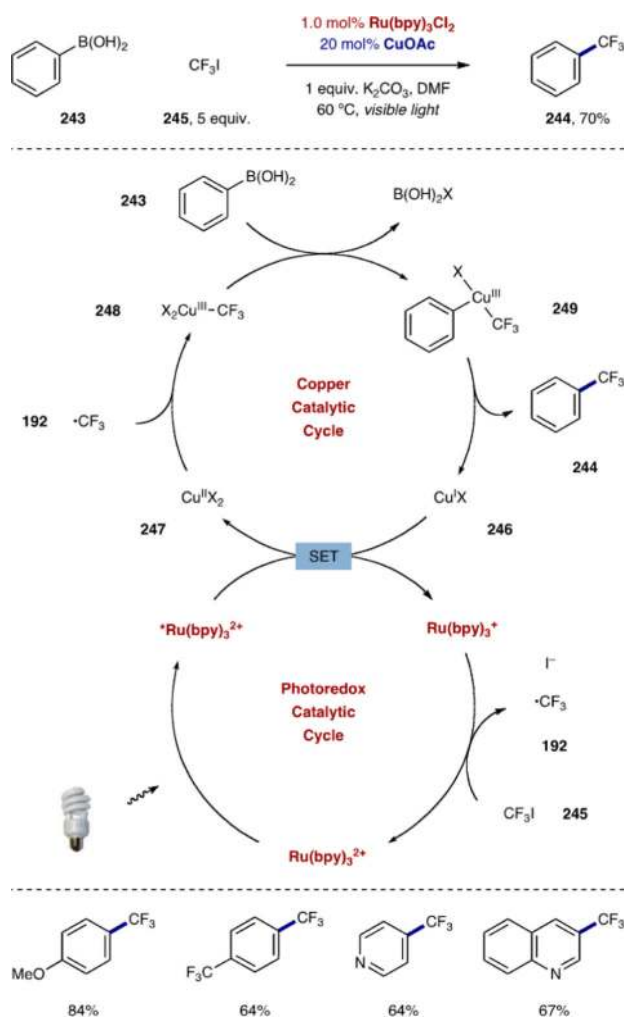


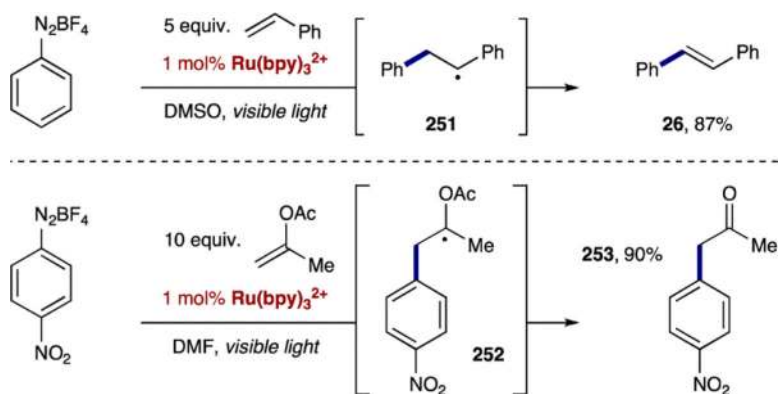
Figure 4.
Photocatalysts employed in arene trifluoromethylation.



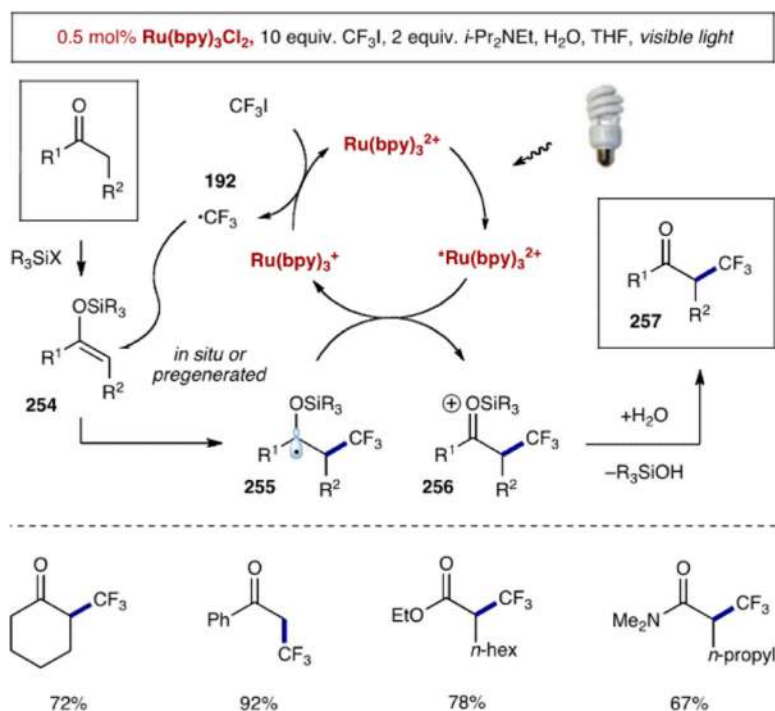
Scheme 52.
Photoredox Trifluoromethylation of Lipitor



Scheme 53.
Merger of Photoredox and High-Valent Copper Catalysis: Trifluoromethylation of Arylboronic Acids

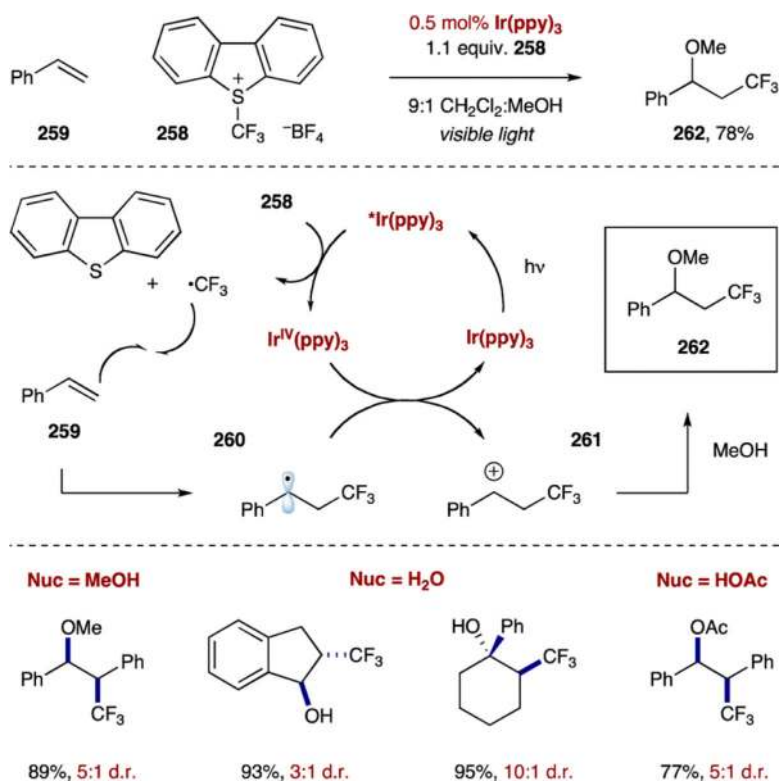


Scheme 54.
Arylation Reactions of Styrenes and Enol Acetates

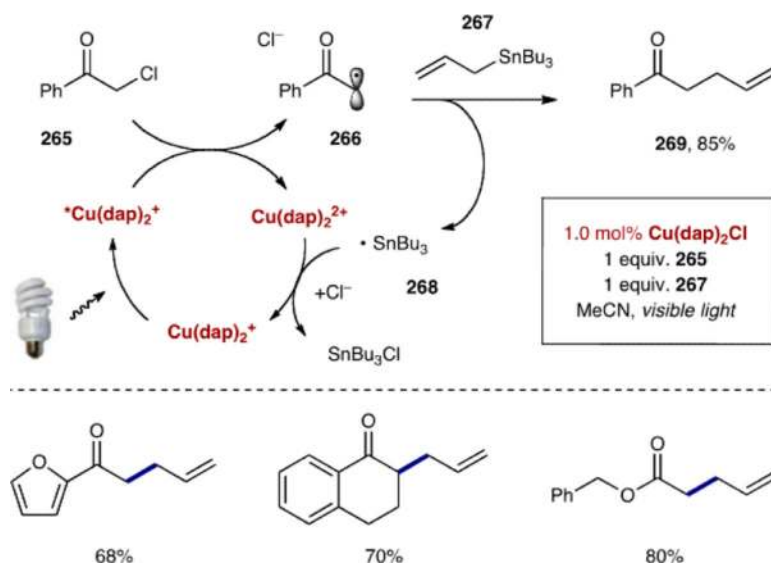


Scheme 55.

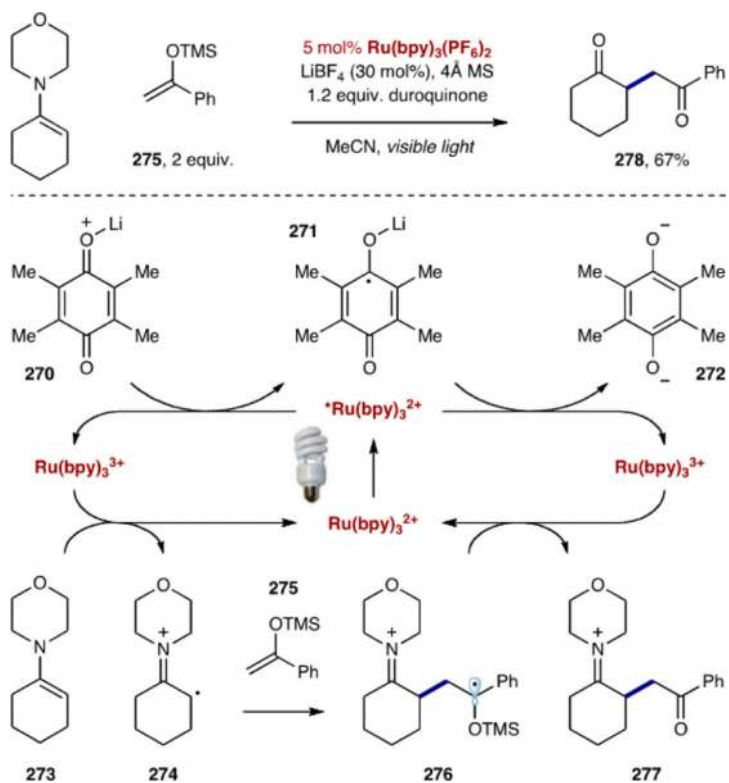
α -Trifluoromethylation of Ketones, Esters, and Amides



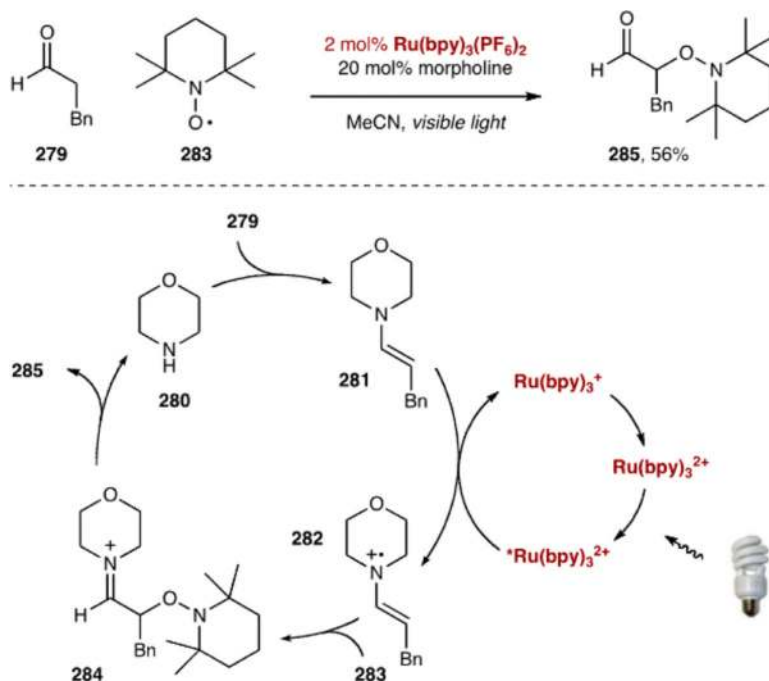
Scheme 56.
Photoredox Oxytrifluoromethylation of Styrenes



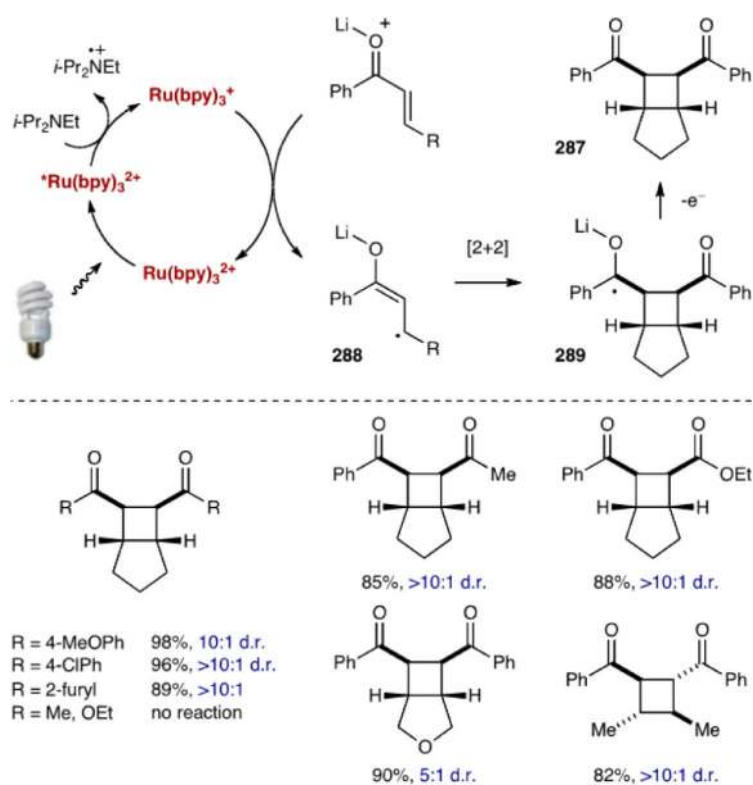
Scheme 57.
Photoredox α -Allylation of α -Halocarbonyls



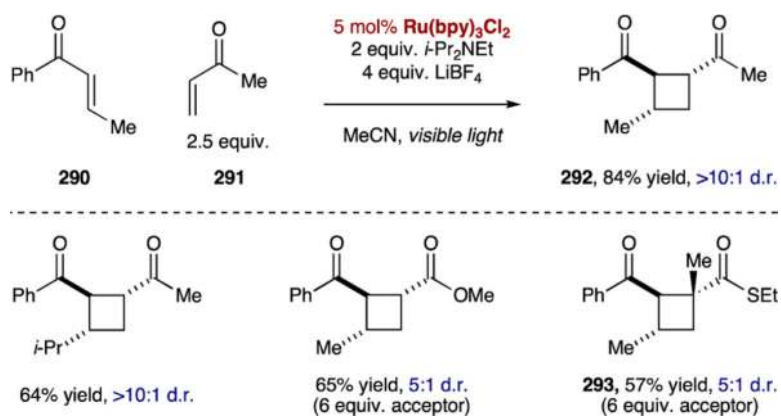
Scheme 58.
Oxidative Coupling of Enamines with Enolsilanes



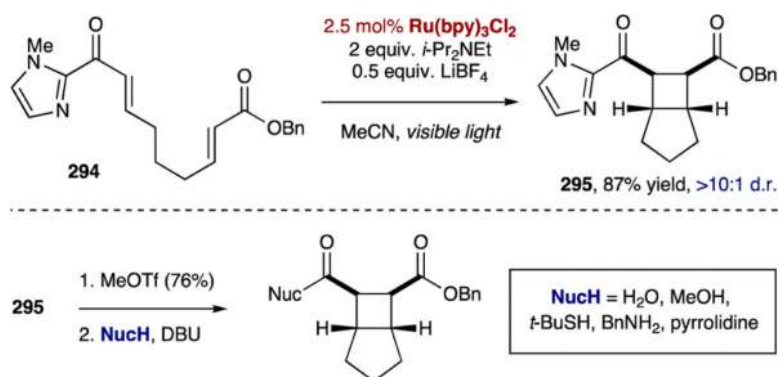
Scheme 59.
 α -Oxyamination of Aldehydes with TEMPO

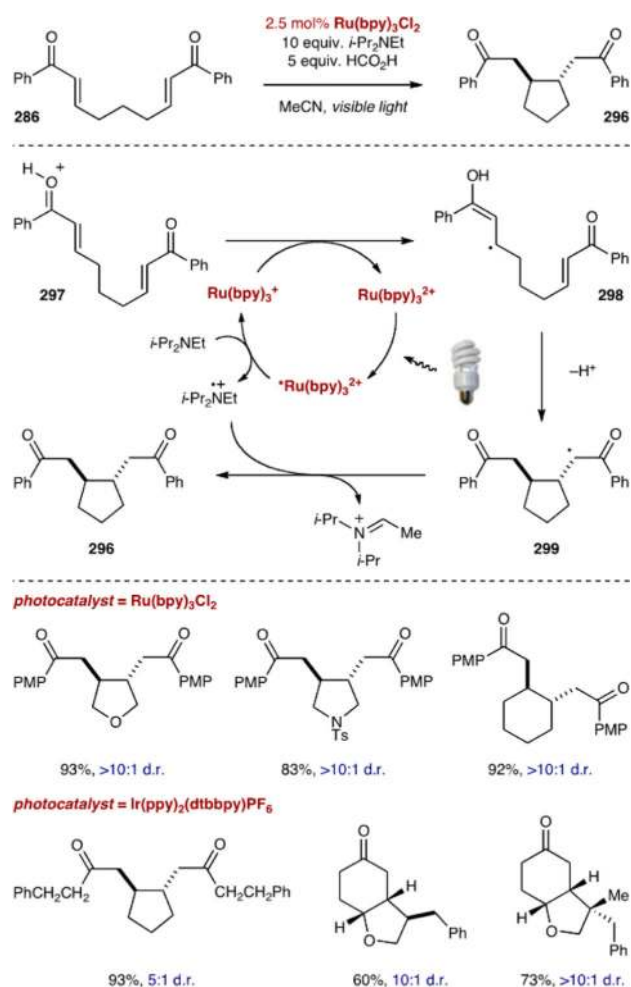
**Scheme 60.**

Yoon's Photoredox Enone [2 + 2] Cycloaddition

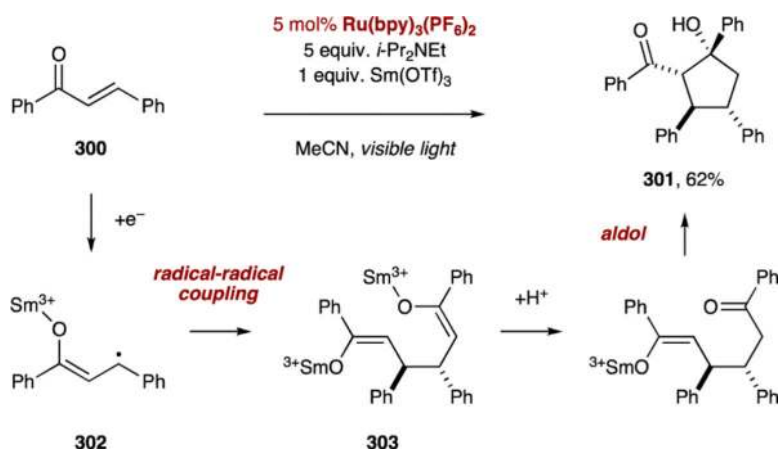
**Scheme 61.**

Crossed Intermolecular [2 + 2] Cycloadditions

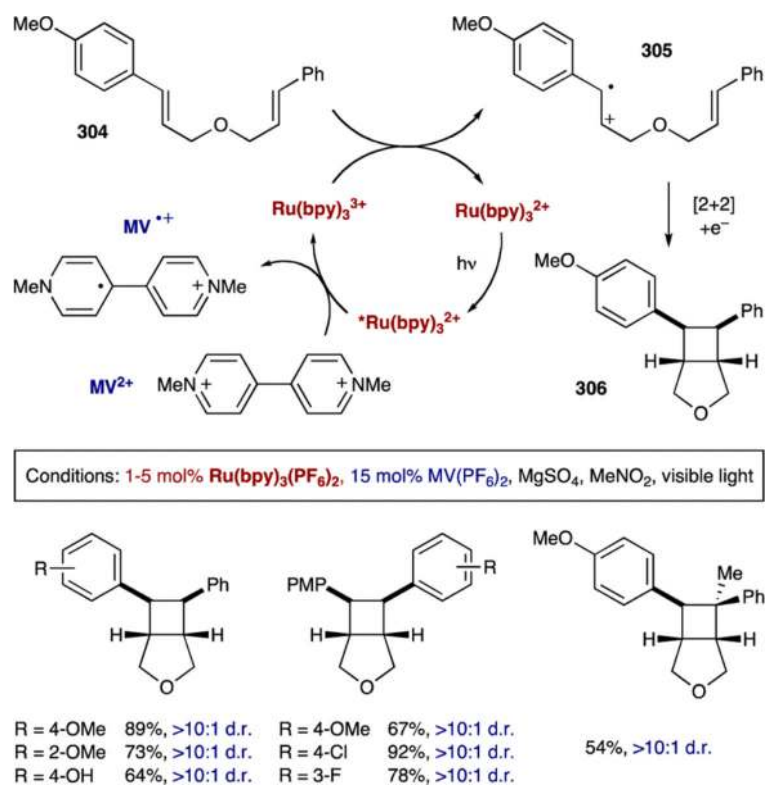
**Scheme 62.**Use of the *N*-Methylimidazolyl Group as a Redox Auxiliary



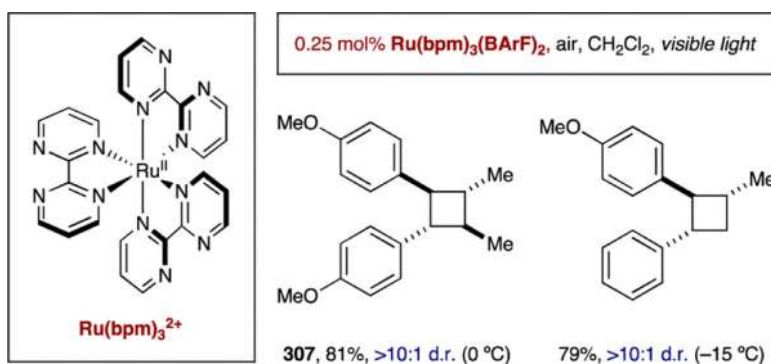
Scheme 63.
Photoredox Reductive Cyclization of Bis(enones)

**Scheme 64.**

Reductive Cyclization of Chalcones to Cyclopentanols

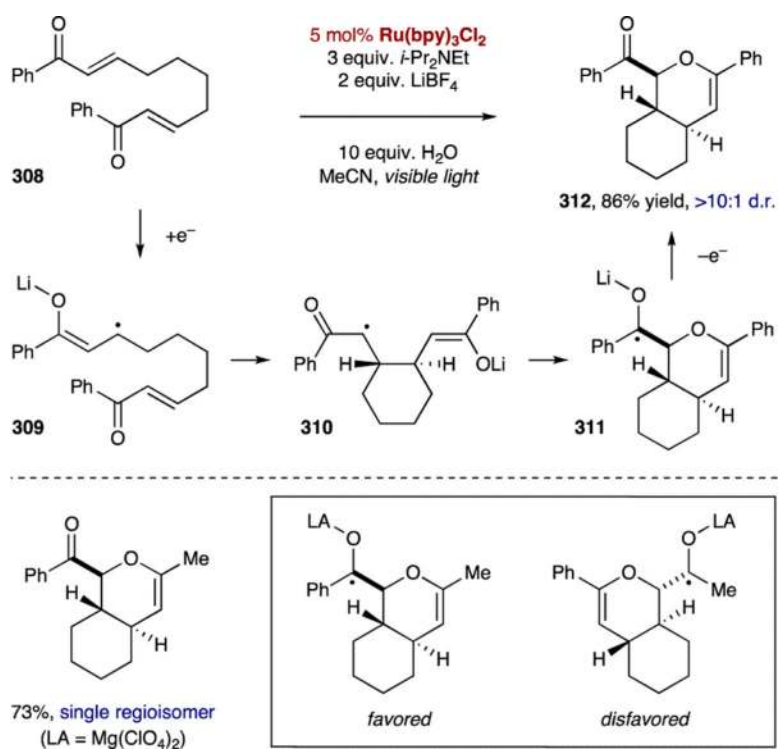
**Scheme 65.**

[2 + 2] Cycloaddition of Electron-Rich Bis(styrenes)

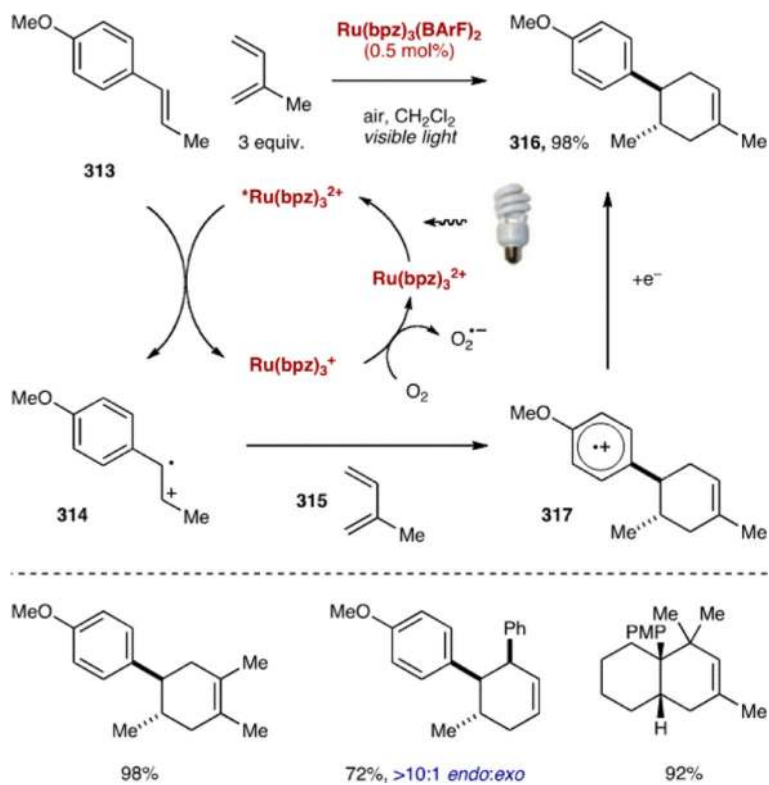


Scheme 66.

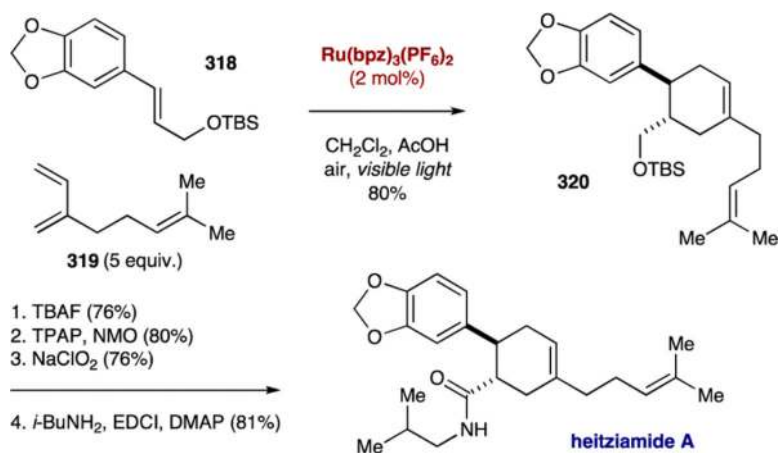
$\text{Ru}(\text{bpm})_3^{2+}$ -Catalyzed Intermolecular [2 + 2] Cycloaddition of Styrenes



Scheme 67.
Radical Anion Hetero-Diels–Alder Reaction of Bis(enones)

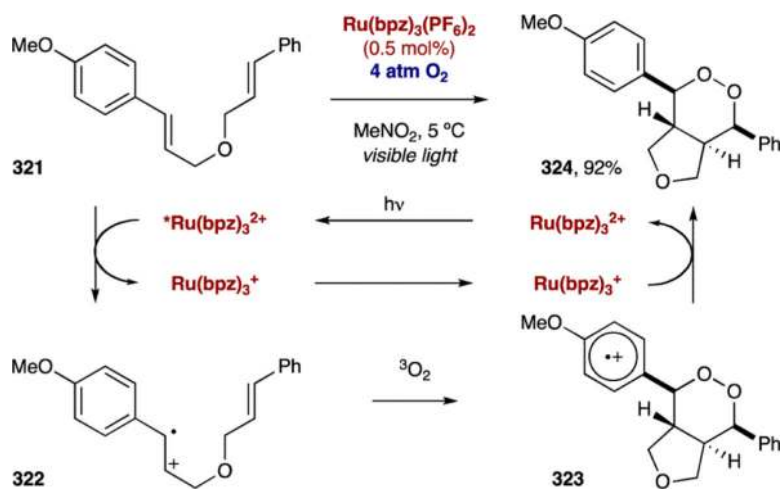


Scheme 68.
Radical Cation Diels–Alder Reaction



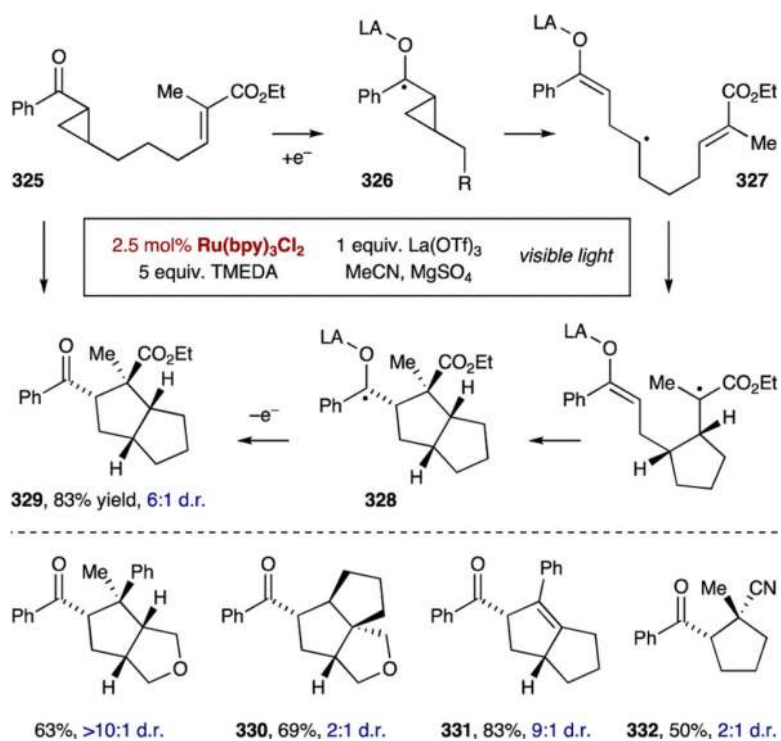
Scheme 69.

Total Synthesis of Heitziamide A via Photoredox Cycloaddition

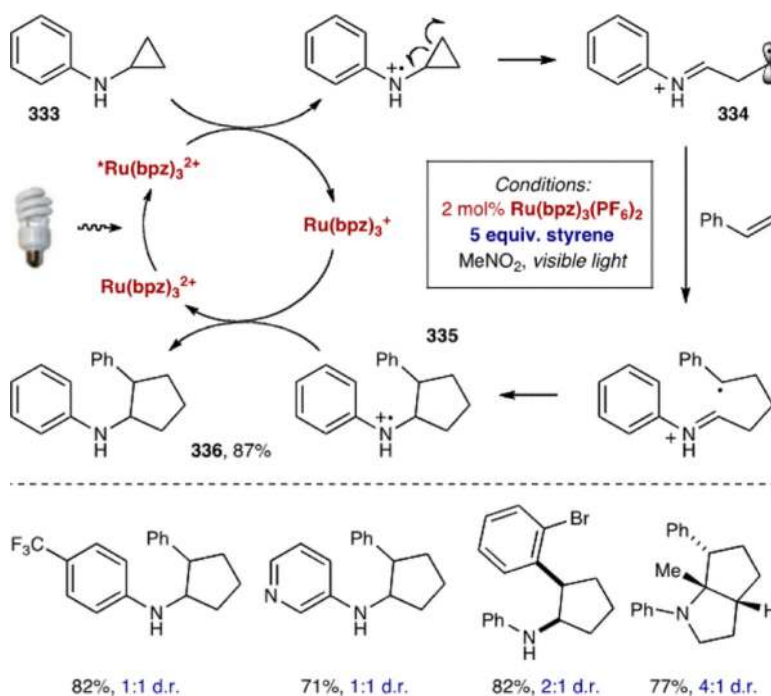


Scheme 70.

Synthesis of Endoperoxides via [2 + 2 + 2] Cycloaddition

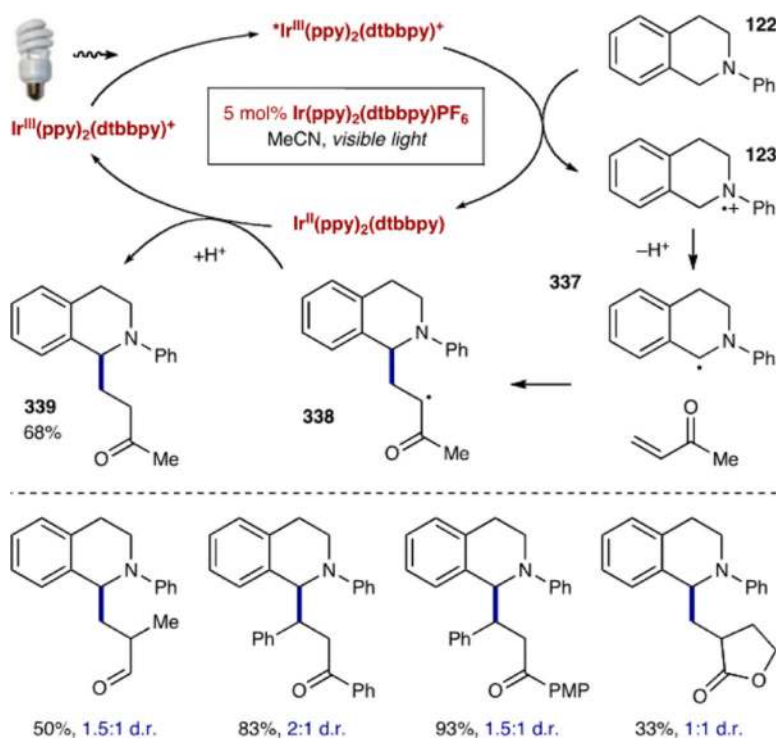
**Scheme 71.**

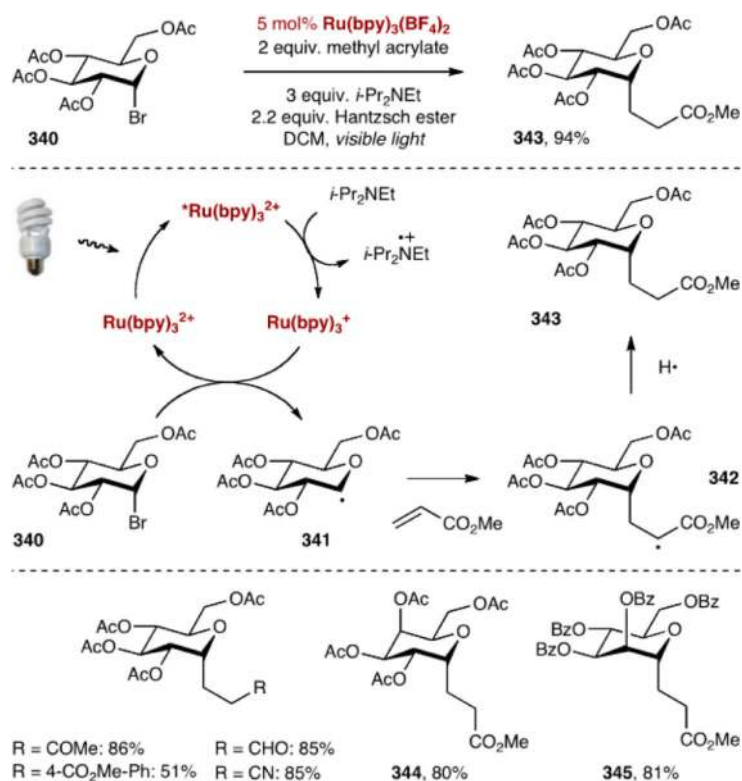
Intramolecular [3 + 2] Cycloaddition of Cyclopropyl Ketones



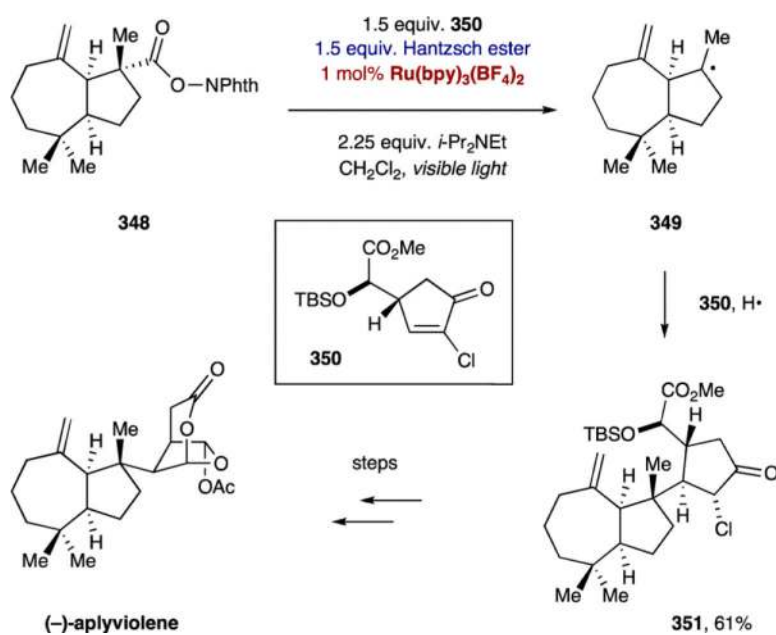
Scheme 72.

Intermolecular [3 + 2] Cycloaddition of Cyclopropylamines

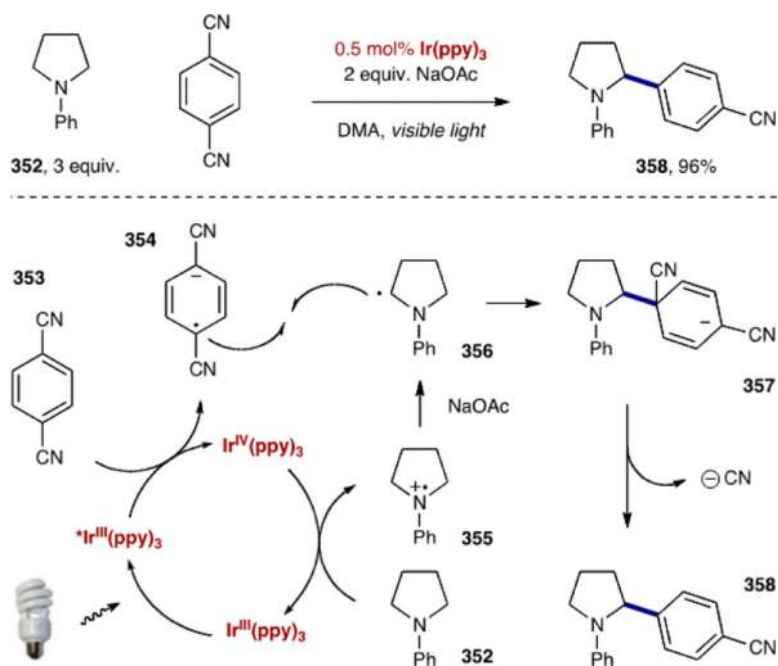
**Scheme 73.***α*-Amino Radical Conjugate Addition to Michael Acceptors



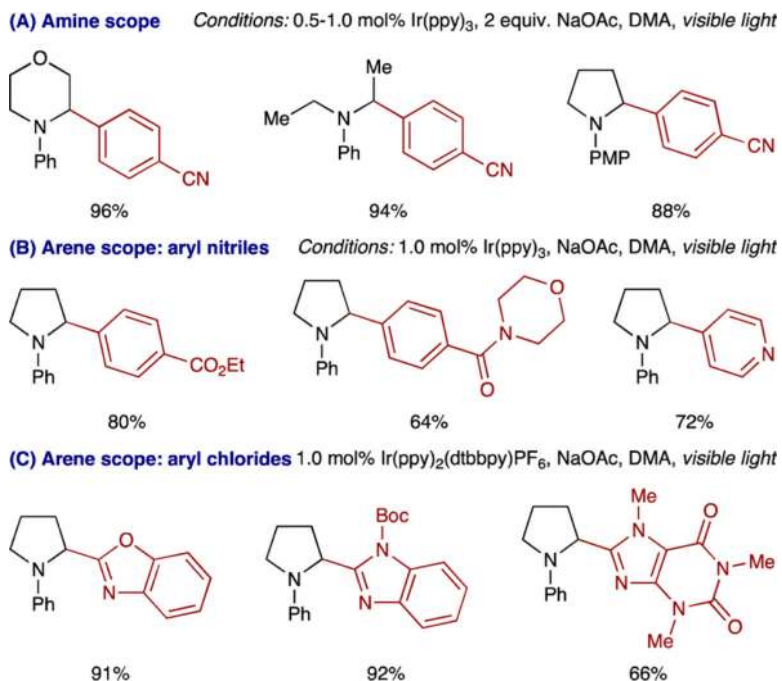
Scheme 74.
Addition of Glycosyl Radicals to Electron-Deficient Olefins

**Scheme 75.**

Photoredox Radical Conjugate Addition Applied to the Total Synthesis of (-)-Aplyviolene

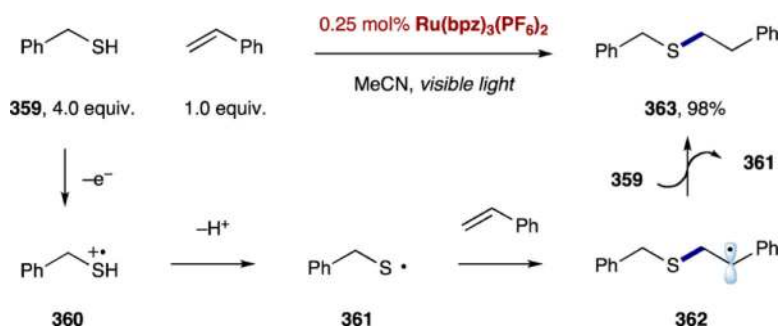


Scheme 76.
Photoredox α -Arylation of Amines with 1,4-Dicyanobenzene

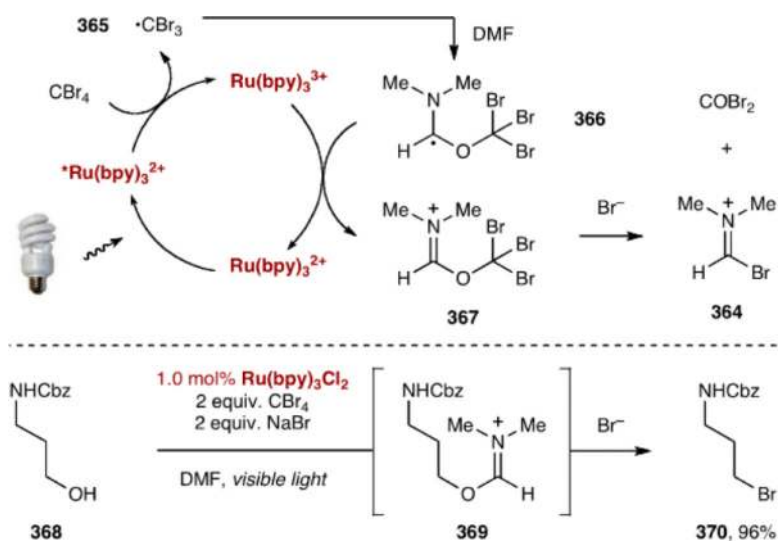


Scheme 77.

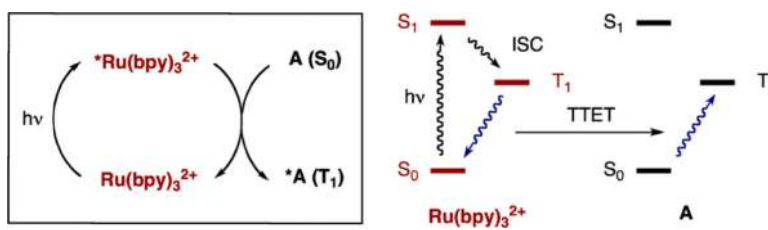
Scope of the Photoredox Amine α -Arylation Reaction



Scheme 78.
Photoredox Hydrothiolation of Alkenes via Thiyl Radicals

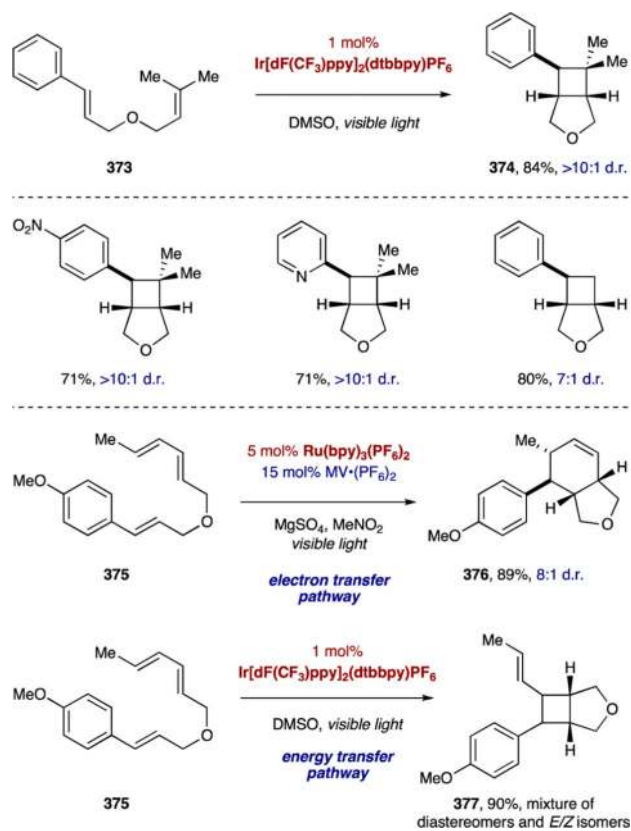


Scheme 79.
Photoredox Generation of the Vilsmeier-Haack Reagent



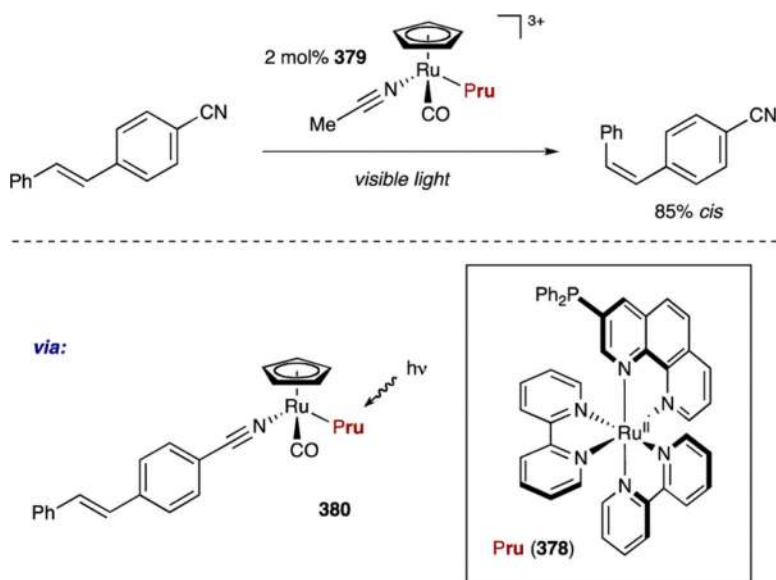
Scheme 80.

Triplet-Triplet Energy Transfer from $^*\text{Ru(bpy)}_3^{2+}$ to Acceptor A



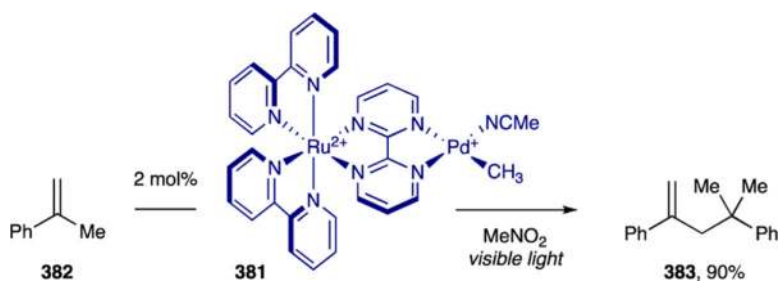
Scheme 81.

[2 + 2] Styrene Cycloadditions Enabled via Energy Transfer



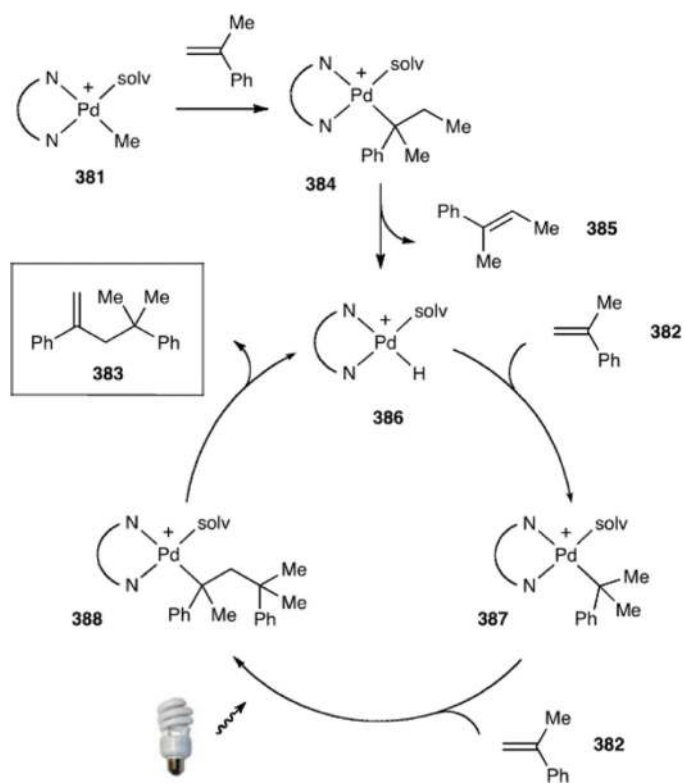
Scheme 82.

Isomerization of trans-4-Cyanostilbene via Energy Transfer from a $\text{Ru}(\text{bpy})_3^{2+}$ -type Ligand



Scheme 83.

Styrene Dimerization Catalyzed by a Bimetallic Ru/Pd Complex



Scheme 84.
 α -Methylstyrene Dimerization by a Bimetallic Ru/Pd Complex

Table 1

Redox Potentials and Selected Photophysical Properties of Commonly Utilized Visible Light Photocatalysts^a

entry	photocatalyst	$E_{1/2}$ (M ⁺ /M [*])	$E_{1/2}$ (M [*] /M ⁻)	$E_{1/2}$ (M ⁺ /M)	$E_{1/2}$ (M/M ⁻)	excited-state lifetime, τ (ns)	excitation λ_{max} (nm)	emission λ_{max} (nm)	ref
1	Ru(bpm) ₃ ²⁺	-0.21	+0.99	+1.69	-0.91	131 ^b	454	639 ^b	161
2	Ru(bpz) ₃ ²⁺	-0.26	+1.45	+1.86	-0.80	740	443	591	55
3	Ru(bpy) ₃ ²⁺	-0.81	+0.77	+1.29	-1.33	1100	452	615	1, 3
4	Ru(phen) ₃ ²⁺	-0.87	+0.82	+1.26	-1.36	500	422	610 ^c	1, 129
5	Ir[dF(CF ₃) ppy] ₂ (dtbbpy) ⁺	-0.89	+1.21	+1.69	-1.37	2300	380	470	77
6	Ir(ppy) ₂ (dtbbpy) ⁺	-0.96	+0.66	+1.21	-1.51	557		581	58, 77
7	Cu(dap) ₂ ⁺	-1.43		+0.62		270		670 ^d	33
8	<i>fac</i> -Ir(ppy) ₃	-1.73	+0.31	+0.77	-2.19	1900	375	494 ^e	38

^a All potentials are given in volts versus the saturated calomel electrode (SCE). Measurements were performed in acetonitrile at room temperature unless otherwise noted.

^b Determined in propylene carbonate.

^c Determined in aqueous solution.

^d Determined in dichloromethane.

^e Determined in 1:1 ethanol/methanol glass at 77 K.